

Fractional θ angle, 't Hooft anomaly, and quantum instantons in charge- q multi-flavor Schwinger model

Tatsuhiro Misumi,^{1,2,3} Yuya Tanizaki,⁴ and Mithat Ünsal⁴

¹*Department of Mathematical Science, Akita University, Akita 010-8502, Japan*

²*iTHEMS Program, RIKEN, Wako 351-0198, Japan*

³*Research and Education Center for Natural Sciences, Keio University, Kanagawa 223-8521, Japan*

⁴*Department of Physics, North Carolina State University, Raleigh, NC 27607, USA*

E-mail: misumi@phys.akita-u.ac.jp, ytaniza@ncsu.edu,
unsal.mithat@gmail.com

ABSTRACT: This work examines non-perturbative dynamics of a 2-dimensional QFT by using discrete 't Hooft anomaly, semi-classics with circle compactification and bosonization. We focus on charge- q N -flavor Schwinger model, and also Wess-Zumino-Witten model. We first apply the recent developments of discrete 't Hooft anomaly matching to theories on \mathbb{R}^2 and its compactification to $\mathbb{R} \times S_L^1$. We then compare the 't Hooft anomaly with dynamics of the models by explicitly constructing eigenstates and calculating physical quantities on the cylinder spacetime with periodic and flavor-twisted boundary conditions. We find different boundary conditions realize different anomalies. Especially under the twisted boundary conditions, there are Nq vacua associated with discrete chiral symmetry breaking. Chiral condensates for this case have fractional θ dependence $e^{i\theta/Nq}$, which provides the Nq -branch structure with soft fermion mass. We show that these behaviors at a small circumference cannot be explained by usual instantons but should be understood by “quantum” instantons, which saturate the BPS bound between classical action and quantum-induced effective potential. The effects of the quantum-instantons match the exact results obtained via bosonization within the region of applicability of semi-classics. We also argue that large- N limit of the Schwinger model with twisted boundary conditions satisfy volume independence.

Contents

1	Introduction and Summary	1
2	Anomaly of charge-q multi-flavor Schwinger model	5
2.1	Symmetry of charge- q N -flavor Schwinger model	5
2.2	't Hooft anomaly of symmetry	8
2.2.1	Background gauge fields of internal symmetry G	8
2.2.2	Computation of anomaly by Stora-Zumino procedure	10
2.2.3	Discrete 't Hooft anomaly and four-fermion interaction	11
2.3	Bosonization and anomaly matching	11
2.3.1	$N = 1$: Charge- q Schwinger model	12
2.3.2	$q = 1$: N -flavor Schwinger model and WZW model	14
2.3.3	General case: $q > 1$ and $N > 1$	15
2.4	Anomaly under S^1 compactifications	16
2.4.1	Thermal compactification	16
2.4.2	Flavor-twisted compactification	17
3	Holonomy effective potentials of massless Schwinger models	19
3.1	Thermal boundary condition	19
3.2	Flavor-twisted boundary condition	20
4	Chiral condensate and Polyakov loop in Schwinger model on $\mathbb{R} \times S^1$	21
4.1	Chiral condensate in thermal boundary condition	23
4.1.1	$q = 1, N = 1$ with thermal b.c.	23
4.1.2	$q = 1, N > 1$ with thermal b.c.	25
4.1.3	$q > 1, N = 1$ with thermal b.c.	26
4.1.4	$q > 1, N > 1$ with thermal b.c.	28
4.2	Chiral condensate in flavor-twisted boundary condition	30
4.2.1	$q = 1, N > 1$ with \mathbb{Z}_N twisted b.c.	30
4.2.2	$q > 1, N > 1$ with \mathbb{Z}_N twisted b.c.	32
4.3	Chiral condensate for generic L	34
4.4	Polyakov loop	35
4.4.1	$q = 1, N \geq 1$ with thermal b.c.	35
4.4.2	$q > 1, N \geq 1$ with thermal b.c.	36
4.4.3	$q \geq 1, N > 1$ with \mathbb{Z}_N twisted b.c.	38
4.5	Discrete anomaly matching	38
5	Quantum instanton on $\mathbb{R} \times S^1$ and chiral condensate	39
5.1	Fractional quantum instanton for thermal boundary condition	40
5.2	Fractional quantum instanton in flavor-twisted boundary condition	42

6	Effect of fermion mass and spontaneous C breaking at $\theta = \pi$	43
6.1	Anomaly and global inconsistency for massive Schwinger model	43
6.2	Dilute fractional-quantum-instanton gas and multi-branched vacua	46
7	Volume independence in $N \rightarrow \infty$ limit and quantum distillations	48
7.1	Interpretation as quantum distillation of Hilbert space	50
8	Twisted-compactification of $SU(N)_k$ Wess-Zumino-Witten model	52
8.1	Wess-Zumino term and topological θ terms	52
8.1.1	$SU(2)$ case	53
8.1.2	$SU(N)$ case	54
8.2	Symmetry, Anomaly, and Energy spectrum	55
9	Conclusion and Outlook	56
A	Two-dimensional Dirac spinor	58
B	Holonomy potential via bosonization	59

1 Introduction and Summary

Low-energy behaviors of quantum gauge theories are still one of the biggest and the most interesting problems in contemporary theoretical physics. Despite the fact that we are getting descriptions of confinement, chiral symmetry breaking, dynamical mass generation in compactified gauge theories on $\mathbb{R}^3 \times S_L^1$ within semi-classics [1], it is still a very hard task to make those ideas into useful tools on \mathbb{R}^4 and obtain reliable computations of physical quantities. Two-dimensional quantum field theories host a number of exactly solvable cases, and may provide useful perspective to deepen such ideas. In that regards, it provides a useful play-ground to understand the non-perturbative dynamics and behavior of the theory upon compactification. With these goals in mind, we examine certain two-dimensional QFTs by using discrete 't Hooft anomaly, semi-classics (including Hamiltonian formalism) and bosonization.

Schwinger model is one of such an example [2]. It is a 2-dimensional QED with one massless Dirac fermion, and the photon excitation becomes massive despite the gauge invariance [2, 3]. Similarities with 4-dimensional QCD are not limited to this phenomenon, and this 2d QED model also shows charge screening/confinement, presence of instantons and θ vacua, and so on [4–6]. Furthermore, massless Schwinger model is exactly solvable on various spacetime, such as cylinder [7, 8], two-sphere [9], and two-torus [10]. Because of this exact solvability, variants of Schwinger models have been used as a benchmark to test methods against the fermion sign problem in numerical Monte Carlo simulations [11–16].

We would like to note that charge-1 1-flavor Schwinger model is analogous to 4d QCD with a 1-flavor fermion. Chiral symmetry does not appear even if we turn off the fermion

mass because of Adler-Bell-Jackiw (ABJ) anomaly [17, 18], and the non-vanishing chiral condensate does not break global symmetry. The situation becomes completely different if we consider $N \geq 2$ flavors of fermions [19, 20], essentially because the theory has $SU(N)_L \times SU(N)_R$ chiral symmetry. Because of Coleman-Mermin-Wagner theorem [21, 22], the chiral condensate must vanish, $\langle \bar{\psi}\psi \rangle = 0$, but still the system shows the algebraic-long-range order, or conformal behavior, as in Kosterlitz-Thouless phase [23]. Fermion mass breaks this chiral symmetry explicitly, and thus it becomes an interesting question to ask how the fermion mass changes the vacuum structure.

In this paper, we take one step further and consider charge- q N -flavor Schwinger models. This extension recently gets some attention since $q = 2$ case is found to appear on the high-temperature domain wall of $\mathcal{N} = 1$ $SU(2)$ super Yang-Mills theory in Refs. [24, 25]. Also, in Ref. [26], the authors propose the string construction of the model with $q = 2$ and $N = 8$ to find the potential between D -brane and orientifold plane in a non-supersymmetric setup. In both papers, the recent development of 't Hooft anomaly matching plays an important role in their analysis, but full structure of anomaly is not yet studied. In this work, we will first figure it out by gauging the whole internal symmetry. Then, we shall discuss its physical consequences with the help of semiclassics after circle compactifications, where we explicitly construct eigenstates under periodic and flavor-twisted boundary conditions. This leads to explicit calculations of chiral condensate and Polyakov loop. For the twisted boundary condition, we find Nq vacua associated with discrete chiral symmetry breaking and chiral condensate with fractional θ dependence $e^{i\theta/Nq}$, leading to the Nq -branch structure with soft fermion mass. We will emphasize that the (fractional) quantum instantons, which saturate the BPS bound between classical action and quantum-induced effective potential, have a direct consequence on the physical quantities. In addition to these outcomes, we will derive the expression of chiral condensate valid for all the range of the circumference, gain new insights into the volume independence, and investigate the twist-compactified WZW models as dual theories of the Schwinger models.

In the following, let us summarize the main results of each section.

In Sec. 2, we discuss symmetry and anomaly of charge- q N -flavor massless Schwinger model. Symmetry group of this theory consists of 1-form symmetry $G^{[1]} = \mathbb{Z}_q^{[1]}$ and 0-form chiral symmetry $G^{[0]}$,

$$G = G^{[1]} \times G^{[0]} = \mathbb{Z}_q^{[1]} \times \frac{SU(N)_L \times SU(N)_R \times (\mathbb{Z}_{qN})_R}{(\mathbb{Z}_N)_V \times (\mathbb{Z}_N)_R}. \quad (1.1)$$

Unlike the case of charge-1 Schwinger model, ABJ anomaly does not spoil $U(1)_R$ chiral symmetry completely, and there is a discrete remnant $(\mathbb{Z}_{Nq})_R$, whose \mathbb{Z}_N subgroup is the same with the center of $SU(N)_R$. We will find the 't Hooft anomaly of G by identifying the 3d topological action that cancels the anomaly by anomaly-inflow mechanism. Through this computation, we find that there is an interesting subgroup,

$$G_{\text{sub}} = \mathbb{Z}_q^{[1]} \times \frac{SU(N)_V}{(\mathbb{Z}_N)_V} \times (\mathbb{Z}_{qN})_R \subset G, \quad (1.2)$$

which has \mathbb{Z}_{Nq} discrete 't Hooft anomaly including \mathbb{Z}_{Nq} two-form gauge fields, and this anomaly is important to discuss the IR realization of chiral symmetry. This \mathbb{Z}_{Nq} 't Hooft anomaly is the refinement of \mathbb{Z}_q anomaly discussed in previous studies [24–26].

In this paper, we put charge- q N -flavor Schwinger model on the cylinder $\mathbb{R} \times S^1$, with the circumference L . For $N \geq 2$, the 't Hooft anomaly on the cylinder depends on the fermion boundary condition, and the result can be summarized as follows:

Fermion b.c.	Anomaly	Prediction on chiral SSB
Thermal	\mathbb{Z}_q	$(\mathbb{Z}_{Nq})_{\text{R}} \rightarrow (\mathbb{Z}_N)_{\text{R}}$
Flavor-twisted	\mathbb{Z}_{Nq}	$(\mathbb{Z}_{Nq})_{\text{R}} \rightarrow 1$

When we take the thermal, or periodic, boundary condition on fermionic fields, only the anomaly involving $\mathbb{Z}_q^{[1]}$ one-form symmetry survives under S^1 -compactification [27]. Although this is already interesting since we can predict the spontaneous symmetry breaking of discrete chiral symmetry as $(\mathbb{Z}_{Nq})_{\text{R}} \rightarrow (\mathbb{Z}_N)_{\text{R}}$, we are losing complete information about continuous chiral symmetry $SU(N)_{\text{L}} \times SU(N)_{\text{R}}$. Taking the flavor-twisted boundary condition, the story becomes more interesting as we can keep the \mathbb{Z}_{Nq} anomaly of G_{sub} [28]. Anomaly predicts the discrete chiral symmetry breaking, $(\mathbb{Z}_{Nq})_{\text{R}} \rightarrow 1$, and this extra \mathbb{Z}_N symmetry breaking is expected to be a remnant of algebraic long-range order on \mathbb{R}^2 . This connection to conformal behavior will be explicitly shown by studying $SU(N)$ Wess-Zumino-Witten model with twisted boundary condition, but it is postponed to Sec. 8 after detailed studies on Schwinger models on $\mathbb{R} \times S^1$.

After some preparation in Sec. 3 by computing holonomy effective potentials, we construct the ground states of charge- q N -flavor Schwinger model on $\mathbb{R} \times S^1$ with both boundary conditions in Sec. 4. Interestingly, the number of classical minima of the classical holonomy potential, which is Nq in the charge $q \geq 1, N \geq 1$ is equal to the number of ground states in the compactified quantum theory. This phenomena is similar to extended $\mathcal{N} = 2$ supersymmetric quantum mechanics [29], where the number of classical and quantum vacua are the same. In our case, this fact arises due to subtle new effects involving the zero mode structure of quantum instantons. Then, we construct the θ vacua $|\theta, k\rangle$ with discrete label k . To contrast the difference between thermal and flavor-twisted compactifications, let us here quote the results only for $N \geq 2$.

In the thermal boundary condition, the fermion bilinear does not condense, $\langle \bar{\psi}_{\text{L}}^f \psi_{\text{R}}^f \rangle = 0$, for any flavors $f = 0, 1, \dots, N-1$, and the leading condensate is the determinant condensate:

$$\frac{\langle \theta, k | \det \bar{\psi}_{\text{L}}^f \psi_{\text{R}}^g | \theta, k \rangle}{\langle \theta, k | \theta, k \rangle} = e^{i \frac{\theta + 2\pi k}{q}} \frac{N!}{L^N} \exp \left(-\frac{N\pi}{Lm_\gamma} \right), \quad (k = 0, 1, \dots, q-1), \quad (1.3)$$

with the photon mass $m_\gamma^2 = Nq^2 e^2 / \pi$. As anomaly predicted, the discrete chiral symmetry is broken as $(\mathbb{Z}_{Nq})_{\text{R}} \rightarrow (\mathbb{Z}_N)_{\text{R}}$, and we have q vacua $|\theta, k\rangle$ with $k = 0, 1, \dots, q-1$ with the fractional θ dependence $e^{i\theta/q}$.

Taking the flavor-twisted boundary condition, instead, the fermion bilinear condensation appears,

$$\frac{\langle \theta, k | \bar{\psi}_L^f \psi_R^f | \theta, k \rangle}{\langle \theta, k | \theta, k \rangle} = \frac{1}{NL} e^{i \frac{\theta + 2\pi k}{Nq}} \exp\left(-\frac{\pi}{NLm_\gamma}\right), \quad (k = 0, 1, \dots, Nq - 1). \quad (1.4)$$

Discrete chiral symmetry is spontaneously broken as $(\mathbb{Z}_{Nq})_R \rightarrow 1$, and the fractional θ dependence becomes $e^{i\theta/Nq}$.

Even though the theta vacua $|\theta, k\rangle$ satisfy the cluster decomposition properties about 2d local correlators, such as those of chiral condensates $\bar{\psi}_L \psi_R$, this is not true for correlators of Polyakov loop $P = \exp(i \int_{S^1} a)$. Indeed, in both boundary conditions, we find that

$$\lim_{\tau \rightarrow \infty} \frac{\langle \theta, k | P(\tau)^\dagger P(0) | \theta, k \rangle}{\langle \theta, k | \theta, k \rangle} = \exp\left(-\frac{\pi m_\gamma L}{2q^2 N}\right), \quad (1.5)$$

while $\langle \theta, k | P | \theta, k \rangle = 0$. Correspondingly, $\mathbb{Z}_q^{[1]}$ one-form symmetry is spontaneously broken in 2d decompactification limit. We further clarify that the impossibility to achieve the cluster decomposition for both $\bar{\psi}_L \psi_R$ and P is exactly the way anomaly matching is satisfied in this theory on $\mathbb{R} \times S^1$.

In Sec. 5, we revisit the computation of chiral symmetry breaking on $\mathbb{R} \times S^1$ with semiclassical approximation of path integral, and we rediscover importance of fractional “quantum” instanton, or fracton by Smilga [30] and by Shifman and Smilga [31]. The exponents of chiral condensates in (1.3) and (1.4) depend on the gauge coupling e as

$$S_{\mathcal{F}} = \frac{\#}{eL}, \quad (1.6)$$

with a numerical constant $\#$ that depends on q, N and boundary conditions, and this is unusual as field-theoretic instanton action, which is typically $\sim 1/e^2$. We show that this has to occur as a BPS bound of Maxwell kinetic term, $\sim 1/e^2$, and quantum-induced 1-loop potential, ~ 1 . It is notable that this semiclassical object has a direct consequence on physical observables.

So far, we have limited ourselves to the massless Schwinger models. In Sec. 6, we discuss the effect of flavor-degenerate soft fermion mass m_ψ . We first show that the charge conjugation \mathcal{C} at $\theta = \pi$ has a mixed anomaly with other symmetries if $qN \geq 2$ is even, and that global inconsistency exists with \mathcal{C} and other symmetries between $\theta = 0$ and π if $qN \geq 3$ is odd. This explains the spontaneous breakdown of \mathcal{C} at $\theta = \pi$. Indeed, taking the flavor-twisted boundary condition, we have Nq branch structure with the (meta-stable) ground-state energies,

$$E_k(\theta) = -2m_\psi \exp\left(-\frac{\pi}{Nm_\gamma L}\right) \cos\left(\frac{\theta + 2\pi k}{Nq}\right). \quad (1.7)$$

For $-\pi < \theta < \pi$, the ground state is uniquely determined as $|\theta, 0\rangle$, but $|\theta, 0\rangle$ and $|\theta, -1\rangle$ are degenerate at $\theta = \pi$. We obtain this result both by mass perturbation and by dilute gas approximation of fractional quantum instantons.

This multi-branch ground state energies can be observed, since $E_n(\theta) - E_0(\theta)$ is nothing but the string tension of charge- n test particle. Especially, string tension for $n = \pm 1$ vanishes for $\theta = \pi$, while others do not vanish, and this is consistent with anomaly or global inconsistency.

In Sec. 7, we discuss the large- N volume independence of multi-flavor Schwinger model. We argue that the large- N volume independence fails for the thermal boundary condition, while it is intact with the flavor-twisted boundary condition.

This paper is organized as follows. In Sec. 2, we discuss symmetry and anomaly of charge- q N -flavor massless Schwinger model. In Sec. 3, we compute the holonomy effective potential on $\mathbb{R} \times S^1$ with thermal and flavor-twisted boundary conditions. In Sec. 4, we perform the quantum-mechanical treatment of this setup, and discuss properties of the ground states, especially about chiral condensate and Polyakov loop. In Sec. 5, we provide their semiclassical interpretation as quantum instanton. In Sec. 6, we discuss the effect of soft fermion mass. In Sec. 7, we discuss the large- N volume independence of charge- q N -flavor Schwinger model. In Sec. 8, we study the $SU(N)$ Wess-Zumino-Witten model in twisted boundary condition, and see the connection between conformal behavior in 2d and ground-state degeneracy on $\mathbb{R} \times S^1$. We conclude in Sec. 9. We fix the convention of 2d Dirac spinor in Appendix A. In Appendix B, we derive the holonomy effective potential in the language of Abelian bosonization.

2 Anomaly of charge- q multi-flavor Schwinger model

The Schwinger model is a $(1 + 1)$ dimensional quantum electrodynamics (QED) of one massless Dirac fermion with minimal electric charge [2]. This model has acquired a lot of attention because it can be exactly solved, while the theory contains many nonperturbative phenomena similar to those of QCD: mass gap of photons, nonvanishing chiral condensate, and so on. Furthermore, various correlation functions can be computed not only on \mathbb{R}^2 , but also on other two-dimensional manifolds, like cylinder $\mathbb{R} \times S^1$ [7, 8] and torus T^2 [10]. Despite its interesting features, the low-energy properties of the usual Schwinger model are rather trivial. This is mainly because the Schwinger model does not have global symmetries except for Poincare symmetry, and thus interesting phenomena like spontaneous symmetry breaking do not occur at all.

We therefore consider generalization of Schwinger model to have an interesting low-energy physics while keeping its solvability. In this section, we discuss general properties of charge- q N -flavor massless Schwinger model, especially by paying attention to symmetry and its 't Hooft anomaly. This generalization of Schwinger model has been recently discussed in Refs. [24–26].

2.1 Symmetry of charge- q N -flavor Schwinger model

The Euclidean action S of charge- q N -flavor massless Schwinger model is given by

$$S = \frac{1}{2e^2} \int_{M_2} |da|^2 + \frac{i\theta}{2\pi} \int_{M_2} da + \sum_{f=1}^N \int_{M_2} d^2x \bar{\psi}^f \gamma^\mu (\partial_\mu + qia_\mu) \psi^f. \quad (2.1)$$

Here, a is the $U(1)$ gauge field, which is canonically normalized as $\int da \in 2\pi\mathbb{Z}$ for any closed two-manifolds, e is the gauge coupling with the mass dimension 1, and ψ^f and $\bar{\psi}^f$ are two-dimensional Dirac fermions with the flavor label $f = 1, \dots, N$. When the flavor structure is evident, the flavor indices are suppressed below. For convention of two-dimensional spinors, see Appendix A. These fermions have charge $q \in \mathbb{Z}$ under the $U(1)$ gauge group. The first term is the Maxwell kinetic term of the photon fields, and the second one is the topological theta term with $\theta \sim \theta + 2\pi$. $U(1)$ gauge transformation of this theory is given by

$$a \mapsto a + d\lambda, \quad \psi \mapsto e^{-qi\lambda}\psi, \quad \bar{\psi} \mapsto \bar{\psi}e^{qi\lambda}, \quad (2.2)$$

where the gauge parameter λ is 2π -periodic compact scalar fields.

Let us identify the internal global symmetry of this theory, including higher-form symmetry. We will show that the theory has the 0-form symmetry

$$G^{[0]} = \frac{SU(N)_L \times SU(N)_R \times (\mathbb{Z}_{qN})_R}{(\mathbb{Z}_N)_V \times (\mathbb{Z}_N)_R}, \quad (2.3)$$

and the 1-form symmetry $G^{[1]} = \mathbb{Z}_q$. Let us denote these symmetries at the same time as

$$G = G^{[1]} \times G^{[0]} = \mathbb{Z}_q^{[1]} \times \frac{SU(N)_L \times SU(N)_R \times (\mathbb{Z}_{qN})_R}{(\mathbb{Z}_N)_V \times (\mathbb{Z}_N)_R}. \quad (2.4)$$

First, we discuss the 0-form symmetry. Since the Dirac fermions ψ are massless, the Lagrangian is invariant under independent unitary transformations on the right-handed fermions ψ_R and the left-handed fermions ψ_L . Therefore, the Lagrangian is invariant under

$$U(N)_L \times U(N)_R = \frac{SU(N)_L \times U(1)_L}{(\mathbb{Z}_N)_L} \times \frac{SU(N)_R \times U(1)_R}{(\mathbb{Z}_N)_R}. \quad (2.5)$$

Since the vector-like $U(1)$ symmetry is gauged, the global symmetry of the classical action is given as¹

$$G_{\text{classical}}^{[0]} = \frac{SU(N)_L \times SU(N)_R \times U(1)_R}{(\mathbb{Z}_N)_V \times (\mathbb{Z}_N)_R}. \quad (2.6)$$

This is, however, not the symmetry of quantum theory, since the path-integral measure $\mathcal{D}\bar{\psi}\mathcal{D}\psi$ is not invariant [33, 34] due to ABJ anomaly [17, 18]. In this case, $U(1)_R$ transformation $\psi_R \mapsto e^{i\alpha}\psi_R$, $\bar{\psi}_R \mapsto e^{-i\alpha}\bar{\psi}_R$ changes the path-integral measure as

$$\mathcal{D}\bar{\psi}\mathcal{D}\psi \mapsto \mathcal{D}\bar{\psi}\mathcal{D}\psi \exp\left(i\alpha \frac{Nq}{2\pi} \int da\right). \quad (2.7)$$

Because $\int da \in 2\pi\mathbb{Z}$, this transformation is the symmetry only if α is quantized to integer multiples of $2\pi/(qN)$. Therefore, $G_{\text{classical}}^{[0]}$ is explicitly broken down to (2.3). The ABJ anomaly indicates that the theta angle can be shifted as $\theta \mapsto \theta + qN\alpha$ by performing chiral

¹Here, we rewrite the Abelian symmetry as $U(1)_L \times U(1)_R = U(1)_V \times U(1)_R$ using the vector-like symmetry $U(1)_V$, but we do not introduce the axial symmetry $U(1)_A$, $\psi \mapsto e^{i\beta\gamma}\psi$. This is because the π rotations of $U(1)_V$ and $U(1)_A$ both give the \mathbb{Z}_2 fermion parity, and thus the group structure becomes slightly complicated as $U(1)_L \times U(1)_R = [U(1)_V \times U(1)_A]/\mathbb{Z}_2$. Similarly, we use $(\mathbb{Z}_N)_L \times (\mathbb{Z}_N)_R = (\mathbb{Z}_N)_V \times (\mathbb{Z}_N)_R$ to find (2.6). Similar identification of symmetry turns out to be useful also for 4-dimensional QCD [32].

transformation once we fix the UV regularization, and thus we can set $\theta = 0$ without loss of generality if massless fermions exist.

Next, we discuss the 1-form symmetry [35]. Before discussing its mathematical construction, let us explain the physical meaning of \mathbb{Z}_q one-form symmetry. We consider the Wilson loop of charge k ,

$$W_k(C) = \exp \left(ik \int_C a \right), \quad (2.8)$$

and we are interested in its behavior as C gets larger. Taking C as rectangle with area $T \times R$, its expectation value measures the potential between test particles with charge k and $-k$ at separated points;

$$-\frac{1}{T} \ln \langle W_k(C) \rangle = V_k(R). \quad (2.9)$$

Since there are dynamical particles with charge q that repeat pair creation/annihilation from vacuum, the electric charge of test particles makes sense only as $k \bmod q$ after quantization. It is therefore natural to expect that we have a symmetry operation to measure the test charge modulo q . The one-form symmetry $\mathbb{Z}_q^{[1]}$ justifies this physical intuition.

In order to construct the $\mathbb{Z}_q^{[1]}$ one-form transformation, we introduce sufficiently fine local patches $\{\mathcal{U}_i\}_i$ of our two-dimensional spacetime M_2 . Gauge field a is a set of \mathbb{R} -valued one-form fields a_i on \mathcal{U}_i with the connection formula,

$$a_j = a_i - ig_{ij}^{-1} dg_{ij}, \quad (2.10)$$

where g_{ij} is the $U(1)$ -valued transition function on the double overlap $\mathcal{U}_{ij} = \mathcal{U}_i \cap \mathcal{U}_j$. The Dirac fields ψ_f are also spinor-valued fields $(\psi_f)_i$ on each local path \mathcal{U}_i with the connection formula,

$$(\psi_f)_j = (g_{ij})^{-q} (\psi_f)_i. \quad (2.11)$$

Since we take sufficiently fine cover of M_2 , the double overlaps \mathcal{U}_{ij} can be regarded as the codimension-1 submanifolds (i.e. walls) of M_2 , and we assign the $U(1)$ transformation g_{ij} on each wall. We require the cocycle condition on the triple overlap $\mathcal{U}_{ijk} = \mathcal{U}_i \cap \mathcal{U}_j \cap \mathcal{U}_k$ as

$$g_{ij} g_{jk} g_{ki} = 1, \quad (2.12)$$

which gives the canonical normalization condition, $\int da \in 2\pi\mathbb{Z}$. This condition says that the $U(1)$ transformations on the walls must satisfy the group multiplication law at the junction \mathcal{U}_{ijk} of three walls, \mathcal{U}_{ij} , \mathcal{U}_{jk} , and \mathcal{U}_{ki} . We can readily find that we can construct the codimension-2 defect by driving a hole at the junction and inserting Aharonov-Bohm flux quantized to $2\pi/q$. That is, we perform the transformation,

$$g_{ij} \mapsto g'_{ij} = g_{ij} e^{2\pi i n_{ij}/q}, \quad (2.13)$$

so that

$$g'_{ij} g'_{jk} g'_{ki} = 1 \quad (2.14)$$

outside the defect but

$$g'_{ij} g'_{jk} g'_{ki} = e^{2\pi i/q}. \quad (2.15)$$

at the defect. Since the connection formulas of gauge fields and dynamical fermions are unaffected by this transformation, insertion of this defect is a topological operation, i.e. a symmetry transformation. Since the test particle can feel the Aharonov-Bohm flux around this defect, the above transformation acts on the Wilson loop as

$$W_k(C) \mapsto W_k(C) e^{2\pi i k/q}, \quad (2.16)$$

when C links to the defect. This operation, $\mathbb{Z}_q^{[1]}$, thus measures the charge of test particle modulo q , as we have expected from physical arguments. We therefore identify the internal symmetry group as (2.4).

2.2 't Hooft anomaly of symmetry

Let us briefly review 't Hooft anomaly matching [36, 37] in a modern terminology [38–40]. We introduce the background gauge field \mathcal{A} for symmetry G , and denote its partition function as $Z_{M_2}[\mathcal{A}]$. In general, this partition function cannot become gauge-invariant under the gauge-transformation of background fields, $\mathcal{A} \mapsto \mathcal{A} + \delta_\theta \mathcal{A}$, and it contains the phase ambiguity,

$$Z_{M_2}[\mathcal{A} + \delta_\theta \mathcal{A}] = Z_{M_2}[\mathcal{A}] \exp \left(i \int_{M_2} f(\theta, \mathcal{A}) \right). \quad (2.17)$$

As indicated in the above expression, if the phase ambiguity depends only on the background fields and their gauge-transformation parameter, we call it an 't Hooft anomaly (of Dijkgraaf-Witten type). An important observation is that the anomaly can be canceled by the boundary contribution of 3-dimensional topological G -gauge theory $S_3[\mathcal{A}]$,

$$\delta_\theta S_3[\mathcal{A}] = \int_{M_2} f(\theta, \mathcal{A}), \quad (2.18)$$

so that $Z_{M_2}[\mathcal{A}] \exp(-iS_3[\mathcal{A}])$ is gauge invariant. This shows the 't Hooft anomaly matching condition by anomaly-inflow mechanism [41]. See, for example, Refs. [24–28, 32, 42–58] for recent applications in various contexts.

In Refs. [24–26], 't Hooft anomaly of charge- q N -flavor Schwinger model has been partly discussed, but the description there is not complete. In this subsection, we are going to give the complete description regarding the 't Hooft anomaly of internal symmetry G .

2.2.1 Background gauge fields of internal symmetry G

To find the 't Hooft anomaly of charge- q N -flavor Schwinger model, we first have to construct the background gauge fields \mathcal{A} of G . It consists of

- A_R : $SU(N)_R$ one-form gauge field,
- A_L : $SU(N)_L$ one-form gauge field,
- $A_\chi = (A_\chi^{(1)}, A_\chi^{(0)})$: $(\mathbb{Z}_{qN})_R$ one-form gauge field,
- $B_V = (B_V^{(2)}, B_V^{(1)})$: (\mathbb{Z}_{qN}) two-form gauge field,

- $B_R = (B_R^{(2)}, B_R^{(1)})$: $(\mathbb{Z}_N)_R$ two-form gauge field.

Here, we regard that the \mathbb{Z}_n p -form gauge field C as a pair of $U(1)$ p -form and $(p-1)$ -form gauge fields $(C^{(p)}, C^{(p-1)})$ that satisfy the constraint, $nC^{(p)} = dC^{(p-1)}$ [59]. Following [60], we embed $SU(N)_{R/L}$ gauge fields into $U(N)_{R/L}$ gauge fields, which locally looks as

$$\tilde{A}_R = A_R + \frac{1}{N}B_V^{(1)} + \frac{1}{N}B_R^{(1)}, \quad \tilde{A}_L = A_L + \frac{1}{N}B_V^{(1)}. \quad (2.19)$$

With these background fields, the fermion kinetic term is replaced as

$$\bar{\psi}_R \gamma^\mu (\partial_\mu + i[qa_\mu + \tilde{A}_{R,\mu} + A_{\chi,\mu}^{(1)}])\psi_R + \bar{\psi}_L \gamma^\mu (\partial_\mu + i[qa_\mu + \tilde{A}_{L,\mu}])\psi_L \quad (2.20)$$

We now postulate the invariance under one-form gauge transformations to find the correct topological structure [60]. On two-form gauge fields, they are defined as

$$\begin{aligned} B_V^{(2)} &\mapsto B_V^{(2)} + d\lambda_V, & B_V^{(1)} &\mapsto B_V^{(1)} + qN\lambda_V, \\ B_R^{(2)} &\mapsto B_R^{(2)} + d\lambda_R, & B_V^{(1)} &\mapsto B_R^{(1)} + N\lambda_R, \end{aligned} \quad (2.21)$$

where the gauge parameters $\lambda_{V/R}$ are $U(1)$ one-form gauge fields. To make consistency with the local expression (2.19) of $U(N)$ gauge fields, we find that

$$\tilde{A}_R \mapsto \tilde{A}_R + q\lambda_V + \lambda_R, \quad \tilde{A}_L \mapsto \tilde{A}_L + q\lambda_V. \quad (2.22)$$

In order to make the gauged fermion kinetic term (2.20) be invariant under 1-form transformations, we have to require that

$$a \mapsto a - \lambda_V, \quad A_\chi^{(1)} \mapsto A_\chi^{(1)} - \lambda_R. \quad (2.23)$$

Since the transformation (2.23) is not consistent with $qNA_\chi^{(1)} = dA_\chi^{(0)}$, we should replace this constraint equation as $q(NA_\chi^{(1)} + B_R^{(1)}) = dA_\chi^{(0)}$.

Now, the field strength da is no longer gauge invariant, and it should be replaced as $da + B_V^{(2)}$ so that the Maxwell term becomes

$$\frac{1}{2e^2} \int_{M_2} |da + B_V^{(2)}|^2 + \frac{i\theta}{2\pi} \int_{M_2} (da + B_V^{(2)}). \quad (2.24)$$

Combined with the fermion kinetic term (2.20), we obtain the gauged action S_{gauged} . Fixing a UV regularization scheme, we can compute the partition function as

$$Z_{M_2}[\mathcal{A}] = \int \mathcal{D}a \mathcal{D}\bar{\psi} \mathcal{D}\psi \exp(-S_{\text{gauged}}). \quad (2.25)$$

Since the background gauge fields \mathcal{A} are chiral, the fermion path integral potentially suffers from non-Abelian chiral anomaly.

2.2.2 Computation of anomaly by Stora-Zumino procedure

To find the chiral anomaly, the easiest way is to use the descent equation of Stora-Zumino chain [61, 62]. It starts from computing 4-dimensional Abelian anomaly density,

$$\begin{aligned}\Omega_4 &= \frac{1}{4\pi} \text{tr}[(qda + \tilde{F}_R + F_\chi)^2] - \frac{1}{4\pi} \text{tr}[(qda + \tilde{F}_L)^2] \\ &= \frac{1}{4\pi} \text{tr}[(\tilde{F}_R + F_\chi)^2 - \tilde{F}_L^2] + \frac{1}{2\pi} qda \wedge (\text{tr}[\tilde{F}_R + F_\chi] - \text{tr}[\tilde{F}_L]) \\ &= \frac{1}{4\pi} \text{tr}[(\tilde{F}_R + F_\chi)^2 - \tilde{F}_L^2] + \frac{q}{2\pi} da \wedge d(B_R^{(1)} + NA_\chi^{(1)}).\end{aligned}\quad (2.26)$$

Here, $\tilde{F}_{R/L} = d\tilde{A}_{R/L} + i\tilde{A}_{R/L}^2$, and $F_\chi = dA_\chi^{(1)}$. Since $q(NA_\chi^{(1)} + B_R^{(1)}) = dA_\chi^{(0)}$, the second term of the last line vanishes identically. Therefore, we obtain

$$\Omega_4 = \frac{1}{4\pi} \text{tr}[(\tilde{F}_R + F_\chi)^2 - \tilde{F}_L^2]. \quad (2.27)$$

Let us apply the descent procedure to Ω_4 . We should find Ω_3^0 , which satisfies $d\Omega_3^0 = \Omega_4$. Ω_3^0 is not uniquely determined, and different ones correspond to different regularization scheme of symmetry generators, so we just have to pick up a favorite one. It is easy to check that either of the following ones satisfies the equation;

$$\Omega_3^0 = \frac{1}{4\pi} \text{tr} \left[(\tilde{A}_R + A_\chi^{(1)}) d \left(d(\tilde{A}_R + A_\chi^{(1)}) + \frac{2i}{3} \tilde{A}_R^2 \right) - \tilde{A}_L \left(d\tilde{A}_L + \frac{2i}{3} \tilde{A}_L^2 \right) \right], \quad (2.28)$$

or

$$\begin{aligned}\Omega_3^0 &= \frac{1}{4\pi} \text{tr} \left[\tilde{A}_R \left(d\tilde{A}_R + \frac{2i}{3} \tilde{A}_R^2 \right) - \tilde{A}_L \left(d\tilde{A}_L + \frac{2i}{3} \tilde{A}_L^2 \right) \right] \\ &\quad + \frac{1}{2\pi} A_\chi^{(1)} \wedge (qNB_V^{(2)} + NB_R^{(2)}) + \frac{N}{4\pi} A_\chi^{(1)} \wedge dA_\chi^{(1)}.\end{aligned}\quad (2.29)$$

In the first expression (2.28), we take the L-R scheme for the whole expression. In the second one (2.29), we take the L-R scheme for the non-Abelian part, and take the V-A scheme for the linear term in terms of $A_\chi^{(1)}$. The difference between them is expressed by the total derivative.

The final step of the descent procedure shows that the three-dimensional topological action,

$$S_3[\mathcal{A}] = \int_{M_3} \Omega_3^0, \quad (2.30)$$

satisfies the anomaly-inflow mechanism so that

$$Z_{M_2}[\mathcal{A}] \exp(-iS_3[\mathcal{A}]) \quad (2.31)$$

is gauge invariant for $\partial M_3 = M_2$, when we take the consistent regularizations. Therefore, Eq. (2.28), or (2.29), characterizes the 't Hooft anomaly of the charge- q N -flavor Schwinger model.

2.2.3 Discrete 't Hooft anomaly and four-fermion interaction

In this part, let us pay attention to a subgroup G_{sub} of the symmetry G :

$$G_{\text{sub}} = \mathbb{Z}_q^{[1]} \times \frac{SU(N)_V}{(\mathbb{Z}_N)_V} \times (\mathbb{Z}_{qN})_R \subset G. \quad (2.32)$$

That is, continuous chiral symmetry $SU(N)_L \times SU(N)_R$ is restricted to its diagonal subgroup $SU(N)_V$, while we keep the discrete axial symmetry $(\mathbb{Z}_{qN})_R$. Any fermion bilinear operators $\bar{\psi}_R \psi_L$, $\bar{\psi}_L \psi_R$ break the discrete chiral symmetry completely, but we can consider four-fermion operators which are invariant under G_{sub} :

$$(\bar{\psi}_R \psi_L)(\bar{\psi}_L \psi_R), \quad \sum_{a=1}^{N^2-1} (\bar{\psi}_R T^a \psi_L)(\bar{\psi}_L T^a \psi_R), \quad (2.33)$$

where T^a are generators of $SU(N)$. By adding this four-fermion interaction to the Lagrangian, we can explicitly break G down to G_{sub} . In the context of 4-dimensional QCD with fundamental fermions, this operator was important to discuss the exotic scenario of chiral symmetry breaking, called Stern phase [32, 63–66]. Also, this restriction of symmetry is important to discuss the application of 2-flavor Schwinger model ($\simeq SU(2)$ level-1 Wess-Zumino-Witten (WZW) model) to $(1+1)$ -dimensional anti-ferromagnetic quantum spin chain in the context of Haldane conjecture [67–70]. Its generalization to N -flavor case is important when we consider the generalization of Haldane conjecture to $SU(N)$ anti-ferromagnetic spin chain [54, 71–74].

We can readily find the anomaly of G_{sub} . We have to set $A_R = A_L \equiv A_V$ for $SU(N)$ gauge fields, and $B_R = 0$. This sets $\tilde{A}_R = \tilde{A}_L \equiv \tilde{A}_V$ with the constraint $\text{tr}[\tilde{A}_V] = B_V^{(1)}$, and $qNA_\chi^{(1)} = dA_\chi^{(0)}$, and we substitute it into (2.29). As a consequence, the anomaly is characterized by

$$S_3[\mathcal{A}_{\text{sub}}] = \int_{M_3} \frac{qN}{2\pi} A_\chi^{(1)} \wedge B_V^{(2)}. \quad (2.34)$$

This action is quantized to \mathbb{Z}_{qN} phase, and thus we find the discrete anomaly of G_{sub} .

Let us make a remark on a related anomaly, which is found in previous studies [24–26]. In those papers, authors only perform gauging of $\mathbb{Z}_q^{[1]}$ and not of $SU(N)_V/\mathbb{Z}_N$. As a consequence, anomalous breaking of discrete chiral symmetry occurs as $\mathbb{Z}_{Nq} \rightarrow \mathbb{Z}_N$ in Refs. [24–26]. In our case, we find a stronger discrete anomaly, since (2.34) says that the discrete chiral symmetry \mathbb{Z}_{Nq} is completely anomalously broken by background gauge fields.

2.3 Bosonization and anomaly matching

In two spacetime dimension, the statistics does not make much sense, and we can interchange descriptions of one field theory with bosonic fundamental field and with fermionic fundamental field. This is called Bose-Fermi duality in two dimension.

In this section, we provide the bosonic description of charge- q N -flavor Schwinger model, and check its anomaly matching explicitly. First, we discuss $N = 1$ case and $q = 1$ case separately, and go into the general case armed with that knowledge.

2.3.1 $N = 1$: Charge- q Schwinger model

One-flavor Dirac fermion $\bar{\psi}\not{\partial}\psi$ can be mapped to the free boson $\frac{1}{8\pi}|\mathrm{d}\phi|^2$ with 2π -periodic compact scalar field by Abelian bosonization [75]. The correspondence of operators are the following: The $U(1)_{V/A}$ conserved currents become

$$\bar{\psi}\gamma^\mu\psi \leftrightarrow \frac{1}{2\pi}\varepsilon^{\mu\nu}\partial_\nu\phi, \quad \bar{\psi}\gamma\gamma^\mu\psi \leftrightarrow \frac{1}{2\pi}\partial^\mu\phi. \quad (2.35)$$

The scalar fermion bilinear operator is related as

$$\bar{\psi}_R\psi_L \leftrightarrow c(\mu)e^{i\phi} \quad (2.36)$$

with some renormalization constant $c(\mu) \propto \mu$, where μ is the renormalization scale, up to some normal ordering.

Applying this Abelian bosonization to the Schwinger model (2.1) with $N = 1$ flavor, we obtain the bosonized action

$$S = \int_{M_2} \left(\frac{1}{2e^2}|\mathrm{d}a|^2 + \frac{1}{8\pi}|\mathrm{d}\phi|^2 + \frac{i}{2\pi}(q\phi + \theta) \wedge \mathrm{d}a \right). \quad (2.37)$$

The discrete axial symmetry $(\mathbb{Z}_q)_R$ becomes the shift symmetry on the scalar field ϕ :

$$\phi \mapsto \phi + \frac{2\pi}{q}. \quad (2.38)$$

Indeed, the change of the action is $\Delta S = i \int \mathrm{d}a \in 2\pi i\mathbb{Z}$, as we expect it from ABJ anomaly, and thus it does not affect path integral weight. We can also explicitly check the discrete anomaly (2.34) in the following way: Let us rewrite the bosonized action as

$$S = \int_{M_2} \left(\frac{1}{2e^2}|\mathrm{d}a|^2 + \frac{1}{8\pi}|\mathrm{d}\phi|^2 + \frac{i\theta}{2\pi}\mathrm{d}a \right) + \frac{iq}{2\pi} \int_{M_3} \mathrm{d}\phi \wedge \mathrm{d}a, \quad (2.39)$$

where M_3 is an arbitrary 3-manifold with $\partial M_3 = M_2$. We gauge $\mathbb{Z}_q^{[1]}$ and $(\mathbb{Z}_q)_R$ by the minimal coupling procedure, $\mathrm{d}a \rightarrow (\mathrm{d}a + B_V^{(2)})$ and $\mathrm{d}\phi \rightarrow (\mathrm{d}\phi + A_\chi^{(1)})$, and then the gauged action becomes

$$\begin{aligned} S_{\text{gauged}} &= \int_{M_2} \left(\frac{1}{2e^2}|\mathrm{d}a + B_V^{(2)}|^2 + \frac{1}{8\pi}|\mathrm{d}\phi + A_\chi^{(1)}|^2 + \frac{i\theta}{2\pi}(\mathrm{d}a + B_V^{(2)}) \right) \\ &\quad + \frac{iq}{2\pi} \int_{M_3} (\mathrm{d}\phi + A_\chi^{(1)}) \wedge (\mathrm{d}a + B_V^{(2)}) \\ &= \int_{M_2} \left(\frac{1}{2e^2}|\mathrm{d}a + B_V^{(2)}|^2 + \frac{1}{8\pi}|\mathrm{d}\phi + A_\chi^{(1)}|^2 + \frac{i\theta}{2\pi}(\mathrm{d}a + B_V^{(2)}) \right) \\ &\quad + \frac{i}{2\pi} \int_{M_3} (q\mathrm{d}\phi \wedge \mathrm{d}a + \mathrm{d}A_\chi^{(0)} \wedge \mathrm{d}a + \mathrm{d}\phi \wedge \mathrm{d}B_V^{(1)}) \\ &\quad + i\frac{q}{2\pi} \int_{M_3} A_\chi^{(1)} \wedge B_V^{(2)}. \end{aligned} \quad (2.40)$$

Except for the last term, which is nothing but $S_3[\mathcal{A}_{\text{sub}}]$ given in (2.34), S_{gauged} does not depend on the extension of fields to M_3 modulo $2\pi i$. This means that the gauge invariance

is satisfied by the anomaly inflow from the three-dimensional topological action $S_3[\mathcal{A}_{\text{sub}}]$, and this implies the 't Hooft anomaly matching.

Let us concretely check how the vacuum structure matches the 't Hooft anomaly. By completing the square in terms of $d\phi$ in (2.37), we can easily find that the photon da gets the mass²

$$m_\gamma^2 = \frac{q^2 e^2}{\pi}. \quad (2.41)$$

To find how the anomaly is matched, we can pay attention only to the IR limit of the theory, and thus we can take the limit $e \rightarrow \infty$, i.e. the mass gap is infinite.

We put our theory on a compact spacetime M_2 , such as torus T^2 . Since any one-point function with nontrivial charge under a symmetry does not develop the expectation value, we get

$$\langle \bar{\psi}_R \psi_L(x) \rangle_{M_2} \sim \langle e^{i\phi(x)} \rangle_{M_2} = 0 \quad (2.42)$$

for $q > 1$. This is the important difference when we compare it with $q = 1$ case: When $q = 1$, the one-instanton sector on M_2 gives the non-zero expectation value [10],

$$\langle e^{i\phi(x)} \rangle_{M_2} \equiv v > 0, \quad (q = 1). \quad (2.43)$$

Next, we discuss the two-point correlation function, $\langle e^{i\phi(x)} e^{-i\phi(y)} \rangle_{M_2}$. Equation of motion of a says that $d\phi = 0$, i.e. ϕ is constant, so that we find that

$$\langle e^{i\phi(x)} e^{-i\phi(y)} \rangle_{M_2} = v^2 > 0, \quad (2.44)$$

whether $q > 1$ or $q = 1$.

We now take the decompactification limit $M_2 \rightarrow \mathbb{R}^2$, and also separate two points $|x - y| \rightarrow \infty$. The above discussion shows that

$$\lim_{|x-y| \rightarrow \infty} \lim_{M_2 \rightarrow \mathbb{R}^2} \left(\langle e^{i\phi(x)} e^{-i\phi(y)} \rangle_{M_2} - |\langle e^{i\phi} \rangle_{M_2}|^2 \right) = \begin{cases} v^2 & (q > 1), \\ 0 & (q = 1). \end{cases} \quad (2.45)$$

Therefore, the cluster decomposition holds for $q = 1$ as shown explicitly in [10], but this is not true for $q > 1$. This is because, for $q > 1$, \mathbb{Z}_q chiral symmetry is spontaneously broken and the vacuum obtained by $M_2 \rightarrow \mathbb{R}^2$ becomes the mixed state of those q vacua. Each pure-state vacuum is labeled by $k = 0, 1, \dots, q - 1$, with

$$\langle e^{i\phi(x)} \rangle_k = v \exp \left(\frac{2\pi k - \theta}{q} i \right), \quad (2.46)$$

and

$$\lim_{M_2 \rightarrow \mathbb{R}^2} \langle \mathcal{O}(x_1, \dots, x_i) \rangle_{M_2} = \frac{1}{q} \sum_k \langle \mathcal{O}(x_1, \dots, x_i) \rangle_k \quad (2.47)$$

²The photon mass m_γ^2 in the general (q, N) model arises from the fermion loop diagram at one-loop order. Compared to the Schwinger model, the mass is enhanced by two factors. Charge at the vertices is replaced with $e \rightarrow qe$, and there are N fermions that can run in the loop, hence, $m_\gamma^2 = \frac{Nq^2 e^2}{\pi}$.

for any local correlators. The existence of q vacua does match the $\mathbb{Z}_q^{[1]} \times (\mathbb{Z}_q)_R$ 't Hooft anomaly. One of the main purpose of this paper is to obtain this fractionalized θ dependence with spontaneous chiral symmetry breaking using semiclassical approach with circle compactifications, following Refs. [30, 31].

The interesting consequence of anomaly (2.34) is that the partition function of these q vacua are related as

$$(\mathbb{Z}_q)_R : Z_k[B_V^{(2)}] \mapsto Z_{k+1}[B_V^{(2)}] = Z_k[B_V^{(2)}] \exp \left(i \int B_V^{(2)} \right). \quad (2.48)$$

The first relation is the very definition of the label k of discrete chiral symmetry breaking, and the second relation represents the mixed 't Hooft anomaly. This relation says that the q vacua are different as symmetry-protected topological (SPT) phases protected by $\mathbb{Z}_q^{[1]}$, and the domain wall between k -th and k' -th vacua supports the charge $(k' - k) \bmod q$ excitation under the $U(1)$ gauge symmetry (see, also, Refs. [46, 76–78] for nontrivial domain walls).

2.3.2 $q = 1$: N -flavor Schwinger model and WZW model

Next, let us consider the ordinary multi-flavor massless Schwinger model. This part is known in literatures, so we just briefly summarize it and include it in the analysis of general cases.

In this case, the symmetry contains only the 0-form symmetry, and it is the continuous chiral symmetry, $G = [SU(N)_L \times SU(N)_R]/(\mathbb{Z}_N)_V$. Essentially, the 't Hooft anomaly (2.29) is just the perturbative non-Abelian chiral anomaly, determined by the 3-dimensional Chern-Simons action:

$$S_3[A_R, A_L] = \frac{1}{4\pi} \int_{M_3} \text{tr} \left[A_R \left(dA_R + \frac{2i}{3} A_R^2 \right) - A_L \left(dA_L + \frac{2i}{3} A_L^2 \right) \right]. \quad (2.49)$$

It is important to notice that the spontaneous symmetry breaking is prohibited by Coleman-Mermin-Wagner theorem since the symmetry group G is continuous [21, 22]. This anomaly can be matched by $SU(N)_1$ WZW model [79–81],

$$S_{\text{WZW}} = \frac{1}{8\pi} \int_{M_2} \text{tr} [dU \wedge \star dU^\dagger] + \frac{i}{12\pi} \int_{M_3} \text{tr} [(U^\dagger dU)^3], \quad (2.50)$$

where U is the $SU(N)$ -valued field on M_2 , which is extended to M_3 for the Wess-Zumino term. This can be explicitly obtained by non-Abelian bosonization to the multi-flavor Schwinger model, and taking the limit $e \rightarrow \infty$, to make the photon mass $m_\gamma^2 = Ne^2/\pi$ infinite. Therefore, the vacuum is unique, and the conformal field theory matches the 't Hooft anomaly.

The four-fermion interaction (2.33) corresponds to the double-trace terms $|\text{tr}(U)|^2$, $|\text{tr}(T^a U)|^2$. Requiring $\text{tr}(U^k) = 0$ on M_2 for $k = 1, \dots, N-1$ as a consequence of such deformations, the $SU(N)_1$ WZW theory can be continuously connected to the flag-manifold sigma model with the target space $SU(N)/U(1)^{N-1}$ with the specific theta angles [54]. The symmetry group is reduced to $G_{\text{sub}} = SU(N)_V/(\mathbb{Z}_N)_V \times (\mathbb{Z}_N)_R$, and the theta terms of the flag sigma model reproduces the discrete anomaly $S_3[\mathcal{A}_{\text{sub}}]$ [54].

2.3.3 General case: $q > 1$ and $N > 1$

The non-Abelian bosonization maps N -flavor Dirac fermion to $U(N)_1$ WZW model [81–83]. The correspondence of the fermion bilinear operator is

$$\psi_L \bar{\psi}_R \sim U, \quad (2.51)$$

where U is the $U(N)$ -valued scalar field. This tells that the element of the 0-form symmetry,

$$[(V_L, V_R, e^{i\alpha_R})] \in \frac{SU(N)_L \times SU(N)_R \times (\mathbb{Z}_{Nq})_R}{(\mathbb{Z}_N)_V \times (\mathbb{Z}_N)_R}, \quad (2.52)$$

acts on U as

$$U \mapsto V_L U V_R^\dagger e^{-i\alpha_R}. \quad (2.53)$$

The bosonized action of the theory is given by

$$\begin{aligned} S = & \frac{1}{2e^2} \int_{M_2} |da|^2 + \frac{1}{8\pi} \int_{M_2} \text{tr}(|dU|^2) \\ & + \frac{i}{12\pi} \int_{M_3} \text{tr}((U^\dagger dU)^3) + \frac{q}{2\pi} \int_{M_3} da \wedge \text{tr}(U^\dagger dU). \end{aligned} \quad (2.54)$$

The first two terms are kinetic terms, and the third term is the level-1 Wess-Zumino term. The last term can be expressed as

$$\int_{M_2} a \wedge \frac{1}{2\pi} d(\ln \det(U)^q), \quad (2.55)$$

and, in the limit $e \rightarrow \infty$, the $U(1)$ gauge field a plays a role of the Lagrange multiplier field, so that $\det(U) \in \mathbb{Z}_q$ and it reproduces the ABJ anomaly $U(1)_R \rightarrow (\mathbb{Z}_{Nq})_R$.

Let us check that the bosonized action has the same anomaly $S_3[\mathcal{A}]$, given in (2.28), including the discrete factors of G . The gauge-invariance of the kinetic terms is evident, and thus let us concentrate on the last two topological terms. The covariant derivative D on U and U^\dagger with background gauge fields \mathcal{A} are given as

$$DU = dU + i\tilde{A}_L U - iU(\tilde{A}_R + A_\chi^{(1)}), \quad DU^\dagger = dU^\dagger + i(\tilde{A}_R + A_\chi^{(1)})U^\dagger - iU^\dagger \tilde{A}_L. \quad (2.56)$$

The naive replacement $U^\dagger dU \rightarrow U^\dagger DU$, etc., is insufficient for the Wess-Zumino term, and we must find an appropriate local counterterm. With some trial-and-error, we can find that the following works well:

$$\begin{aligned} \Gamma_{\text{WZ}} \equiv & \frac{1}{12\pi} \text{tr}((U^\dagger DU)^3) - i\frac{q}{2\pi} (da + B_V^{(2)}) \wedge \text{tr}(U^\dagger DU) \\ & + \frac{1}{4\pi} \text{tr}[(UDU^\dagger) \wedge i(\tilde{F}_L - qB_V^{(2)}) - (U^\dagger DU) \wedge i(\tilde{F}_R + dA_\chi^{(1)} - qB_V^{(2)})]. \end{aligned} \quad (2.57)$$

The gauge invariance both under the ordinary and 1-form transformations is manifest in this expression. A straightforward computation shows that

$$\begin{aligned} \Gamma_{\text{WZ}} = & \frac{1}{12\pi} \text{tr}[(U^\dagger U)^3] - \frac{i}{2\pi} da \wedge \left(\text{tr}[U^\dagger dU] - q(NA_\chi^{(1)} + B_R^{(1)}) \right) \\ & + d \left(\frac{i}{4\pi} \text{tr} \left[U^\dagger dU(\tilde{A}_R + A_\chi^{(1)}) - U dU^\dagger \tilde{A}_L + iU^\dagger \tilde{A}_L U(\tilde{A}_R + A_\chi^{(1)}) \right] \right) \\ & - \frac{1}{4\pi} \text{tr} \left[(\tilde{A}_R + A_\chi^{(1)}) d \left(d(\tilde{A}_R + A_\chi^{(1)}) + \frac{2i}{3} \tilde{A}_R^2 \right) - \tilde{A}_L \left(d\tilde{A}_L + \frac{2i}{3} \tilde{A}_L^2 \right) \right]. \end{aligned} \quad (2.58)$$

The last line is equal to the topological action, $S_3[\mathcal{A}]$, given in (2.28). Other terms on the right-hand-side is defined on M_2 modulo 2π . This shows that the gauge invariance is established by anomaly inflow from the three-dimensional bulk action, $S_3[\mathcal{A}]$, and thus it has the same 't Hooft anomaly with the massless Schwinger model.

2.4 Anomaly under S^1 compactifications

In the later sections, we will establish the semiclassical understandings of nonperturbative phenomena in charge- q N -flavor Schwinger model. In order to validate the semiclassical treatment, we need to put the theory on the cylinder with small compactification radius [30, 31]. We have seen that the two-dimensional model has the 't Hooft anomaly and it constrains the vacuum structures and the massless excitations. We would like to retain those 't Hooft anomalies as much as possible, and we shall see that the appropriate flavor-twisted boundary condition plays an important role [28, 50, 84].

2.4.1 Thermal compactification

Let us put our theory on $M_2 = M_1 \times S^1 \ni (x^1, x^2) =: (\tau, x)$, and assume that the size of S^1 is much smaller than that of M_1 . We then obtain the effective field theory on M_1 , and would like to understand its properties. We first consider the ordinary boundary condition³ along the compactified direction $x \sim x + L$:

$$\psi^f(\tau, x + L) = -\psi^f(\tau, x), \quad (2.59)$$

$$a(\tau, x + L) = a(\tau, x) + d\lambda(\tau), \quad (2.60)$$

where λ is a 2π -periodic scalar on $\tau \in M_1$.

To discuss the 't Hooft anomaly of the 1-dimensional effective theory on M_1 , we first need to identify the symmetries. This boundary condition does not affect the 0-form symmetry $G^{[0]}$. What is important for gauge theories is that Polyakov-loop operators become local gauge-invariant operators under S^1 -compactification;

$$P(\tau) = \exp \left(i \int_0^L a_2(\tau, x) dx \right). \quad (2.61)$$

The 1-form symmetry, $\mathbb{Z}_q^{[1]}$, in two-dimensions provides the additional 0-form symmetry, $\mathbb{Z}_q^{[0]}$, in one-dimensions, and it is given by

$$P(\tau) \mapsto e^{2\pi i/q} P(\tau), \quad (2.62)$$

so that the symmetry G in two-dimensions induces

$$G \rightsquigarrow G_{\text{1d}} = \mathbb{Z}_q^{[0]} \times \frac{SU(N)_L \times SU(N)_R \times (\mathbb{Z}_{qN})_R}{(\mathbb{Z}_N)_V \times (\mathbb{Z}_N)_R}. \quad (2.63)$$

³Here, we take the anti-periodic boundary condition for the fundamental fermion fields. We, however, would like to point out that the overall $U(1)$ phase of the boundary condition does not affect the physics since the $U(1)$ symmetry is gauged, and thus periodic and anti-periodic boundary conditions play the same role. In other words, since the local gauge-invariant operators are all bosonic, the above difference of boundary conditions does not change physics. This point will be discussed more in detail in Sec. 3.

In this thermally compactified theory, the $SU(N)_{L/R}$ chiral anomalies in two-dimensions disappear in one-dimensions and do not imply the anomaly matching condition. To see this, let us remind that, for instance, the $SU(N)_R$ two-dimensional anomalies take the form

$$\frac{1}{4\pi} \int_{M_3} \text{tr} \left(A_R \left(dA_R + \frac{2i}{3} A_R^2 \right) \right). \quad (2.64)$$

When we gauge $SU(N)_R$ symmetry as a symmetry of one-dimensional theory, A_R depends only on τ and should not show any x dependence. As a consequence, the gauge fields on M_3 do not have x dependence, and we identically obtain $A_R dA_R + \frac{2i}{3} A_R^3 \equiv 0$ since it becomes the 3-form of 2-dimensional functions.

The anomaly of higher-form symmetries is exceptional in this viewpoint [27]. Let us gauge $\mathbb{Z}_q^{[0]}$, and we denote its gauge field as

$$A_{c(q)} = A_{c(q),1}(\tau) d\tau. \quad (2.65)$$

Although this is the one-form gauge field on M_1 , it acts on Polyakov loops and thus its two-dimensional origin is $B_V^{(2)}$:

$$B_V^{(2)} = A_{c(q)} \wedge \frac{dx}{L}. \quad (2.66)$$

Substituting this expression into (2.29), we find that the discrete anomaly survives:

$$\Omega_3^0 = \frac{q}{2\pi} (N A_\chi^{(1)}) \wedge A_{c(q)} \wedge \frac{dx}{L}, \quad (2.67)$$

and then the anomaly inflow is controlled by the two-dimensional $\mathbb{Z}_q \times \mathbb{Z}_q$ Dijkgraaf-Witten action,

$$\int \Omega_3^0 = \frac{q}{2\pi} \int (N A_\chi^{(1)}) \wedge A_{c(q)}. \quad (2.68)$$

This describes the mixed anomaly of

$$\mathbb{Z}_q^{[0]} \times \left(\frac{\mathbb{Z}_{Nq}}{\mathbb{Z}_N} \right)_R \subset G_{1d}. \quad (2.69)$$

We therefore conclude that the discrete anomaly survives under thermal compactification when $q > 1$. However, we completely lose the information about continuous chiral anomaly under this compactification. Especially, when $q = 1$, we do not have the discrete anomaly, and the vacuum structure becomes completely trivial.

2.4.2 Flavor-twisted compactification

If possible, we would like to keep the nontrivial structure of two-dimensional field theories as much as possible under S^1 compactification. If we take the thermal boundary condition for fermion fields, however, the information about continuous chiral symmetry is completely lost. Many recent studies of asymptotically free theories [1, 85–115] suggest that we can keep the nontrivial vacuum structure of the original theory by taking the appropriate symmetry-twisted boundary condition. This is, indeed, noticed much earlier than these recent works in the context of multi-flavor Schwinger model by Shifman and Smilga [31],

but its full generality is appreciated by aforementioned works, and it is referred to as adiabatic continuity [1]. We here provide its interpretation in view of 't Hooft anomaly following Ref. [28].

We put the flavor-twisted boundary condition on the fundamental fermion fields,

$$\psi'^f(\tau, x + L) = e^{2\pi i f/N} \psi'^f(\tau, x), \quad (2.70)$$

and we simply denote this as $\psi'(\tau, x + L) = \Omega_F \psi'(\tau, x)$ introducing the diagonal matrix $\Omega_F = \text{diag}(1, e^{2\pi i/N}, \dots, e^{2\pi i(N-1)/N})$. This is related to the fermion field with the periodic boundary condition as

$$\psi'^f(\tau, x) = e^{2\pi i f x/NL} \psi^f(\tau, x), \quad (2.71)$$

and the fermion kinetic term is given as

$$\int_{M_1} d\tau \int_0^L dx \sum_{f=1}^N \bar{\psi}^f \left(\gamma^\mu \partial_\mu + \gamma^1 i q a_1 + \gamma^2 i \left(q a_2 + \frac{2\pi f}{NL} \right) \right) \psi^f. \quad (2.72)$$

In this way, we can interpret the flavor-twisted boundary condition as the background $SU(N)_V$ holonomy. We will use both descriptions in the following of the paper.

In this boundary condition, the symmetry acting on the Polyakov loop $P(\tau)$ is not just $\mathbb{Z}_q^{[0]}$, but it is further extended to $\mathbb{Z}_{Nq}^{[0]}$ with the following transformation:

$$a_2 \mapsto a_2 + \frac{2\pi}{NqL}, \quad (2.73)$$

and it is intertwined with the shift transformation,

$$\psi^f \mapsto \psi^{f+1} \quad (f = 1, \dots, N-1), \quad \psi^N \mapsto e^{-2\pi i x/L} \psi^1. \quad (2.74)$$

The ordinary flavor symmetry $G^{[0]}$ is explicitly broken to its maximal Abelian subgroup because of this boundary condition,

$$\frac{U(1)_L^{N-1} \times U(1)_R^{N-1} \times (\mathbb{Z}_{Nq})_R}{(\mathbb{Z}_N)_V \times (\mathbb{Z}_N)_R} \subset G^{[0]}. \quad (2.75)$$

Then, the full symmetry group is

$$\mathbb{Z}_{Nq}^{[0]} \ltimes \frac{U(1)_L^{N-1} \times U(1)_R^{N-1} \times (\mathbb{Z}_{Nq})_R}{(\mathbb{Z}_N)_V \times (\mathbb{Z}_N)_R}. \quad (2.76)$$

It is important for later applications that this symmetry group contains $\mathbb{Z}_{Nq}^{[0]} \times (\mathbb{Z}_{Nq})_R$ as a subgroup.

As we have discussed in gauging $\mathbb{Z}_q^{[0]}$, the $\mathbb{Z}_{Nq}^{[0]}$ background gauge field, $A_{c(Nq)}$, is embedded into the two-form gauge field as

$$B_V^{(2)} = A_{c(Nq)} \wedge \frac{dx}{L}. \quad (2.77)$$

Substituting this into the anomaly-inflow action (2.29) in two-dimensions, we find that the effective theory on M_1 with the twisted boundary condition has the anomaly, which is determined by $\mathbb{Z}_{Nq} \times \mathbb{Z}_{Nq}$ Dijkgraaf-Witten action,

$$\frac{Nq}{2\pi} \int A_\chi^{(1)} \wedge A_{c(Nq)}. \quad (2.78)$$

Unlike the thermal boundary condition, this anomaly persists even for $q = 1$ multi-flavor Schwinger model.

3 Holonomy effective potentials of massless Schwinger models

As a preparation of quantum mechanical treatment in Sec. 4, we compute the effective potential of the Polyakov loop, $\exp(iLa)$, by integrating out fermions. Below, we describe two physically different compactification of the charge- q N flavor Schwinger model: Thermal and flavor-twisted boundary conditions denoted with $SU(N)_V$ flavor matrix, Ω_F .

3.1 Thermal boundary condition

Let us first discuss that the overall $U(1)$ phase of fermion boundary conditions is unphysical in Schwinger models. More generally, this is true for Spin^c gauge theories. In text-books, it is sometimes asserted that the thermal boundary conditions are necessarily anti-periodic for fermionic fields. Here, let us take a more general boundary condition on $\mathbb{R} \times S^1$,

$$\psi(\tau, x + L) = e^{i\alpha} \psi(\tau, x), \quad (3.1)$$

and $\alpha = \pi$ corresponds to the usual thermal boundary condition. We perform the “improper” gauge transformation,

$$a \mapsto a' = a + \frac{\alpha}{qL}, \quad \psi \mapsto \psi' = e^{-i\alpha x/L} \psi, \quad (3.2)$$

and then the form of the Lagrangian is not changed, but the fields satisfy the periodic boundary condition. Local gauge-invariant operators, $\star da = \partial_\tau a(\tau)$, $\bar{\psi}\psi$, etc., do not change under this transformation, and the only change on gauge-invariant operators appears as the phase of Polyakov loop,

$$e^{iLa} \mapsto e^{i\alpha/q} e^{iLa}. \quad (3.3)$$

Therefore, the computation with periodic boundary condition gives sufficient information to obtain the result with general α , and the overall phase α is unphysical in this sense. In Hilbert space interpretation, these boundary conditions correspond to the computation of $\text{tr}(e^{-LH} e^{i(\alpha+\pi)F})$, where F is fermion number. However, there are no gauge invariant fermionic states in the Hilbert space of the model, and hence,

$$\text{tr}(e^{-LH} e^{i(\alpha+\pi)F}) = \text{tr}(e^{-LH}), \quad (3.4)$$

because $F \equiv 0$ on physical Hilbert space.

We now compute the holonomy effective potential, using periodic boundary condition for fermionic fields, $\alpha = 0$. Since this is 2d $U(1)$ gauge theory, the holonomy potential is induced solely by fermions:

$$V(a) = -\ln \text{Det}(\gamma^\mu D_\mu) = -N \ln \text{Det}(\gamma^1 \partial_\tau + \gamma^2 (\partial_x + ia)). \quad (3.5)$$

In the statistical-mechanics language, the potential takes the form:

$$\begin{aligned} V(a) &= -\frac{N}{L} \int \frac{dp}{2\pi} \left(\log(1 + e^{-L|p| + iLqa + i\pi}) + \text{c.c.} \right) \\ &= \frac{2N}{\pi L^2} \sum_{n=1}^{\infty} \frac{1}{n^2} \cos(Lqan) \\ &= \min_{k \in \mathbb{Z}} \frac{2N}{\pi L^2} \left(\frac{1}{4} (Lqa + \pi(2k+1))^2 - \frac{\pi^2}{12} \right) \end{aligned} \quad (3.6)$$

In the first line, the over-all minus sign is related to Pauli-exclusion principle. The $e^{i\pi}$ arises from the periodic boundary conditions on fermions. In Appendix B, we derive the same result in the bosonized theory.

The minimal value of the potential, (3.6), is the thermal free energy density:

$$\mathcal{F}_{\text{thermal}} = -\frac{2N}{L^2} \frac{\pi}{12}, \quad (3.7)$$

and this is the Stefan-Boltzmann law for black-body radiation for N species of Dirac fermions.

We make two comments on (3.6).

- In the usual Schwinger model, $(q, N) = (1, 1)$ and its multiflavor thermal version $(1, N > 1)$, the holonomy potential has a unique minimum in its fundamental domain located at $La = \pi$.
- In the $(q > 1, N \geq 1)$ with p.b.c. for all flavors, the holonomy potential has q minima in the fundamental domain given by $La = \frac{2\pi}{q}(p + \frac{1}{2})$, with $p = 0, 1, \dots, q-1$. These minima are separated by $L\Delta a = \frac{2\pi}{q}$.

Unlike a purely bosonic system in which the q -fold perturbative degeneracy would generically be lifted due to non-perturbative instanton effects, in the present case the degeneracy will survive. This is guaranteed by the persistent mixed anomaly and is realized through fermionic zero-mode structure of fractional instantons. This is the subject matter of Sec. 4.1.

3.2 Flavor-twisted boundary condition

A boundary condition twisted by the genuine global symmetry has crucial physical consequences. Now, consider the fermions with flavor-twisted boundary conditions:

$$\psi(\tau, x + L) = \Omega_F \psi(\tau, x) \quad (3.8)$$

In the operator formalism, this will correspond to a grading and quantum distillation over the Hilbert space [84]. The holonomy potential is given by

$$V_{\Omega_F}(a) = \frac{1}{\pi L^2} \sum_{n=1}^{\infty} \frac{1}{n^2} (e^{iLqan \text{tr}(\Omega_F^n)} + \text{c.c.}), \quad (3.9)$$

and we now substitute $\Omega_F = \text{diag}(1, e^{2\pi i/N}, \dots, e^{2\pi i(N-1)/N})$. All terms in (3.9), but $n = Nn'$, are zero due to Ω_F -twist matrix. As a result, the potential takes the form:

$$\begin{aligned} V_{\Omega_F}(a) &= \frac{2}{\pi L^2} \frac{1}{N} \sum_{n'=1}^{\infty} \frac{1}{n'^2} \cos(NLqan') \\ &= \min_{k \in \mathbb{Z}} \frac{2}{\pi L^2 N} \left(\frac{1}{4} \left(qNL a + \pi(2k+1) \right)^2 - \frac{\pi^2}{12} \right) \end{aligned} \quad (3.10)$$

We make various comments for the minima of the holonomy potential:

- In the $(q = 1, N > 1)$ with Ω_F twist, the holonomy potential has N minima in the fundamental domain $La \in [0, 2\pi)$, given by $La = \frac{2\pi}{N}(p + \frac{1}{2})$, $p = 0, 1, \dots, N-1$. These minima are separated by $L\Delta a = \frac{2\pi}{N}$.
- For the most general $(q > 1, N \geq 1)$ with Ω_F twist, the holonomy potential has qN minima in the fundamental domain, and those minima are given by $La = \frac{2\pi}{qN}(p + \frac{1}{2})$, $p = 0, 1, \dots, qN-1$, which are separated by $L\Delta a = \frac{2\pi}{qN}$.

Unlike a purely bosonic theory in which the qN -fold perturbative degeneracy would generically be lifted due to instanton effects, in the present case the qN -fold degeneracy is not lifted due to fermion zero mode structure of the instantons, and also as dictated by anomalies. The mechanism that will be described is similar to $\mathcal{N} = 2$ supersymmetric quantum mechanics, in which, the degeneracy of the classical vacua persists despite the instanton effects [29]. This is also explained by using Picard–Lefschetz theory applied to multi-instantons [116]. This will be crucial in realizing the mixed anomalies in reduced quantum mechanics.

The free energy density with Ω_F twist is given by

$$\mathcal{F}_{\Omega_F} = -\frac{2}{N} \frac{\pi}{12} \frac{1}{L^2} = \frac{1}{N^2} \mathcal{F}_{\text{thermal}} \quad (3.11)$$

4 Chiral condensate and Polyakov loop in Schwinger model on $\mathbb{R} \times S^1$

Chiral symmetry breaking and chiral condensates in Schwinger model on $\mathbb{R} \times S^1$ were investigated in [10, 30, 31]. In particular, Shifman and Smilga [31] investigated the 2-flavor cases with the flavor-twisted boundary condition, with emphasis on the contributions from fractional instantons. It is of great importance to review their results and extend them to the charge- q N -flavor cases.

Firstly, let us review the chiral condensate in the simplest case, or the massless $N = 1$ Schwinger model with $q = 1$ on \mathbb{R}^2 . The chiral condensate for this case is exactly calculated as

$$\langle \bar{\psi} \psi \rangle = -\frac{m_\gamma}{2\pi} e^\gamma, \quad (4.1)$$

where $m_\gamma \equiv e/\sqrt{\pi}$ and $\gamma \simeq 0.5771$ is the Euler-Mascheroni constant. There are several techniques to derive the chiral condensate [7, 9, 10, 117–120], including bosonization, functional integral around instanton backgrounds, and the cluster decomposition of the four-point correlators.

We here obtain the chiral condensates for charge- q N -flavor Schwinger models with thermal b.c. (or, periodic b.c., p.b.c.) and \mathbb{Z}_N t.b.c. on $\mathbb{R} \times S^1$ by use of quantum mechanical techniques. We first note that we can choose $a_1 = 0$ by use of gauge degrees of freedom (i.e. temporal gauge). Moreover, we here focus on the case

$$eL \ll 1, \quad (4.2)$$

and can drop the higher Kaluza-Klein (KK) modes of a_2 . So, we will work on position-independent a_2 denoted just as $a_2 \equiv a$ below.

The associated Dirac equation for general cases with charge- q and N -flavor is

$$\left[i \frac{\partial}{\partial t} + \sigma_3 \left(i \frac{\partial}{\partial x} - qa \right) \right] \psi = 0. \quad (4.3)$$

Here we denote the energy of k -th state as $E^{(k)}$ with assuming $\psi \sim e^{-iE^{(k)}t} \psi_k(x)$. We here call the compactified direction as $x^2 = x$, and introduce a Minkowski time t to study the system quantum-mechanically. The equation is then rewritten as

$$E^{(k)} \psi_k(x) = -\sigma_3 \left(i \frac{d}{dx} - qa \right) \psi_k(x). \quad (4.4)$$

The solution of eigenfunctions $\psi_k(x)$ depends on boundary conditions, charges and flavors, thus we below discuss distinct cases separately.

An important consequence in Secs. 4.1 and 4.2 is that the chiral condensate on $\mathbb{R} \times S^1$ with (4.2) behaves as

$$\langle \bar{\psi} \psi \rangle \sim \frac{\#}{L} \exp \left(-\frac{\#}{eL} \right), \quad (4.5)$$

where $\#$'s are numerical constants that depend on q , N , and boundary conditions. In this section, we will find their explicit forms by quantum mechanical computations, since this is important to understand the degeneracy of ground states. In Sec. 5, we shall reinterpret this behavior using the path-integral approach with semiclassical approximations. It is notable that the exponent of chiral condensates behaves as $\sim 1/e$, instead of the usual field-theoretic instanton action $\sim 1/e^2$. We shall interpret this as a manifestation of “quantum” instanton in Sec. 5.

In Sec. 4.1, we construct theta vacua for cluster-decomposition properties about correlators of chiral condensates for thermal boundary conditions. In Sec. 4.2, we do the same analysis for flavor-twisted boundary condition, and we will see that the vacuum structures are different as a consequence of different anomalies. In Sec. 4.4, however, the Polyakov-loop correlators are studied, and we show that they do not satisfy the cluster decomposition with theta vacua if the discrete chiral symmetry is spontaneously broken. We shall see in Sec. 4.5 that this matches the 't Hooft anomaly discussed in Sec. 2.4.

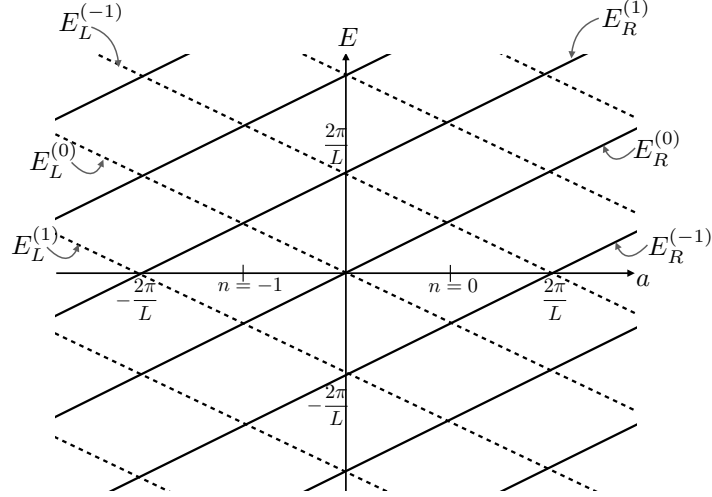


Figure 1. One-particle energy levels as a function of a for $q = 1$, $N = 1$ with periodic boundary condition. The black solid line stands for $E_R^{(k)}$ while the black broken line is $E_L^{(k)}$.

4.1 Chiral condensate in thermal boundary condition

4.1.1 $q = 1$, $N = 1$ with thermal b.c.

We review the results for this case by following the argument in the reference [31]. The eigenfunction satisfying the periodic boundary condition for this case is

$$\psi_k(x) \propto \frac{1}{\sqrt{L}} \exp\left(i \frac{2\pi k}{L} x\right), \quad (4.6)$$

and the one-particle energy of k -th level for the left-handed and right handed fermions is

$$E_R^{(k)} = \frac{2\pi k}{L} + a, \quad E_L^{(k)} = -\frac{2\pi k}{L} - a. \quad (4.7)$$

When one of the k -th states for the left-handed fermion is filled, we denote the state as $|1_L, k\rangle$. These energies are depicted in Fig. 1 as a function of a . The black solid line stands for $E_R^{(k)}$ while the black broken line is $E_L^{(k)}$. It is notable that the periodicity of a is

$$\frac{2\pi}{L}, \quad (4.8)$$

which reflects the invariance under large gauge transformation,

$$a \mapsto a + \frac{2\pi}{L}, \quad \psi(x) \mapsto e^{-\frac{2\pi i}{L} x} \psi(x). \quad (4.9)$$

The spectrum also indicates that the minimum of the induced potential $V_{\text{eff}}(a)$ is

$$a = \frac{\pi(2n+1)}{L}, \quad (4.10)$$

with $n \in \mathbb{Z}$. Since the effective potential $V_{\text{eff}}(a)$ in the vicinity of the n -th minimum is derived from the regularized zero-point energy (Casimir energy) E_0 , we take a sum over all the negative energy levels with the appropriate regularization with a small number ϵ as

$$\begin{aligned} E_0|_{a \sim \frac{\pi(2n+1)}{L}} &= \sum_{k=-n}^{\infty} E_L^{(k)} \exp(-\epsilon |E_L^{(k)}|) + \sum_{k=-\infty}^{-n-1} E_R^{(k)} \exp(-\epsilon |E_R^{(k)}|) \\ &= \frac{L}{2\pi} \left(a - \frac{\pi(2n+1)}{L} \right)^2 + \mathcal{O}(\epsilon) + \text{const.}, \end{aligned} \quad (4.11)$$

which corresponds to $E_0 = LV(a)$ in (3.6). Then one finds that the induced effective theory around the n -th potential minima is a simple harmonic oscillator,

$$H_{\text{eff}} = -\frac{\pi m_\gamma^2}{2L} \left(\frac{d}{da} \right)^2 + \frac{L}{2\pi} \left(a - \frac{\pi(2n+1)}{L} \right)^2, \quad (4.12)$$

with $m_\gamma^2 \equiv e^2/\pi$. Therefore the eigenstate (wavefunction) of the n -th ground state is given by

$$\begin{aligned} \langle a|n \rangle &= \left(\frac{L}{\pi^2 m_\gamma} \right)^{1/4} \exp \left[-\frac{1}{2\pi m_\gamma L} \left(La - \pi(2n+1) \right)^2 \right] \\ &\times \prod_{k=-n}^{+\infty} |1_L, k \rangle \prod_{k=-\infty}^{-n-1} |1_R, k \rangle. \end{aligned} \quad (4.13)$$

By shifting $a \rightarrow a + 2\pi/L$ (large gauge transformation), one left-handed particle and one right-handed hole emerge as seen from Fig. 1, where we find out $\Delta Q = 0$ and $\Delta Q_5 = 2$. It is nothing but manifestation of the $U(1)_A$ axial (or ABJ) anomaly. The vacuum state invariant under the large gauge transformation is obtained as a linear combination of $|n\rangle$ with the vacuum angle θ as

$$|\theta\rangle = \sum_n e^{in\theta} |n\rangle \quad (4.14)$$

The bilinear chiral condensate in this vacuum states is calculated as

$$\frac{\langle \theta | \bar{\psi}_L \psi_R | \theta \rangle}{\langle \theta | \theta \rangle} = e^{i\theta} \langle n-1 | \bar{\psi}_L \psi_R | n \rangle = e^{i\theta} \frac{1}{L} \exp \left(-\frac{\pi}{Lm_\gamma} \right). \quad (4.15)$$

This is clearly seen from $\Delta Q_5 = 2$ under $a \rightarrow a + 2\pi/L$. It is also notable that the bilinear chiral condensate vanishes if $\Delta Q_5 > 2$ under this shift. We will see such cases for multi-flavor Schwinger models below.

It is instructive to calculate the four-point fermion correlator as

$$\begin{aligned} \lim_{\tau \rightarrow \infty} \frac{\langle \theta | \bar{\psi}_L \psi_R e^{-H\tau} \bar{\psi}_R \psi_L | \theta \rangle}{\langle \theta | \theta \rangle} &= \langle n | \bar{\psi}_L \psi_R | n+1 \rangle \langle n+1 | \bar{\psi}_R \psi_L | n \rangle \\ &= \frac{1}{L^2} \exp \left(-\frac{2\pi}{Lm_\gamma} \right), \end{aligned} \quad (4.16)$$

which clearly shows the cluster-decomposition property of the theta vacua [10],

$$\lim_{\tau \rightarrow \infty} \langle \theta | \bar{\psi}_L \psi_R(\tau) \bar{\psi}_R \psi_L(0) | \theta \rangle = |\langle \theta | \bar{\psi}_L \psi_R | \theta \rangle|^2. \quad (4.17)$$

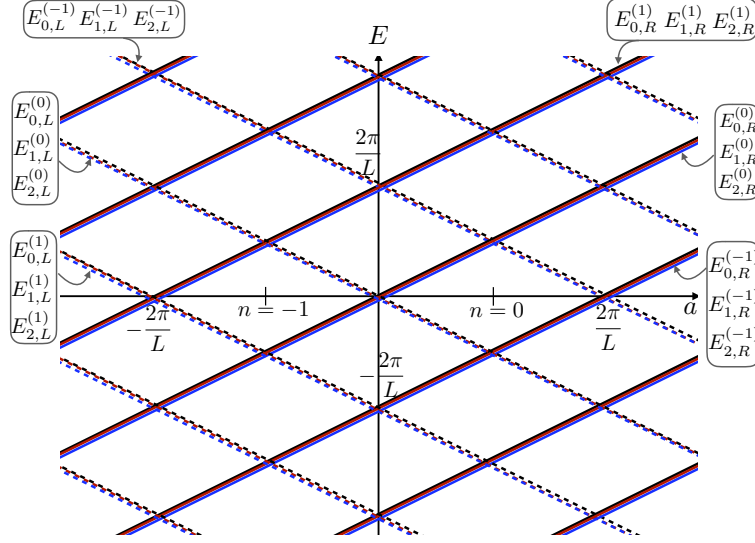


Figure 2. One-particle energy levels as a function of a for $q = 1, N = 3$ with periodic boundary condition. Black, red and blue solid lines stands for $E_{f,R}^{(k)}$ with $f = 0, 1, 2$ while black, red and blue broken lines are $E_{f,L}^{(k)}$ with $f = 0, 1, 2$.

4.1.2 $q = 1, N > 1$ with thermal b.c.

The eigenfunction satisfying p.b.c. is

$$\psi_{f,k} \propto \frac{1}{\sqrt{L}} \exp\left(i \frac{2\pi k}{L} x\right), \quad (4.18)$$

where subscript f is used to specify the flavor as $f = 0, 1, \dots, N-1$. The one-particle energy of k -th state for the left-handed and right handed fermions for each flavor is

$$E_{f,R}^{(k)} = \frac{2\pi k}{L} + a, \quad E_{f,L}^{(k)} = -\frac{2\pi k}{L} - a. \quad (4.19)$$

When one of the k -th states for the left-handed f -flavor is filled, we denote the state as $|1_L^f, k\rangle$. These energies for $N = 3$ are shown in Fig. 2. Black, red and blue solid lines stands for $E_{f,R}^{(k)}$ with $f = 0, 1, 2$ while black, red and blue broken lines are $E_{f,L}^{(k)}$ with $f = 0, 1, 2$. It is obvious that the energy levels for three flavors are degenerate for this case. The periodicity of a is again $\frac{2\pi}{L}$, reflecting invariance under the large gauge transformation, $a \mapsto a + \frac{2\pi}{L}$, $\psi(x) \mapsto e^{-\frac{2\pi i}{L}x} \psi(x)$. The minimum of the induced potential $V_{\text{eff}}(a)$ is $a = \frac{\pi(2n+1)}{L}$ with $n \in \mathbb{Z}$. Then the induced effective Hamiltonian around the n -th potential minima is

$$H_{\text{eff}} = -\frac{\pi m_\gamma^2}{2NL} \left(\frac{d}{da}\right)^2 + \frac{NL}{2\pi} \left(a - \frac{\pi(2n+1)}{L}\right)^2, \quad (4.20)$$

with $m_\gamma^2 \equiv Ne^2/\pi$. The eigenfunction of the n -th ground state is expressed as

$$\begin{aligned} \langle a|n\rangle &= \left(\frac{NL}{\pi^2 m_\gamma}\right)^{1/4} \exp\left[-\frac{N}{2\pi m_\gamma L}\left(La - \pi(2n+1)\right)^2\right] \\ &\times \prod_{f=0}^{N-1} \left(\prod_{k=-n}^{+\infty} |1_L^f, k\rangle \prod_{k=-\infty}^{-n-1} |1_R^f, k\rangle \right). \end{aligned} \quad (4.21)$$

By shifting $a \rightarrow a + 2\pi/L$, N left-handed particle and N right-handed hole emerge, where we have $\Delta Q = 0$ and $\Delta Q_5 = 2N$. The vacuum states invariant under the large gauge transformation is obtained as a linear combination of $|n\rangle$ with the vacuum angle θ as $|\theta\rangle = \sum_n e^{in\theta} |n\rangle$. For this case one finds that the bilinear chiral condensate vanishes as

$$\langle \theta | \bar{\psi}_L^f \psi_R^f | \theta \rangle = 0, \quad (4.22)$$

since $\Delta Q_5 = 2N$ under $a \rightarrow a + 2\pi/L$. It means that the axial subgroup of $SU(N)_L$ and $SU(N)_R$ flavor symmetry is not broken, which is consistent with Coleman's theorem.

4.1.3 $q > 1$, $N = 1$ with thermal b.c.

The eigenfunction satisfying the boundary condition is $\exp(i\frac{2\pi k}{L}x)$ and the one-particle energy of k -th state for the left-handed and right-handed fermions is

$$E_R^{(k)} = \frac{2\pi k}{L} + qa, \quad E_L^{(k)} = -\frac{2\pi k}{L} - qa. \quad (4.23)$$

These energies for $q = 2$ are shown in Fig. 3. A black solid line stands for $E_R^{(k)}$ while a black broken line is $E_L^{(k)}$. The periodicity of a is

$$\frac{2\pi}{qL}, \quad (4.24)$$

which reflects the \mathbb{Z}_q one-form symmetry [24–26]

$$a \rightarrow a + \frac{2\pi}{qL}, \quad \psi(x) \rightarrow e^{-\frac{2\pi i}{L}x} \psi(x), \quad (4.25)$$

which results in \mathbb{Z}_q 0-form symmetry under compactification. The spectrum indicates that the minimum of the induced potential $V_{\text{eff}}(a)$ is

$$a = \frac{\pi(2n+1)}{qL}. \quad (4.26)$$

and the induced effective hamiltonian around the n -th potential minimum is

$$H_{\text{eff}} = -\frac{\pi m_\gamma^2}{2q^2 L} \frac{d^2}{da^2} + \frac{q^2 L}{2\pi} \left(a - \frac{\pi(2n+1)}{qL} \right)^2, \quad (4.27)$$

with $m_\gamma^2 \equiv q^2 e^2/\pi$. The eigenfunction of the n -th ground state is expressed as

$$\begin{aligned} \langle a|n\rangle &= \left(\frac{q^2 L}{\pi^2 m_\gamma}\right)^{1/4} \exp\left[-\frac{q^2}{2\pi m_\gamma L}\left(La - \frac{\pi(2n+1)}{q}\right)^2\right] \\ &\times \prod_{k=-n}^{+\infty} |1_L, k\rangle \prod_{k=-\infty}^{-n-1} |1_R, k\rangle. \end{aligned} \quad (4.28)$$

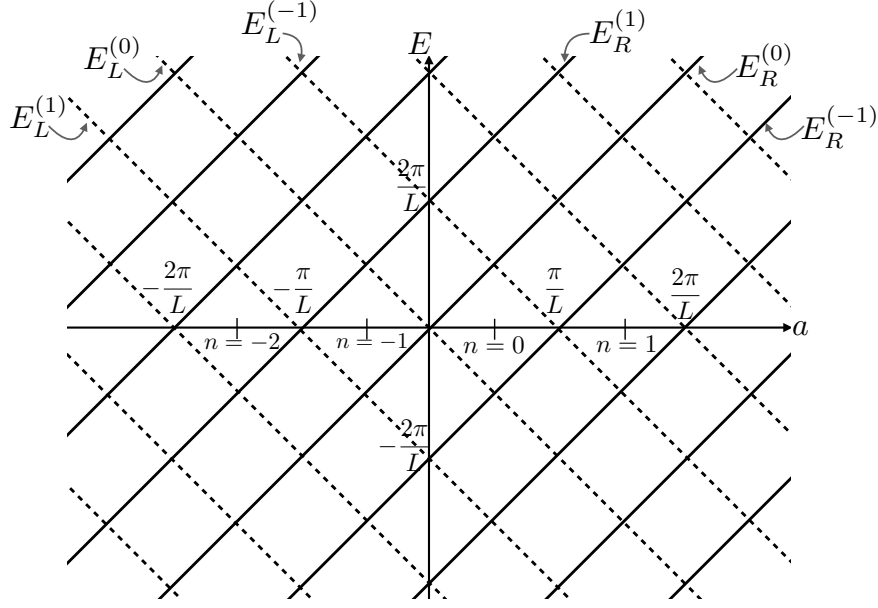


Figure 3. One-particle energy levels as a function of a for $q = 2, N = 1$ with periodic boundary condition. A black solid line stands for $E_R^{(k)}$ while a black broken line is $E_L^{(k)}$.

By shifting $a \rightarrow a + 2\pi/(qL)$, one left-handed particle and one right-handed hole emerge, where we have $\Delta Q = 0$ and $\Delta Q_5 = 2$ as seen from Fig. 3.

The physical vacuum states are constructed as linear combinations of $|n\rangle$ with the vacuum angle θ so that they are invariant under the large-gauge transformation, $a \mapsto a + 2\pi/L$. We obtain q different physical vacua as

$$|\widetilde{\ell, \theta}\rangle = \sum_{m \in \mathbb{Z}} e^{im\theta} |\ell + qm\rangle, \quad (4.29)$$

for $\ell = 0, 1, \dots, q-1$, and they are related under $\mathbb{Z}_q^{[1]}$ transformation as $\ell \mapsto \ell + 1$. We take the linear combinations of these q vacua so that they become eigenstates of $\mathbb{Z}_q^{[1]}$ symmetry:

$$\begin{aligned} |\theta, k\rangle &= \sum_{\ell=0}^{q-1} e^{i\frac{\theta+2\pi k}{q}\ell} |\widetilde{\ell, \theta}\rangle \\ &= \sum_{\ell=0}^{q-1} e^{i\frac{\theta+2\pi k}{q}\ell} \left(\sum_{m \in \mathbb{Z}} e^{im\theta} |\ell + qm\rangle \right) \\ &= \sum_{n \in \mathbb{Z}} e^{i\frac{\theta+2\pi k}{q}n} |n\rangle, \end{aligned} \quad (4.30)$$

with $k = 0, 1, \dots, q-1$. It is notable that their dependence on vacuum angle θ is fractional, $\tilde{\theta} \equiv \theta/q$, and then $|\theta + 2\pi, k\rangle = |\theta, k+1\rangle$. The bilinear chiral condensate is thus calculated

as

$$\frac{\langle \theta, k | \bar{\psi}_L \psi_R | \theta, k \rangle}{\langle \theta, k | \theta, k \rangle} = e^{i(\theta+2\pi k)/q} \langle n-1 | \bar{\psi}_L \psi_R | n \rangle = \frac{1}{L} e^{i(\theta+2\pi k)/q} \exp\left(-\frac{\pi}{Lm_\gamma}\right). \quad (4.31)$$

This is clearly seen from $\Delta Q_5 = 2$ under $a \mapsto a + 2\pi/(qL)$. This condensate spontaneously breaks the discrete chiral symmetry $(\mathbb{Z}_q)_R$ [24, 25]. The emergence of fractionalized action $\pi/(Lm_\gamma)$ and fractionalized vacuum angle $\tilde{\theta} = \theta/q$ originates in the contribution of the fractional instantons to chiral condensate. The four-point fermion correlator is also calculated as

$$\lim_{\tau \rightarrow \infty} \frac{\langle \theta, k | \bar{\psi}_L \psi_R e^{-H\tau} \bar{\psi}_R \psi_L | \theta, k \rangle}{\langle \theta, k | \theta, k \rangle} = \frac{1}{L^2} \exp\left(-\frac{2\pi}{Lm_\gamma}\right), \quad (4.32)$$

and thus the cluster decomposition is satisfied for these vacua. More generally,

$$\lim_{M_2 \rightarrow \mathbb{R} \times S^1} \langle \mathcal{O}(x_1, \dots, x_n) \rangle_{M_2} = \frac{1}{q} \sum_{k=0}^{q-1} \frac{\langle \theta, k | \mathcal{O}(x_1, \dots, x_n) | \theta, k \rangle}{\langle \theta, k | \theta, k \rangle} \quad (4.33)$$

for any two-dimensional local n -point functions \mathcal{O} , and the cluster decomposition holds for each sector $|\theta, k\rangle$.

4.1.4 $q > 1$, $N > 1$ with thermal b.c.

The eigenfunction $\exp(i\frac{2\pi k}{L}x)$ satisfying the p.b.c. leads to the energy of k -th state for the right-handed and left-handed fermions for each flavor, $E_{f,R}^{(k)} = \frac{2\pi k}{L} + qa$, $E_{f,L}^{(k)} = -\frac{2\pi k}{L} - qa$. These one-particle energies for $q = 2, N = 3$ are depicted in Fig. 4. Black, red and blue solid lines stands for $E_{f,R}^{(k)}$ with $f = 0, 1, 2$ and black, red and blue broken lines are $E_{f,L}^{(k)}$ with $f = 0, 1, 2$, where the energy levels for three flavors are degenerate for this case. The periodicity $\frac{2\pi}{qL}$ is a remnant of the \mathbb{Z}_q one-form symmetry $a \mapsto a + \frac{2\pi}{qL}$, $\psi(x) \mapsto e^{-\frac{2\pi i}{L}x} \psi(x)$. The spectrum indicates that the minimum of the induced potential $V_{\text{eff}}(a)$ is $a = \frac{\pi(2n+1)}{qL}$ and the induced effective hamiltonian around the n -th potential minimum is given by

$$H_{\text{eff}} = -\frac{\pi m_\gamma^2}{2q^2 NL} \frac{d^2}{da^2} + \frac{q^2 NL}{2\pi} \left(a - \frac{\pi(2n+1)}{qL}\right)^2, \quad (4.34)$$

where

$$m_\gamma^2 \equiv Nq^2 e^2 / \pi. \quad (4.35)$$

The eigenfunction of the n -th ground state is expressed as

$$\begin{aligned} \langle a | n \rangle &= \left(\frac{q^2 NL}{\pi^2 m_\gamma} \right)^{1/4} \exp \left[-\frac{q^2 N}{2\pi m_\gamma L} \left(La - \frac{\pi(2n+1)}{q} \right)^2 \right] \\ &\times \prod_{f=0}^{N-1} \left(\prod_{k=-n}^{+\infty} |1_L^f, k\rangle \prod_{k=-\infty}^{-n-1} |1_R^f, k\rangle \right). \end{aligned} \quad (4.36)$$

By shifting $a \rightarrow a + 2\pi/(qL)$, N left-handed particle and N right-handed hole emerge, where we have $\Delta Q = 0$ and $\Delta Q_5 = 2N$ as seen from Fig. 4. The physical vacuum states are obtained as a linear combination of $|n\rangle$ with the vacuum angle θ as

$$|\theta, k\rangle = \sum_n e^{i\frac{\theta+2\pi k}{q}n} |n\rangle, \quad (4.37)$$

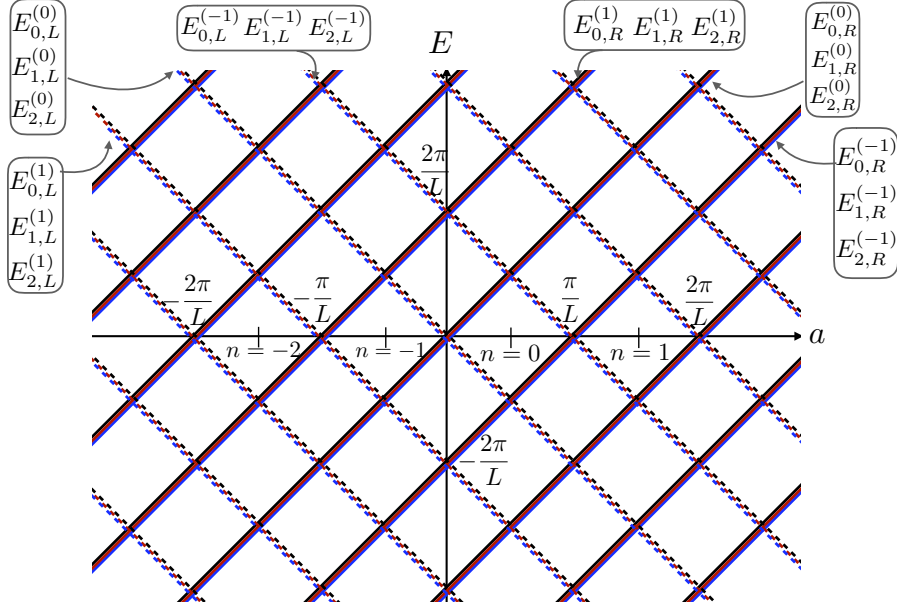


Figure 4. One-particle energy levels as a function of a for $q = 2, N = 3$ with periodic boundary condition. Black, red and blue solid lines stands for $E_{f,R}^{(k)}$ with $f = 0, 1, 2$ while black, red and blue broken lines are $E_{f,L}^{(k)}$ with $f = 0, 1, 2$.

with $k = 0, 1, \dots, q - 1$. The bilinear chiral condensate for this case vanishes due to $\Delta Q_5 = 2N$ under $a \rightarrow a + 2\pi/(qL)$ as

$$\langle \theta, k | \bar{\psi}_L^f \psi_R^f | \theta, k \rangle = 0. \quad (4.38)$$

The axial subgroup of $SU(N)_L$ and $SU(N)_R$ flavor symmetry is not broken, which is consistent with Coleman's theorem. As shown in [24, 25], however, there emerges the determinant condensate $\det \bar{\psi}_L^f \psi_R^g$, which breaks the discrete chiral symmetry $(\mathbb{Z}_q)_R$. This is exactly analogous to QCD with adjoint fermions on small $\mathbb{R}^3 \times S^1$ [86]. The reason of existence of the determinant condensate composed of $2N$ fermion operators again originates in $\Delta Q_5 = 2N$ under $a \rightarrow a + 2\pi/(qL)$ in Fig. 4. We can compute its explicit form as

$$\begin{aligned} \frac{\langle \theta, k | \det \bar{\psi}_L^f \psi_R^g | \theta, k \rangle}{\langle \theta, k | \theta, k \rangle} &= e^{i \frac{\theta + 2\pi k}{q}} N! \langle n - 1 | \prod_f \bar{\psi}_L^f \psi_R^f | n \rangle \\ &= e^{i \frac{\theta + 2\pi k}{q}} \frac{N!}{L^N} \exp \left(-\frac{N\pi}{Lm_\gamma} \right). \end{aligned} \quad (4.39)$$

This condensate are saturated by configuration with one fractional instanton.

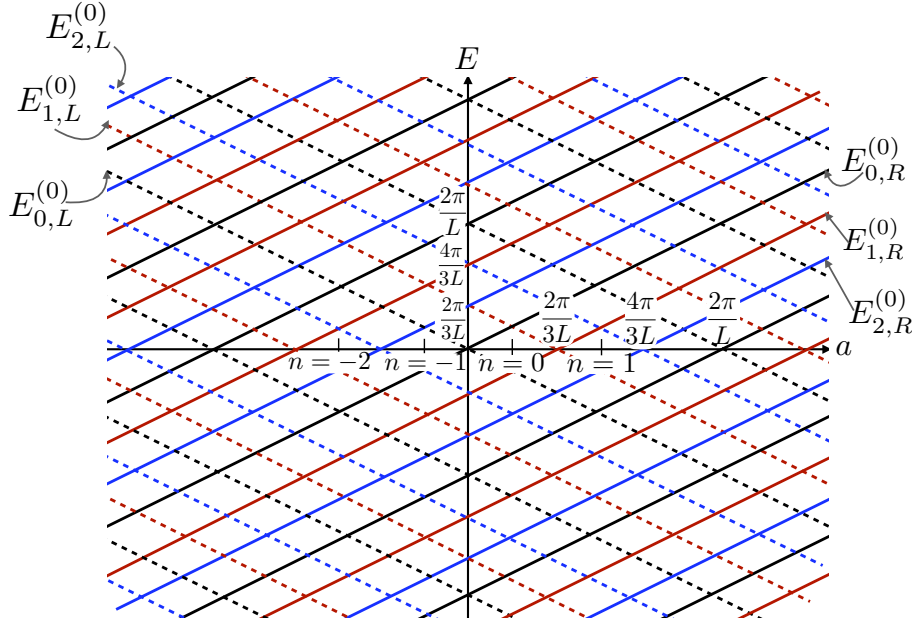


Figure 5. One-particle energy levels as a function of a for $q = 1, N = 3$ with \mathbb{Z}_N twisted boundary condition. Black, red and blue solid lines stands for $E_{f,R}^{(k)}$ with $f = 0, 1, 2$ while black, red and blue broken lines are $E_{f,L}^{(k)}$ with $f = 0, 1, 2$.

4.2 Chiral condensate in flavor-twisted boundary condition

4.2.1 $q = 1, N > 1$ with \mathbb{Z}_N twisted b.c.

The eigenfunction satisfying \mathbb{Z}_N t.b.c. is

$$\psi_{f,k} \propto \frac{1}{\sqrt{L}} \exp \left(i \frac{2\pi(Nk - f)}{NL} x \right), \quad (4.40)$$

with $f = 0, 1, \dots, N - 1$. The one-particle energy of k -th state for the right-handed and left-handed fermions for each flavor is

$$E_{f,R}^{(k)} = \frac{2\pi(Nk - f)}{NL} + a, \quad E_{f,L}^{(k)} = -\frac{2\pi(Nk - f)}{NL} - a. \quad (4.41)$$

When one of the k -th states for the left-handed f -flavor is filled, we denote the state as $|1_L^f, k\rangle$. These energies for $N = 3$ are depicted in Fig. 5. Black, red and blue solid lines stands for $E_{f,R}^{(k)}$ with $f = 0, 1, 2$ while black, red and blue broken lines are $E_{f,L}^{(k)}$ with $f = 0, 1, 2$. We note that the degeneracy of the energy levels for flavors is lifted in this case. The periodicity of a is

$$\frac{2\pi}{NL}, \quad (4.42)$$

reflecting the \mathbb{Z}_N one-form symmetry, given in (2.73) and (2.74),

$$a \mapsto a + \frac{2\pi}{NL}, \quad \psi_f(x) \mapsto e^{-\frac{2\pi i}{NL} x} \psi_{f+1}(x), \quad (4.43)$$

which results in \mathbb{Z}_N zero-form symmetry in the compactified theory. The minimum of the induced potential $V_{\text{eff}}(a)$ is

$$a = \frac{\pi(2n+1)}{NL}, \quad (4.44)$$

with $n \in \mathbb{Z}$. Then the induced effective Hamiltonian around the n -th potential minimum is

$$H_{\text{eff}} = -\frac{\pi m_\gamma^2}{2NL} \left(\frac{d}{da} \right)^2 + \frac{NL}{2\pi} \left(a - \frac{\pi(2n+1)}{NL} \right)^2, \quad (4.45)$$

with $m_\gamma^2 \equiv Ne^2/\pi$. Let us consider the eigenfunction of the n -th ground state. We here denote n as $n = N\ell + j$ with $\ell \in \mathbb{Z}$ and $j = 0, 1, \dots, N-1$, since the properties of the vacua depend on $n \bmod N$. The eigenfunction is expressed as

$$\begin{aligned} \langle a|n\rangle &= \langle a|N\ell + j\rangle \\ &= \left(\frac{NL}{\pi^2 m_\gamma} \right)^{1/4} \exp \left[-\frac{N}{2\pi m_\gamma L} \left(La - \frac{\pi(2(N\ell + j) + 1)}{N} \right)^2 \right] \\ &\quad \times \prod_{f=0}^j \left(\prod_{k=-\ell}^{\infty} |1_L^f, k\rangle \prod_{k=-\infty}^{-\ell-1} |1_R^f, k\rangle \right) \prod_{f'=j+1}^{N-1} \left(\prod_{k=1-\ell}^{+\infty} |1_L^{f'}, k\rangle \prod_{k=-\infty}^{-\ell} |1_R^{f'}, k\rangle \right). \end{aligned} \quad (4.46)$$

By shifting $a \rightarrow a + 2\pi/(NL)$, one left-handed particle and one right-handed hole emerge, where we have $\Delta Q = 0$ and $\Delta Q_5 = 2$.

The physical vacuum states are invariant under the large-gauge transformation, $a \mapsto a + 2\pi/L$, and they are obtained as a linear combination of $|n\rangle$ with the vacuum angle θ as,

$$|\widetilde{j, \theta}\rangle = \sum_{\ell \in \mathbb{Z}} e^{i\ell\theta} |N\ell + j\rangle. \quad (4.47)$$

The eigenstates under $\mathbb{Z}_N^{[0]}$ shift-center symmetry are given by

$$\begin{aligned} |\theta, k\rangle &= \sum_{j=0}^{N-1} e^{i\frac{\theta+2\pi k}{N}j} |\widetilde{j, \theta}\rangle \\ &= \sum_{n \in \mathbb{Z}} e^{in\frac{\theta+2\pi k}{N}} |n\rangle, \end{aligned} \quad (4.48)$$

with $k = 0, 1, \dots, N-1$, and their dependence on θ becomes fractional as $\tilde{\theta} = \theta/N$. The bilinear chiral condensate is thus calculated as

$$\begin{aligned} \frac{\langle \theta, k | \bar{\psi}_L^f \psi_R^f | \theta, k \rangle}{\langle \theta, k | \theta, k \rangle} &= e^{i\frac{\theta+2\pi k}{N}} \frac{\langle N\ell + f - 1 | \bar{\psi}_L^f \psi_R^f | N\ell + f \rangle}{\sum_{f'} \langle N\ell + f | N\ell + f \rangle} \\ &= \frac{1}{NL} e^{i\frac{\theta+2\pi k}{N}} \exp \left(-\frac{\pi}{NLm_\gamma} \right). \end{aligned} \quad (4.49)$$

This is due to $\Delta Q_5 = 2$ under $a \rightarrow a + 2\pi/(NL)$. This result was first derived in [31]. This condensate breaks the discrete chiral symmetry $(\mathbb{Z}_N)_R$. The emergence of fractional vacuum angle $\tilde{\theta} = \theta/N$ originates in the contribution of the $1/N$ fractional instantons

to chiral condensate. We note that $q > 1$, $N = 1$ with p.b.c. and $q = 1$, $N > 1$ with \mathbb{Z}_N t.b.c. share the properties including symmetries, chiral condensates and symmetry breaking patterns. The four-point fermion correlator is

$$\lim_{\tau \rightarrow \infty} \frac{\langle \theta, k | \bar{\psi}_L^f \psi_R^f e^{-H\tau} \bar{\psi}_R^f \psi_L^f | \theta, k \rangle}{\langle \theta, k | \theta, k \rangle} = \frac{1}{N^2 L^2} \exp \left(-\frac{2\pi}{NLm_\gamma} \right) \quad (4.50)$$

which shows the cluster decomposition property⁴.

4.2.2 $q > 1$, $N > 1$ with \mathbb{Z}_N twisted b.c.

The eigenfunction satisfying \mathbb{Z}_N t.b.c. is $\exp(i\frac{2\pi k}{NL}x)$ and the one-particle energy of k -th state for the right-handed and left-handed fermions for each flavor is

$$E_{f,R}^{(k)} = \frac{2\pi(Nk - f)}{NL} + qa, \quad E_{f,L}^{(k)} = -\frac{2\pi(Nk - f)}{NL} - qa. \quad (4.51)$$

These energies for $q = 2$, $N = 3$ are depicted in Fig. 6. Black, red and blue solid lines stands for $E_{f,R}^{(k)}$ with $f = 0, 1, 2$ while black, red and blue broken lines are $E_{f,L}^{(k)}$ with $f = 0, 1, 2$. We note that the degeneracy of the energy levels for flavors is again lifted in this case. The periodicity of a is

$$\frac{2\pi}{qNL}, \quad (4.52)$$

reflecting the \mathbb{Z}_{qN} one-form symmetry

$$a \rightarrow a + \frac{2\pi}{qNL}, \quad \psi_f(x) \rightarrow e^{-\frac{2\pi i}{NL}x} \psi_{f+1}(x), \quad (4.53)$$

which results in \mathbb{Z}_{qN} zero-form symmetry in the compactified theory. The minimum of the induced potential $V_{\text{eff}}(a)$ is

$$a = \frac{\pi(2n+1)}{qNL}, \quad (4.54)$$

with $n \in \mathbb{Z}$. Then the induced effective Hamiltonian around the n -th potential minimum is

$$H_{\text{eff}} = -\frac{\pi m_\gamma^2}{2q^2 NL} \left(\frac{d}{da} \right)^2 + \frac{q^2 NL}{2\pi} \left(a - \frac{\pi(2n+1)}{qNL} \right)^2, \quad (4.55)$$

with $m_\gamma^2 \equiv Nq^2 e^2 / \pi$. Let us consider the eigenfunction of the n -th ground state. We again denote n as $n = N\ell + j$ with $\ell \in \mathbb{Z}$ and $j = 0, 1, 2$. Then the eigenfunction is expressed as

$$\begin{aligned} \langle a | n \rangle &= \langle a | N\ell + j \rangle \\ &= \left(\frac{q^2 NL}{\pi^2 m_\gamma} \right)^{1/4} \exp \left[-\frac{q^2 N}{2\pi m_\gamma L} \left(La - \frac{\pi(2n+1)}{qN} \right)^2 \right] \\ &\quad \times \prod_{f=0}^j \left(\prod_{k=-\ell}^{\infty} |1_L^f, k\rangle \prod_{k=-\infty}^{-\ell-1} |1_R^f, k\rangle \right) \prod_{f'=j+1}^{N-1} \left(\prod_{k=1-\ell}^{+\infty} |1_L^{f'}, k\rangle \prod_{k=-\infty}^{-\ell} |1_R^{f'}, k\rangle \right). \end{aligned} \quad (4.56)$$

⁴In the case of $(0+1)$ d quantum mechanics, the breakdown of cluster decomposition means degenerate ground states as in the case of spontaneous symmetry breaking in higher dimensions, however, it does not lead the superselection rule unlike higher-dimensional case. This notice becomes important in discussion on Polyakov-loop correlators in Sec. 4.4. Because of this special nature in $(0+1)$ d, the degeneracy related to $(\mathbb{Z}_N)_R$ discrete chiral symmetry does not mean the breakdown of $U(1)^{N-1}$ axial symmetry in the symmetry group (2.76). This point will be discussed in more detail in Sec. 8.

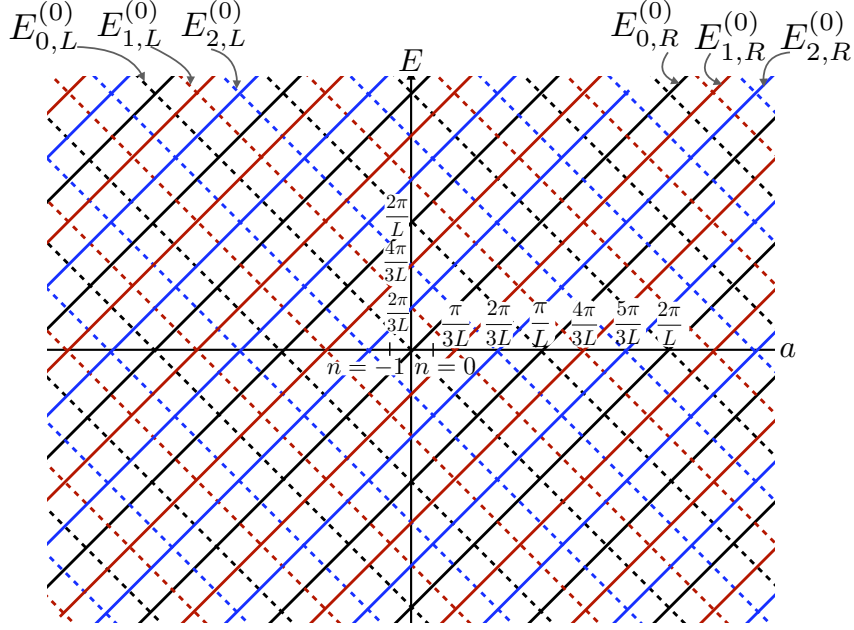


Figure 6. One-particle energy levels as a function of a for $q = 2, N = 3$ with \mathbb{Z}_N twisted boundary condition. Black, red and blue solid lines stands for $E_{f,R}^{(k)}$ with $f = 0, 1, 2$ while black, red and blue broken lines are $E_{f,L}^{(k)}$ with $f = 0, 1, 2$.

By shifting $a \rightarrow a + 2\pi/(qNL)$, one left-handed particle and one right-handed hole emerge, where we have $\Delta Q = 0$ and $\Delta Q_5 = 2$. The physical vacuum state is obtained as a linear combination of $|n\rangle$ with the vacuum angle θ as

$$|\theta, k\rangle = \sum_n e^{in \frac{\theta + 2\pi k}{Nq}} |n\rangle, \quad (4.57)$$

with $k = 0, 1, \dots, Nq - 1$. This vacuum angle $\tilde{\theta}$ satisfies $\tilde{\theta} = \theta/(qN)$. The bilinear chiral condensate is calculated as

$$\begin{aligned} \frac{\langle \theta, k | \bar{\psi}_L^f \psi_R^f | \theta, k \rangle}{\langle \theta, k | \theta, k \rangle} &= e^{i \frac{\theta + 2\pi k}{Nq}} \frac{\langle N\ell + f - 1 | \bar{\psi}_L^f \psi_R^f | N\ell + f \rangle}{\sum_{f'} \langle N\ell + f' | N\ell + f' \rangle} \\ &= \frac{1}{NL} e^{i \frac{\theta + 2\pi k}{Nq}} \exp\left(-\frac{\pi}{NLm_\gamma}\right). \end{aligned} \quad (4.58)$$

This is due to $\Delta Q_5 = 2$ under $a \rightarrow a + 2\pi/(NL)$. This condensate breaks the discrete chiral symmetry $(\mathbb{Z}_{qN})_R$. The emergence of fractionalized action $\pi/(NLm_\gamma)$ and fractionalized vacuum angle $\tilde{\theta} = \theta/(qN)$ originates in the contribution of the $1/(qN)$ fractional instantons to chiral condensate. The four-point fermion correlator is

$$\lim_{\tau \rightarrow \infty} \frac{\langle \theta, k | \bar{\psi}_L^f \psi_R^f e^{-H\tau} \bar{\psi}_R^f \psi_L^f | \theta, k \rangle}{\langle \theta, k | \theta, k \rangle} = \frac{1}{N^2 L^2} \exp\left(-\frac{2\pi}{NLm_\gamma}\right) \quad (4.59)$$

which shows the cluster-decomposition property.

4.3 Chiral condensate for generic L

The chiral condensate in Schwinger models on $\mathbb{R} \times S^1$ with arbitrary eL was discussed in Refs. [7, 10, 31] via the bosonization, the four-point fermion correlators and the fracton path integral. We below show the results extended to $q \geq 1$ and $N \geq 1$ with thermal and flavor-twisted boundary conditions and compare them to what we have obtained in the previous subsections.

Following the arguments in [10, 31], we find that the chiral condensate for generic L for $q \geq 1$ and $N = 1$ is expressed as

$$\begin{aligned} |\langle \bar{\psi}_L \psi_R \rangle| &= \frac{1}{L} \exp\left(-\frac{\pi}{Lm_\gamma}\right) \exp\left[\gamma + \frac{\pi}{Lm_\gamma} + \log \frac{Lm_\gamma}{4\pi} - I(Lm_\gamma)\right] \\ &= \frac{m_\gamma e^\gamma}{4\pi} \exp[-I(Lm_\gamma)], \end{aligned} \quad (4.60)$$

with

$$I(x) = \int_0^\infty \frac{dt}{\sqrt{t^2 + x^2}} \left(\coth \frac{\sqrt{t^2 + x^2}}{2} - 1 \right) = \begin{cases} \gamma + \frac{\pi}{x} + \log \frac{x}{4\pi} & (x \sim 0) \\ 0 & (x \rightarrow \infty) \end{cases}, \quad (4.61)$$

with $m_\gamma^2 = q^2 e^2 / \pi$ ⁵. This smoothly connects the chiral condensate $e^{-\frac{\pi}{Lm_\gamma}} / L$ for small L in the previous subsections to $m_\gamma e^\gamma / (4\pi)$ in $L \rightarrow \infty$ on \mathbb{R}^2 .

For $q \geq 1$, $N > 1$ with thermal boundary condition, we find that the chiral condensate vanishes even for $eL \not\ll 1$,

$$|\langle \bar{\psi}_L \psi_R \rangle| = 0, \quad (4.62)$$

which is consistent with the vanishing chiral condensate for small L in the previous subsections.

For $q \geq 1$, $N > 1$ with the flavor-twisted boundary condition, we find the chiral condensate for generic L ,

$$\begin{aligned} |\langle \bar{\psi}_L \psi_R \rangle| &= \frac{1}{NL} \exp\left(-\frac{\pi}{NLm_\gamma}\right) \exp\left[\frac{1}{N} \left(\gamma + \frac{\pi}{Lm_\gamma} + \log \frac{Lm_\gamma}{4\pi} - I(Lm_\gamma) \right)\right] \\ &= \frac{1}{NL} \left(\frac{Lm_\gamma e^\gamma}{4\pi} \right)^{1/N} \exp\left[-\frac{I(Lm_\gamma)}{N}\right], \end{aligned} \quad (4.63)$$

with $m_\gamma^2 = Nq^2 e^2 / \pi$. This smoothly connects the chiral condensate $e^{-\frac{\pi}{NLm_\gamma}} / (NL)$ for small eL in the previous subsections to the scaling behavior $\langle \bar{\psi}_L \psi_R \rangle \sim L^{-(N-1)/N} \rightarrow 0$ in $L \rightarrow \infty$. This is because the flavor-twisted boundary condition becomes irrelevant in a $L \rightarrow \infty$ limit, where the chiral condensate vanishes for $N > 1$ in Schwinger models. We note that the scaling exponent $(N-1)/N$ is nothing but the scaling dimension of the primary operator of $SU(N)_1$ WZW model.

In Fig. 7, we compare the exact result for the chiral condensate (blue solid curves) with the result with fractional quantum-instanton for $(q, N) = (1, 1)$ and $(q, N) = (1, 3)$ with flavor-twisted boundary condition (orange solid and yellow dashed curves). We can

⁵In [10], the same function $I(x)$ is expressed as a distinct form $I(x) = \int_0^\infty \frac{2}{e^{x \cosh t} - 1} dt$.

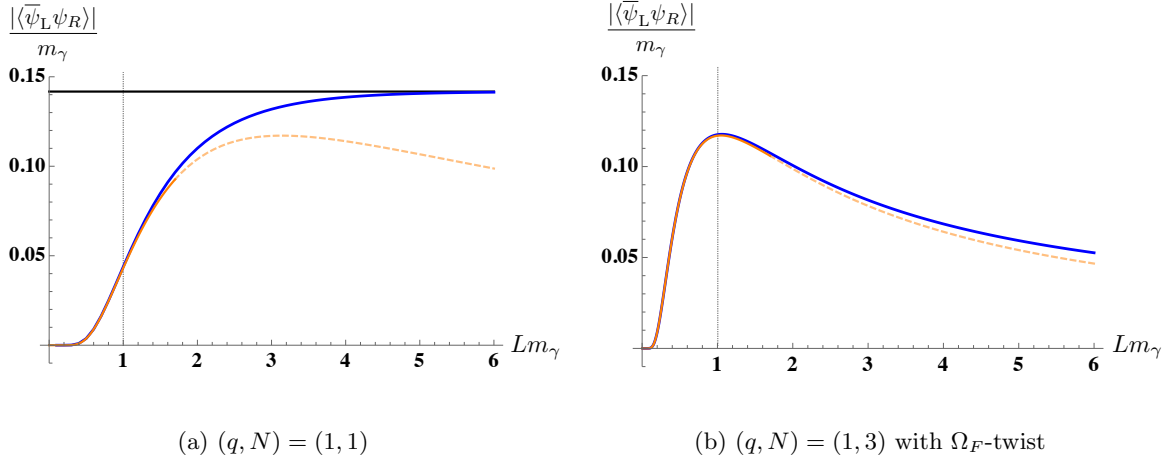


Figure 7. Behaviors of chiral condensate $|\langle\psi_L\psi_R\rangle|/m_\gamma$ as a function of $m_\gamma L$ for $(q, N) = (1, 1)$ in the left figure (a) and for $(q, N) = (1, 3)$ with the flavor-twisted boundary condition in the right figure (b). Blue solid curves are the exact results. The orange solid curves are the semiclassical result with $m_\gamma L < 2$ and the yellow dashed curves are its extrapolation to $m_\gamma L > 2$.

see that when $m_\gamma L \ll 1$, those results behave in the exactly same way. Moreover, it is notable that, under the flavor-twisted boundary condition, the approximate expression of the chiral condensate $e^{-\frac{\pi}{NLm_\gamma}}/(NL)$ which is in principle valid for small eL behaves in a manner similar to the exact result even for large eL as seen in Fig. 7(b).

4.4 Polyakov loop

In this section, we discuss the behavior of Polyakov loops on $\mathbb{R} \times S^1$. Since we neglect the higher KK modes for the gauge fields $a_2(\tau, x) = a(\tau)$, the Polyakov loop can be expressed as

$$P(\tau) = \exp\left(i \int_0^L a_2(\tau, x) dx\right) = \exp(iLa(\tau)). \quad (4.64)$$

This is an order parameter of $\mathbb{Z}_q^{[0]}$ or $\mathbb{Z}_{Nq}^{[0]}$ (shift-)center symmetry depending on whether we take thermal or twisted boundary condition.

4.4.1 $q = 1, N \geq 1$ with thermal b.c.

We first consider the case $q = 1$ and $N \geq 1$ with periodic boundary condition. In this case, there is no nontrivial symmetry that acts on Polyakov loop, and thus its non-zero expectation value is naturally expected. This is still a good exercise to look at how we can compute the Polyakov loop, and its computation can be extended for other nontrivial cases.

The n -th ground-state wave function is given in (4.13) for $N = 1$ and in (4.21) for

$N > 1$ with the periodic boundary condition. It is then easy to find that

$$\begin{aligned}
\langle n|P|n\rangle &= \int da e^{iLa} \sqrt{\frac{NL}{\pi^2 m_\gamma}} e^{-\frac{N}{\pi m_\gamma L} (La - \pi(2n+1))^2} \\
&= \int da e^{iLa + \pi i(2n+1)} \sqrt{\frac{NL}{\pi^2 m_\gamma}} e^{-\frac{N}{\pi m_\gamma L} (La)^2} \\
&= -\exp\left(-\frac{\pi m_\gamma L}{4N}\right).
\end{aligned} \tag{4.65}$$

and other matrix elements vanish, $\langle m|P|n\rangle = 0$ with $m \neq n$, because of the mismatch of fermionic wave functions. Taking the θ vacuum, we obtain

$$\frac{\langle \theta|P|\theta\rangle}{\langle \theta|\theta\rangle} = \langle n|P|n\rangle = -\exp\left(-\frac{\pi m_\gamma L}{4N}\right). \tag{4.66}$$

We can also check that the cluster decomposition holds as

$$\lim_{\tau \rightarrow \infty} \frac{\langle \theta|P(\tau)^\dagger P(0)|\theta\rangle}{\langle \theta|\theta\rangle} = \langle n|P^\dagger|n\rangle \langle n|P|n\rangle = \left| \frac{\langle \theta|P|\theta\rangle}{\langle \theta|\theta\rangle} \right|^2, \tag{4.67}$$

which again suggests the uniqueness of the ground state. This reproduces the result of [10]⁶ when $N = 1$.

4.4.2 $q > 1, N \geq 1$ with thermal b.c.

We next consider the case $q > 1$ and $N \geq 1$ with periodic boundary condition. In this case, there exists $\mathbb{Z}_q^{[0]}$ symmetry that acts on Polyakov loop.

The n -th ground-state wave function is given by (4.28) for $N = 1$ and by (4.36) for $N > 1$ with periodic boundary condition. Therefore,

$$\begin{aligned}
\langle n|P|n\rangle &= \int da e^{iLa} \sqrt{\frac{q^2 NL}{\pi^2 m_\gamma}} e^{-\frac{q^2 N}{\pi m_\gamma L} \left(La - \frac{\pi(2n+1)}{q}\right)^2} \\
&= \int da e^{iLa + \frac{\pi(2n+1)}{q} i} \sqrt{\frac{q^2 NL}{\pi^2 m_\gamma}} e^{-\frac{q^2 N}{\pi m_\gamma L} (La)^2} \\
&= e^{(2n+1)\pi i/q} \exp\left(-\frac{\pi m_\gamma L}{4q^2 N}\right),
\end{aligned} \tag{4.68}$$

and $\langle m|P|n\rangle = 0$ for $m \neq n$. Unlike the chiral condensate, the Polyakov loop is not diagonalized by the theta vacua $|\theta, k\rangle$ given in (4.30). Indeed,

$$\begin{aligned}
\frac{\langle \theta, k'|P|\theta, k\rangle}{\langle \theta, k|\theta, k\rangle} &= \frac{1}{\langle \theta, k|\theta, k\rangle} \sum_n e^{-i\frac{\theta+2\pi k'}{q}} e^{i\frac{\theta+2\pi k}{q}} \langle n|P|n\rangle \\
&= \frac{1}{\langle \theta, k|\theta, k\rangle} e^{\pi i/q} e^{-\pi m_\gamma L/(4q^2 N)} \sum_n e^{\frac{2\pi i}{q}(1+k-k')n} \\
&= \delta_{k', k+1} e^{\pi i/q} e^{-\pi m_\gamma L/(4q^2 N)},
\end{aligned} \tag{4.69}$$

⁶In this section, we take the periodic boundary condition for Dirac fields instead of the anti-periodic boundary condition, and thus the Polyakov loop gets the negative sign while it is positive in Ref. [10]. We again emphasize that this difference is not physical, since these boundary conditions are related by the shift of a as $qa \rightarrow qa + \pi$.

and thus the diagonal elements vanish, $\langle \theta, k | P | \theta, k \rangle = 0$. We emphasize that the Polyakov loop correlators converge to the non-zero constant as

$$\lim_{\tau \rightarrow \infty} \frac{\langle \theta, k | P(\tau)^\dagger P(0) | \theta, k \rangle}{\langle \theta, k | \theta, k \rangle} = \exp \left(-\frac{\pi m_\gamma L}{2q^2 N} \right). \quad (4.70)$$

Therefore, each theta vacuum $|\theta, k\rangle$ satisfies the cluster decomposition for two-dimensional local correlators, such as chiral condensates, but does not for Polyakov-loop correlators. We shall revisit this point in Sec. 4.5.

The non-vanishing two-point correlator of Polyakov loops suggests that the string tension of test particles with charge-1 vanish, and the Wilson loop operator obeys perimeter law. This fact is not limited to the theory on $\mathbb{R} \times S^1$ with $eL \ll 1$. Indeed, using Abelian bosonizations, we can show that \mathbb{Z}_q one-form symmetry is spontaneously broken even if the decompactification limit on \mathbb{R}^2 is taken. We emphasize that this phenomenon should not be understood by string breaking because all dynamical particles have charge q . The impossibility of string breaking by pair production is exactly why the theory has \mathbb{Z}_q one-form symmetry: when it is possible, such loop operators are not order parameter for higher-form symmetries. Instead, this screening phenomenon should be understood by vacuum polarization. Although it was known for a long time that fractional charged particles show screening with massless dynamical fermions while confinement occurs without them [2, 4, 6], its correct interpretation as vacuum polarization was first clearly given in [121], to our best knowledge. In Ref. [122], this is interpreted as spontaneous \mathbb{Z}_q symmetry breaking.

This seems to be a rare example that realizes spontaneous breakdown of $\mathbb{Z}_n^{[d-1]}$ symmetry in d spacetime dimensions, so let us explain this point in detail. Indeed, there is a folklore that the discrete $(d-1)$ form symmetry cannot be spontaneously broken [35], and our result disagrees with it. The origin of this folklore would come from another folklore that symmetry cannot be broken in quantum mechanics since the ground state is unique. However, uniqueness of the ground state can be shown only in limited situations, and there exist counterexamples: double-well quantum mechanics with infinite barrier, free particle on a circle with $\theta = \pi$, etc. One of the standard proof of the uniqueness is to apply Perron-Frobenius theorem to the imaginary-time Feynman kernel in certain basis, and the sufficient condition for this to be true is that the classical potential is non-singular and that the path integral has no sign problem. In our situation, dynamical massless fermions disconnect topologically distinct sectors of the gauge fields, which breaks strong ergodicity, and this is indeed the origin of 't Hooft anomaly to have multiple ground states in massless Schwinger model with discrete anomaly.

We, still, would like to emphasize that, unlike the case $d \geq 2 + 1$, the spontaneous breakdown of one-form symmetry does not lead topological order in two dimensions. This is because it has a mixed anomaly with the 0-form discrete chiral symmetry, which is also spontaneously broken, and the anomaly is saturated by having multiple vacua connected by discrete chiral transformation. For more details, see Sec. 4.5.

4.4.3 $q \geq 1, N > 1$ with \mathbb{Z}_N twisted b.c.

We next consider the case $q \geq 1$ and $N > 1$ with flavor twisted boundary condition. In this case, there exists $\mathbb{Z}_{qN}^{[0]}$ symmetry that acts on Polyakov loop.

The n -th ground-state wave function is given by (4.56). Therefore,

$$\begin{aligned}\langle n|P|n\rangle &= \int da e^{iLa} \sqrt{\frac{q^2 NL}{\pi^2 m_\gamma}} e^{-\frac{q^2 N}{\pi m_\gamma L} \left(La - \frac{\pi(2n+1)}{qN}\right)^2} \\ &= \int da e^{iLa + \frac{\pi(2n+1)}{qN} i} \sqrt{\frac{q^2 NL}{\pi^2 m_\gamma}} e^{-\frac{q^2 N}{\pi m_\gamma L} (La)^2} \\ &= e^{(2n+1)\pi i/(qN)} \exp\left(-\frac{\pi m_\gamma L}{4q^2 N}\right),\end{aligned}\tag{4.71}$$

and $\langle m|P|n\rangle = 0$ for $m \neq n$. Unlike the chiral condensate, the Polyakov loop is not diagonalized by the theta vacua $|\theta, k\rangle$ given in (4.57). Indeed,

$$\begin{aligned}\frac{\langle \theta, k'|P|\theta, k\rangle}{\langle \theta, k|\theta, k\rangle} &= \frac{1}{\langle \theta, k|\theta, k\rangle} \sum_n e^{-i\frac{\theta+2\pi k'}{qN}} e^{i\frac{\theta+2\pi k}{qN}} \langle n|P|n\rangle \\ &= \frac{1}{\langle \theta, k|\theta, k\rangle} e^{\pi i/(qN)} e^{-\pi m_\gamma L/(4q^2 N)} \sum_n e^{\frac{2\pi i}{qN}(1+k-k')n} \\ &= \delta_{k', k+1} e^{\pi i/(qN)} e^{-\pi m_\gamma L/(4q^2 N)},\end{aligned}\tag{4.72}$$

and thus the diagonal elements vanish, $\langle \theta, k|P|\theta, k\rangle = 0$. We emphasize that the Polyakov loop correlators converge to the non-zero constant as

$$\lim_{\tau \rightarrow \infty} \frac{\langle \theta, k|P(\tau)^\dagger P(0)|\theta, k\rangle}{\langle \theta, k|\theta, k\rangle} = \exp\left(-\frac{\pi m_\gamma L}{2q^2 N}\right).\tag{4.73}$$

Again, each theta vacuum $|\theta, k\rangle$ satisfies the cluster decomposition for two-dimensional local correlators, such as chiral condensates, but does not for Polyakov-loop correlators.

4.5 Discrete anomaly matching

Let us discuss how the discrete anomaly (2.68) or (2.78) is matched in the explicit construction of ground states.

Let us denote S and C as the generators of $\mathbb{Z}_{Nq}^{[0]}$ and of $(\mathbb{Z}_{Nq})_R$, respectively, and then the anomaly (2.78) indicates that $\mathbb{Z}_{Nq} \times \mathbb{Z}_{Nq}$ symmetry is projectively realized: $S^{Nq} = C^{Nq} = 1$ and

$$SC = e^{-2\pi i/Nq} CS.\tag{4.74}$$

By definition, the θ vacuum $|\theta, k\rangle$ is the eigenstate of $\mathbb{Z}_{Nq}^{[0]}$, which satisfies

$$S|\theta, k\rangle = e^{-2\pi i k/Nq} |\theta, k\rangle.\tag{4.75}$$

Since k labels the phase of the chiral condensate, the discrete chiral transformation acts as

$$C|\theta, k\rangle = |\theta, k+1\rangle.\tag{4.76}$$

Therefore, comparison between

$$SC|\theta, k\rangle = S|\theta, k+1\rangle = e^{-2\pi i(k+1)/Nq}|\theta, k+1\rangle, \quad (4.77)$$

and

$$CS|\theta, k\rangle = e^{-2\pi i k/Nq}C|\theta, k\rangle = e^{-2\pi i k/Nq}|\theta, k+1\rangle, \quad (4.78)$$

shows that (4.74) holds.

The existence of projective phase forbids the simultaneous eigenstate under the center and discrete chiral symmetries. Since $|\theta, k\rangle$ is constructed as an eigenstate of the center symmetry, the Polyakov loop does not have the diagonal expectation value. Indeed,

$$\langle\theta, k|P|\theta, k\rangle = \langle\theta, k|S^\dagger PS|\theta, k\rangle = e^{2\pi i/Nq}\langle\theta, k|P|\theta, k\rangle, \quad (4.79)$$

and this gives

$$\langle\theta, k|P|\theta, k\rangle = 0. \quad (4.80)$$

We can extend this discussion to see that the only possible nonzero amplitude is given by $\langle\theta, k+1|P|\theta, k\rangle$. In this sense, the Polyakov loop P behaves in the same manner as C up to an overall normalization. We can do the same argument about the chiral condensate $\bar{\psi}_L\psi_R$, and find that the only possible nonzero amplitude is given by $\langle\theta, k|\bar{\psi}_L\psi_R|\theta, k\rangle \sim e^{2\pi i k/Nq}$. Again, up to an overall normalization, the chiral condensate behaves in the similar manner as S , and these relations are nothing but the consequence of mixed 't Hooft anomaly.

5 Quantum instanton on $\mathbb{R} \times S^1$ and chiral condensate

We usually call instantons as bosonic classical solutions with nontrivial topological charge. For well-definedness, we put the theory on the two-torus, $M_2 = T^2 = S^1_\beta \times S^1_L$, and let us discuss instantons of Schwinger model. For a given topological charge,

$$Q = \frac{1}{2\pi} \int da \in \mathbb{Z}, \quad (5.1)$$

the $U(1)$ gauge field a can be decomposed as [10]

$$a = \frac{2\pi Q}{\beta L} \tau dx + \frac{2\pi}{\beta} h_1 d\tau + \frac{2\pi}{L} h_2 dx + \star d\phi + d\lambda, \quad (5.2)$$

where $h_{1,2} \in [0, 1)$ denote constant holonomies, ϕ is the \mathbb{R} -valued scalar field without zero-mode, and λ is the gauge parameter. Using this expression, the Maxwell action is bounded from below as

$$S = \frac{1}{2e^2} \int_{T^2} d^2x \left((\Delta\phi)^2 + \left(\frac{2\pi Q}{\beta L} \right)^2 \right) \geq \frac{2\pi^2}{e^2 \beta L} Q^2. \quad (5.3)$$

Since e^2 has mass dimension two, βL in the denominator of (5.3) is necessary to make the action dimensionless. In the \mathbb{R}^2 limit, the instanton action actually vanishes.

In this section, we give a path-integral interpretation of the results in Sec. 4. There, we will see that “quantum” instanton plays an essential role to describe the spontaneous discrete chiral symmetry breaking in a semiclassical manner [30, 31].

5.1 Fractional quantum instanton for thermal boundary condition

Let us take the periodic boundary condition for fermions. In (4.39), we obtain that $\det(\bar{\psi}_L^f \psi_R^{f'})$ condenses as the following matrix element is nonzero,

$$\langle n-1 | \det(\bar{\psi}_L^f \psi_R^{f'}) | n \rangle \neq 0. \quad (5.4)$$

It breaks \mathbb{Z}_q discrete chiral symmetry if $q > 1$. Integrating out fermion fields, the holonomy potential is induced as (3.6), and we denote the effective potential for quantum mechanics of $a_2(\tau, x) = a(\tau)$ as

$$V_{\text{eff}}(a) \equiv L(V(a) - \mathcal{F}_{\text{thermal}}) = \frac{q^2 N}{2\pi L} \min_k \left(La + \frac{2\pi(k + \frac{1}{2})}{q} \right)^2. \quad (5.5)$$

The boundary condition for gauge fields $a(\tau)$ becomes

$$a(-\infty) = \frac{\pi(2n+1)}{qL}, \quad a(+\infty) = \frac{\pi(2n-1)}{qL}, \quad (5.6)$$

by (5.4), and this is also because the chiral condensate behaves as the generator of $\mathbb{Z}_q^{[0]}$ center symmetry at low energies due to mixed 't Hooft anomaly as we have seen in Sec. 4.5. We can evaluate the lower bound of the Euclidean action by completion of the square (or, BPS trick) as follows:

$$\begin{aligned} S &= \int_{-\infty}^{\infty} d\tau \left(\frac{L}{2e^2} \left(\frac{\partial a}{\partial \tau} \right)^2 + V_{\text{eff}}(a) \right) \\ &= \int d\tau \left\{ \frac{\sqrt{L/2}}{e} \frac{\partial a}{\partial \tau} \mp \sqrt{V_{\text{eff}}(a)} \right\}^2 \pm \frac{\sqrt{2L}}{e} \int d\tau \sqrt{V_{\text{eff}}(a)} \frac{\partial a}{\partial \tau} \\ &\geq \frac{\sqrt{2L}}{e} \left| \int da \sqrt{V_{\text{eff}}(a)} \right|. \end{aligned} \quad (5.7)$$

The lower bound for the given boundary condition is saturated as

$$S_{\mathcal{F}} = \frac{\pi^{3/2} N^{1/2}}{qeL} = \frac{\pi N}{m_{\gamma} L}, \quad \text{where } m_{\gamma} = \frac{N^{1/2} qe}{\pi^{1/2}}. \quad (5.8)$$

The topological charge of this configurations is $Q = -1/q$. Unlike usual instanton, we balance the classical kinetic term and the quantum-induced potential to find this configuration with fractional topological charge, so let us call it fractional quantum instanton, or fracton⁷ following Ref. [31]. From the index theorem, we can deduce that each fracton supports $2N$ fermionic zero modes and this is consistent as we find it in the computation of the determinant condensate.

In Figs. 8a and 8b, we can see the quantum induced potentials and corresponding quantum instantons for $(q, N) = (1, 1)$ and $(q, N) = (2, 1)$, respectively. When $(q, N) =$

⁷Note that this naming has no relation with fracton phases in condensed matter literatures.

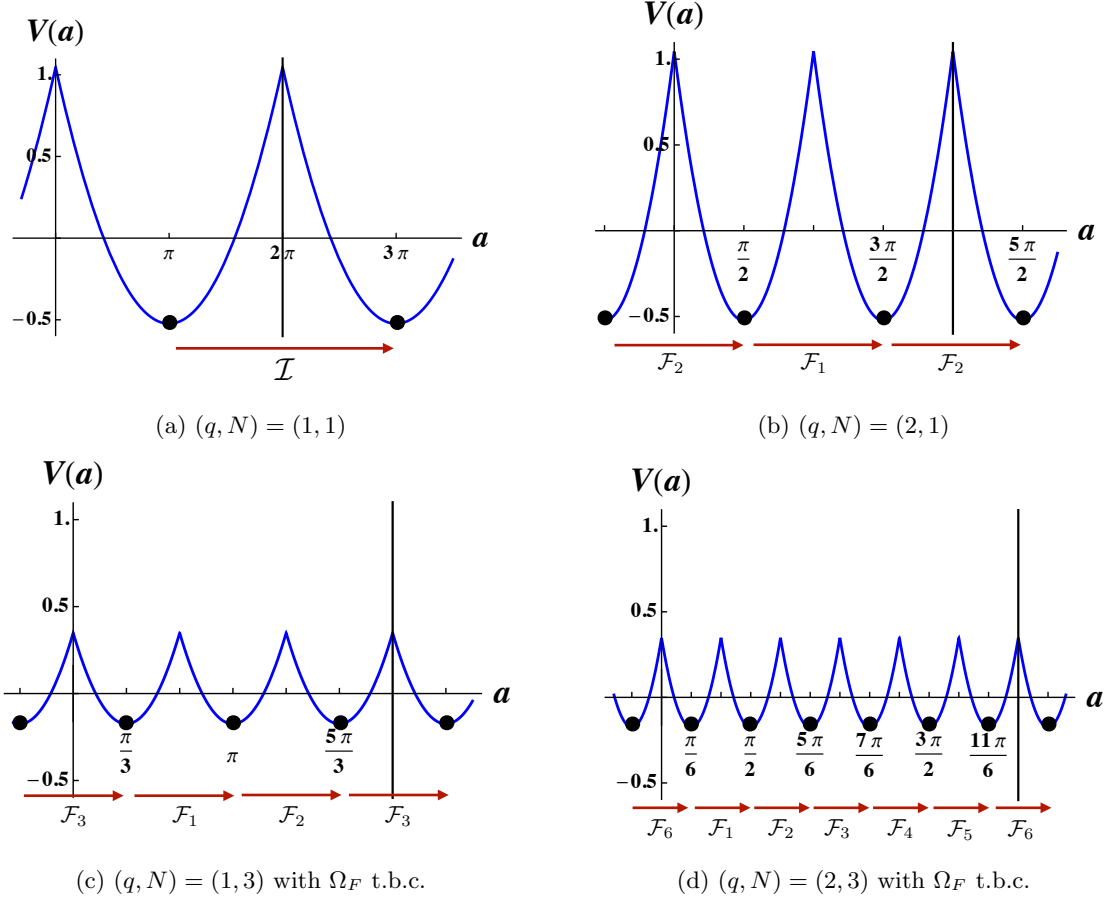


Figure 8. Quantum instantons in various setups: (a) Quantum instanton for $(q, N) = (1, 1)$, which contributes to $\langle \bar{\psi}_L \psi_R \rangle = L^{-1} e^{i\theta} e^{-S_{\mathcal{F}}}$, as a consequence of ABJ anomaly. No symmetry breaking occurs. (b) Fractional quantum instantons (= fractons) for $(q, N) = (2, 1)$, which contributes to $\langle \bar{\psi}_L \psi_R \rangle = L^{-1} e^{i\theta/q} e^{-S_{\mathcal{F}}}$. The fractional θ dependence reflects the spontaneous \mathbb{Z}_q discrete chiral symmetry breaking. (c)(d) Fractons for $(q, N) = (1, 3)$ and $(q, N) = (2, 3)$ with the flavor-twisted boundary condition Ω_F , which contribute to $\langle \bar{\psi}_L^f \psi_R^f \rangle = (NL)^{-1} e^{i\theta/Nq} e^{-S_{\mathcal{F}}}$. The fractional θ dependence reflects the spontaneous \mathbb{Z}_{Nq} discrete chiral symmetry breaking.

$(1, 1)$, we reproduce the result, $\langle \bar{\psi}_L \psi_R \rangle = L^{-1} \exp(-\frac{\pi}{m_\gamma L} + i\theta)$, in [10], and this condensate is the consequence of ABJ anomaly. For charge-2 case in Fig. 8b, fracton contributes to the fermion bilinear condensate, $\langle \bar{\psi}_L \psi_R \rangle = L^{-1} \exp(-\frac{\pi}{m_\gamma L} + i\theta/2)$, so that the θ dependence is fractionalized and \mathbb{Z}_2 discrete chiral symmetry is spontaneously broken.

Since we balance the kinetic term of $O(1/e^2)$ and the quantum induced potential of $O(1)$, the fracton action $S_{\mathcal{F}}$ is of order $1/e$. This has the big difference with usual field-theoretic extended configurations, which are typically of order $1/e^2$. It is notable that the fracton action $S_{\mathcal{F}}$ exactly gives the exponent of (4.39) and the fractional topological charge explains the θ dependence $e^{i\theta/q}$. Therefore, we can directly observe the fracton contribution by measuring this condensate on $\mathbb{R} \times S^1$.

5.2 Fractional quantum instanton in flavor-twisted boundary condition

With the insertion of a Ω_F twist, we now have the quark-bilinear condensate (4.58) sourced by the matrix element

$$\langle N\ell + f - 1 | \bar{\psi}_L^f \psi_R^f | N\ell + f \rangle \neq 0. \quad (5.9)$$

Let us first integrate our fermions again when evaluating this amplitude on $\mathbb{R} \times S^1$, then the holonomy potential takes the form (3.10). We denote the effective potential for quantum mechanics of $a_2(\tau, x) = a(\tau)$ as

$$V_{\text{eff}, \Omega_F}(a) \equiv L(V_{\Omega_F}(a) - \mathcal{F}_{\Omega_F}) = \frac{q^2 N}{2\pi L} \min_k \left(La + \frac{2\pi(k + \frac{1}{2})}{qN} \right)^2, \quad (5.10)$$

and the boundary condition is

$$a(-\infty) = \frac{\pi(2(N\ell + f) + 1)}{Nq}, \quad a(+\infty) = \frac{\pi(2(N\ell + f) - 1)}{Nq}. \quad (5.11)$$

We now evaluate the lower bound of the Euclidean effective action with V_{eff, Ω_F} with the given boundary condition. The BPS trick gives

$$\begin{aligned} S &= \int_{-\infty}^{\infty} d\tau \left(\frac{L}{2e^2} \left(\frac{\partial a}{\partial \tau} \right)^2 + V_{\text{eff}, \Omega_F}(a) \right) \\ &\geq \frac{\sqrt{2L}}{e} \left| \int da \sqrt{V_{\text{eff}, \Omega_F}(a)} \right|. \end{aligned} \quad (5.12)$$

Evaluating this lower bound for the given boundary condition, we obtain the fracton action,

$$S_{\mathcal{F}} = \frac{\pi^{3/2}}{N^{3/2} q e L} = \frac{\pi}{N m_{\gamma} L}, \quad (5.13)$$

and this is nothing but the exponent of the chiral condensate (4.58). The topological charge of this configurations is $Q = -1/Nq$, and this gives the fractional θ dependence, $e^{i\theta/Nq}$. From the index theorem, we can deduce that each fracton supports 2 fermionic zero modes and this is consistent as we find it in the computation of the fermion-bilinear condensate.

The behavior of fractons can be seen in Figs. 8c and 8d for $(q, N) = (1, 3)$ and $(q, N) = (2, 3)$ with symmetry twisted boundary condition, respectively. When we take the twisted boundary condition, we can clearly see in the figure that the height of effective potential becomes shallow of $O(1/N)$, while the local fluctuation of a feels the harmonic potential of $O(N)$. Let us compare the thermal and twisted boundary conditions in the table:

	Barrier height	Width Δa	Fracton action
Thermal	$O(N)$	$2\pi/q$	$S_{\mathcal{F}} = \frac{\pi N}{m_{\gamma} L}$
Ω_F twisted	$O(N^{-1})$	$2\pi/qN$	$S_{\mathcal{F}} = \frac{\pi}{N m_{\gamma} L}$

Differences of the potential barrier by $1/N^2$ and of the potential width by $1/N$ give the factor $\sqrt{1/N^2} \times 1/N = 1/N^2$ in the fracton action in the twisted boundary condition compared with that of the thermal one.

This N dependence of $S_{\mathcal{F}}$ affects the region of validity of our approximation for chiral condensate. Note that the region of validity of the one-loop holonomy potential and the one of the semi-classical instanton analysis are parametrically different. The one-loop analysis is reliable provided $Lm_\gamma \ll 1$. However, the semi-classical quantum-instanton analysis is reliable provided the quantum-instanton amplitude is small, $e^{-S_{\mathcal{F}}} \ll 1$. In the N -flavor Ω_F twisted case, the smallness of this amplitude is valid provided ($N L m_\gamma \ll 1$), and then the region of validity $L \lesssim \frac{1}{m_\gamma N} \rightarrow 0$ in the $N \rightarrow \infty$ limit. This is an imprint of large- N volume independence in the N flavor twisted Schwinger model. In the thermal model, semi-classical approximation is always valid within the domain of validity of one-loop analysis.

6 Effect of fermion mass and spontaneous C breaking at $\theta = \pi$

In this section, we introduce the flavor-degenerate soft mass m_ψ to Dirac fermions and discuss its physical effects by using symmetry, anomaly and global inconsistency, mass perturbation on $\mathbb{R} \times S^1$, and dilute fractional-quantum-instanton gas approximation also on $\mathbb{R} \times S^1$. Unlike massless case, the ground-state energy is affected by the θ angle, and the ground state is unique for generic θ angles. At $\theta = \pi$, we shall see that the charge-conjugation symmetry C is spontaneously broken when $qN \geq 3$ or $q \geq 2$. For $q = 1$ and $N = 2$, we shall see that C is spontaneous broken on $\mathbb{R} \times S^1$, but it is believed to go back to $SU(2)_1$ WZW model on \mathbb{R}^2 at $\theta = \pi$, which is related to the Haldane conjecture.

6.1 Anomaly and global inconsistency for massive Schwinger model

Before the concrete analysis of massive Schwinger model, let us discuss the kinematical constraint by symmetry. We add the fermion mass term,

$$m_\psi \sum_f \int d^2x (\bar{\psi}_L^f \psi_R^f + \bar{\psi}_R^f \psi_L^f), \quad (6.1)$$

to the Lagrangian (2.1), and we assume $m_\psi > 0$ so that the θ angle has the definite meaning. This fermion mass term explicitly breaks the chiral symmetry $G^{[0]}$ in (2.3) to its vector-like subgroup completely, and we get

$$\mathbb{Z}_q^{[1]} \times \frac{SU(N)_V}{\mathbb{Z}_N} \subset G. \quad (6.2)$$

Since this symmetry is vector like, this subgroup has no anomaly, and we do not have any interesting constraint on the vacuum structure so far.

Let us now consider the charge conjugation symmetry C . This \mathbb{Z}_2 internal symmetry is generated by

$$C : \psi \mapsto i\gamma^2 \bar{\psi}^T, \quad \bar{\psi} \mapsto \psi^T i\gamma^2, \quad a \mapsto -a. \quad (6.3)$$

In the chiral notation, C acts as

$$\begin{aligned} \psi_R &\mapsto \bar{\psi}_R, \quad \psi_L \mapsto -\bar{\psi}_L, \\ \bar{\psi}_R &\mapsto \psi_R, \quad \bar{\psi}_L \mapsto -\psi_L. \end{aligned} \quad (6.4)$$

Examples of C-odd observables are $da, \bar{\psi}_R \psi_L - \bar{\psi}_L \psi_R$. Especially, the θ term flip its sign under C, and thus this is symmetry only when $\theta = 0$ or $\theta = \pi$.

The group structure including C [74] is given by the semidirect product,

$$\left(\mathbb{Z}_q^{[1]} \times \frac{SU(N)_V}{\mathbb{Z}_N} \right) \rtimes (\mathbb{Z}_2)_C, \quad (6.5)$$

if $q \geq 3$ or $N \geq 3$, and otherwise it is given by the direct product,

$$\left(\mathbb{Z}_q^{[1]} \times \frac{SU(N)_V}{\mathbb{Z}_N} \right) \times (\mathbb{Z}_2)_C. \quad (6.6)$$

Especially when $q = 1$ and $N = 2$, the group structure $SO(3) \times \mathbb{Z}_2 = O(3)$ is the same with that of discrete chiral transformation.

Let us discuss the mixed anomaly, and to find it we gauge $\mathbb{Z}_q^{[1]} \times PSU(N)_V$ first, and we perform C after that [45]. The background gauge field consists of

- A_V : $SU(N)$ one-form gauge field, and
- B_V : \mathbb{Z}_{Nq} two-form gauge field.

In the description of Sec. 2.2.1, we have to set $A_L = A_R = A_V$, and set other gauge fields to be zero other than B_V . All the terms in the gauged Lagrangian is manifestly gauge-invariant and C-invariant, except for the θ term,

$$\frac{i\theta}{2\pi} \int (da + B_V^{(2)}). \quad (6.7)$$

This shows that the gauged partition functions at $\theta = 0$ and $\theta = \pi$ behave under C as

$$Z_{M_2, \theta=0}[A_V, B_V] \mapsto Z_{M_2, \theta=0}[A_V, B_V], \quad (6.8)$$

$$Z_{M_2, \theta=\pi}[A_V, B_V] \mapsto Z_{M_2, \theta=\pi}[A_V, B_V] \exp \left(i \int B_V^{(2)} \right). \quad (6.9)$$

Thus, the partition function at $\theta = \pi$ gets the \mathbb{Z}_{Nq} phase under C. We have to judge whether this is genuine anomaly or not by studying possible local counter terms.

The only possible local counterterm is $ik \int B_V$ with $k = 0, 1, \dots, Nq - 1$. We then find

$$Z_{M_2, \theta=\pi}[A_V, B_V] e^{ik \int B_V^{(2)}} \mapsto \left(Z_{M_2, \theta=\pi}[A_V, B_V] e^{ik \int B_V^{(2)}} \right) \exp \left(i(1 - 2k) \int B_V^{(2)} \right), \quad (6.10)$$

and thus C-invariance is established if and only if $2k - 1 = 0 \pmod{Nq}$ for some k . If Nq is even, no such counter term exists, and thus $\theta = \pi$ has a mixed 't Hooft anomaly.

When Nq is odd, we can solve $2k = 1 \pmod{Nq}$ as

$$k = \frac{Nq + 1}{2}, \quad (6.11)$$

and thus there is no anomaly at $\theta = \pi$. However, since the coefficient of the local counterterm is quantized, we cannot take the simultaneous UV regularization so that the gauged partition functions at $\theta = 0$ and $\theta = \pi$ are both C invariant. This is called global inconsistency condition [27, 44, 123]. The matching condition for global inconsistency [123] is

- The vacua at $\theta = 0$ and $\theta = \pi$ are different as symmetry-protected topological states, or
- either of $\theta = 0$ or $\theta = \pi$ has nontrivial vacuum as in the case of 't Hooft anomaly.

It is easy to see that the anomaly and global inconsistency is matched by SSB of \mathbb{C} at $\theta = \pi$ in the massive Schwinger model with $qN \geq 2$ on $\mathbb{R} \times S^1$. Here, let us restrict our attention to the case with the Ω_F -twisted boundary condition, so that the theory has $\mathbb{Z}_{Nq}^{[0]}$ symmetry. We have constructed the θ vacua, $|\theta, k\rangle$ with $k = 0, 1, \dots, Nq - 1$, in the massless limit in Sec. 4.2.2, and the chiral condensates are given in (4.58). For sufficiently small mass, then, we find the ground-state energy $E_k(\theta)$ of $|\theta, k\rangle$ by mass perturbation as

$$\begin{aligned} E_k(\theta) &= -Lm_\psi \sum_f \frac{\langle \theta, k | (\bar{\psi}_L^f \psi_R^f + \bar{\psi}_R^f \psi_L^f) | k, \theta \rangle}{\langle \theta, k | \theta, k \rangle} \\ &= -2m_\psi \exp\left(-\frac{\pi}{Nm_\gamma L}\right) \cos\left(\frac{\theta + 2\pi k}{Nq}\right). \end{aligned} \quad (6.12)$$

We thus find that the ground state is unique for generic θ , but $\theta = \pi$ is doubly degenerate if $Nq \geq 2$.

Although our explicit computation of the ground-state energy is limited to the semi-classical regime $eL \ll 1$, the constraint via anomaly and global inconsistency is valid even when the decompactification limit $L \rightarrow \infty$ is taken. The ground-state energy on \mathbb{R}^2 with small fermion mass m_ψ takes the complicated form as shown in Refs. [19, 124, 125], but those results are indeed consistent with anomaly and global inconsistency.

For $-\pi < \theta < \pi$, the ground state is uniquely determined to $k = 0$, $|\theta, 0\rangle$. As we have studied in Sec. 4.4, the Polyakov loop vanishes for this vacuum,

$$\langle \theta, 0 | P | \theta, 0 \rangle = 0. \quad (6.13)$$

Unlike massless case, this is the unique vacuum, and thus $\mathbb{Z}_{Nq}^{[0]}$ symmetry is unbroken. This is consistent with the fact that the string tension does not vanish without massless fermions. If we study the two-point function of n -th Polyakov loop P^n , it roughly behaves in $\tau \rightarrow \infty$ as

$$\begin{aligned} &\langle \theta, 0 | P^{-n}(\tau) P^n(0) | \theta, 0 \rangle \\ &\sim \exp[-\tau(E_n(\theta) - E_0(\theta))] \\ &= \exp\left[-2m_\psi \tau e^{-\pi/Nm_\gamma L} \left\{ \cos\left(\frac{\theta + 2\pi n}{Nq}\right) - \cos\left(\frac{\theta}{Nq}\right) \right\}\right], \end{aligned} \quad (6.14)$$

and it goes to zero unless $n = 0 \bmod Nq$. The exponent, $E_n(\theta) - E_0(\theta)$, corresponds to the string tension of the charge- n test particle. It would be worth to mention that $\theta = \pi$ is again exceptional in this regard, since the exponent vanishes at $\theta = \pi$ with $n = -1 \bmod Nq$. The corresponding statement is true for Wilson loops in the 2d decompactification limit [26].

6.2 Dilute fractional-quantum-instanton gas and multi-branched vacua

Let us reproduce the above result as a semiclassical approximation of the path integral. We first discuss the holonomy potential. Introducing mass term modifies $e^{-L|p|}$ in (3.6) and (3.9) into $e^{-L\sqrt{p^2+m_\psi^2}}$. As a result, the thermal holonomy potential takes the form,

$$V_{\text{thermal}}(a, m_\psi) = \frac{2N}{\pi L^2} \sum_{n=1}^{\infty} \frac{1}{n^2} (m_\psi L n) K_1(m_\psi L n) \cos(qan), \quad (6.15)$$

and similarly, in the Ω_F background, the potential takes the form:

$$V_{\Omega_F}(a, m_\psi) = \frac{2}{\pi L^2} \frac{1}{N} \sum_{n'=1}^{\infty} \frac{1}{n'^2} (m_\psi L N n') K_1(m_\psi L N n') \cos(Nqan'). \quad (6.16)$$

Here, we denote La simply by a , and $K_1(z)$ is the modified Bessel function of the first kind, whose asymptotic behaviors are

$$K_1(z) \sim \begin{cases} \frac{1}{z} + \frac{1}{4}z(2\ln(z) + 2\gamma - 1 - 2\ln(2)) + O(z^2), & z \rightarrow 0 \\ \sqrt{\frac{\pi}{2z}} e^{-z}(1 + O(1/z)), & z \rightarrow \infty. \end{cases} \quad (6.17)$$

For concreteness, we consider the massive Schwinger model with Ω_F background in the following. The presence of mass smoothens the cusp that is present in the potential with massless fermions, but otherwise, the vacuum structures are extremely similar at this level: We have Nq minima of the potential, which we denote as a_j with $j = 0, 1, \dots, Nq - 1$. Writing $j = Nm + f$ with $m = 0, \dots, q - 1$ and $f = 0, \dots, N - 1$, the perturbative ground state around a_j corresponds to

$$|a_j\rangle = \sum_{\ell \in \mathbb{Z}} e^{i\theta\ell} |N(q\ell + m) + f\rangle, \quad (6.18)$$

in the notation of Sec. 4.2.2.

The crucial difference between massless and massive cases is that, in the latter, the vacuum degeneracy will be lifted by quantum tunneling. In the massless case, this is prohibited since $|a_j\rangle$ with different j have different charged under \mathbb{Z}_{Nq} discrete chiral symmetry. In other words, the would-be tunneling process is fractional quantum instanton, which has $\Delta Q_5 = 2$, and it does not contribute to the partition function. Adding fermion mass, this symmetry is explicitly broken so that quantum tunneling process occurs.

The theory on small circle, $eL \ll 1$, reduces to a simple quantum mechanical problem for the a field. This is the quantum mechanics of a particle moving on a circle S^1 in the presence of a potential with Nq minima given in (6.16) in its fundamental domain $a \in [0, 2\pi)$. There is no harm in simplifying the potential into

$$V(a) \sim \cos(Nqa). \quad (6.19)$$

and there exists an Aharonov-Bohm flux passing through the center of the circle, which captures the topological θ angle.

The partition function, $Z(\beta) = \text{tr}[\exp(-\beta H)]$, in the $\beta \rightarrow \infty$ limit is dominated by the lowest- Nq states. To all orders in perturbation theory, the harmonic states at the minima of the potential (6.19) are exactly degenerate. To simplify the discussion, we can forget about higher states in the spectrum within Born-Oppenheimer approximations, because instanton induced splittings $\sim \omega e^{-S_{\mathcal{F}}}$ is much smaller than perturbative gap in the spectrum ($\sim \omega$). The path-integral representation of the partition function is

$$Z(\beta) = \int_{a(\beta)=a(0)} \mathcal{D}a \exp(-S[a]), \quad (6.20)$$

and this is a sum over paths obeying the periodic boundary condition, $a(\beta) = a(0)$. The maps $S^1_\beta \rightarrow S^1$ are classified by the winding numbers, $\pi_1(S^1) = \mathbb{Z}$, which is nothing but the topological charge $Q = \frac{1}{2\pi} \int da \in \mathbb{Z}$ in 2d language.

The essence of the matter is following: The partition function is a sum over integer topological charge configurations $Q \in \mathbb{Z}$, yet, in the problem, there are classical solutions with fractional topological charges quantized in $1/Nq$, which we call fractional quantum instanton with the action $S_{\mathcal{F}}$. A single fractional instanton does not contribute to the partition function because of the mismatch of boundary condition, and this introduces a constraint when considering the dilute gas approximation as a semiclassical approximation of $Z(\beta)$. In the dilute fractional-instanton gas approximation of $Z(\beta)$, we must sum over all configurations with n fracton, \bar{n} anti-fracton satisfying the constraint $n - \bar{n} - WNq = 0$, where $W \in \mathbb{Z}$ is the winding number. This guarantees that the gauge field is a connection of $U(1)$ bundle.

In the dilute gas approximation, the partition function can therefore be written as

$$Z(\beta) = Nq \sum_{W \in \mathbb{Z}} \sum_{n=0}^{\infty} \sum_{\bar{n}=0}^{\infty} \frac{1}{n!} \frac{1}{\bar{n}!} \left(\beta K e^{-S_{\mathcal{F}} + i\theta/Nq} \right)^n \left(\beta K e^{-S_{\mathcal{F}} - i\theta/Nq} \right)^{\bar{n}} \delta_{n-\bar{n}-WNq}, \quad (6.21)$$

where K denotes the 1-loop determinant multiplied by the volume of internal moduli, and it is given as $K = m_\psi$ for soft fermion mass. The constraint $n - \bar{n} - WqN = 0$ guarantees that the θ angle dependence over any configuration contributing to path integral is of the form $(e^{i\theta/Nq})^{n-\bar{n}} = e^{iW\theta}$, $W \in \mathbb{Z}$ as it must be. The overall factor Nq is due to Nq distinct classical minima in the fundamental domain.

We can convert the constrained sum (6.21) into a sum on the space of representation of \mathbb{Z}_{Nq} , by using $\text{Hom}(\mathbb{Z}_{Nq}, U(1)) = \mathbb{Z}_{Nq}$, and hence,

$$\sum_{W \in \mathbb{Z}} \delta_{n-\bar{n}-WNq} = \frac{1}{Nq} \sum_{k=0}^{Nq-1} e^{i2\pi k(n-\bar{n})/Nq}. \quad (6.22)$$

We can now express the partition function as

$$\begin{aligned} Z(\beta) &= \sum_{k=0}^{Nq-1} \sum_{n=0}^{\infty} \sum_{\bar{n}=0}^{\infty} \frac{1}{n!} \frac{1}{\bar{n}!} \left(\beta K e^{-S_{\mathcal{F}} + i\frac{\theta+2\pi k}{Nq}} \right)^n \left(\beta K e^{-S_{\mathcal{F}} - i\frac{\theta+2\pi k}{Nq}} \right)^{\bar{n}} \\ &= \sum_{k=0}^{Nq-1} e^{2\beta K e^{-S_{\mathcal{F}}} \cos \frac{\theta+2\pi k}{Nq}} \end{aligned} \quad (6.23)$$

This is the contribution of the Nq lowest lying states to the partition function, which were degenerate to all orders in perturbation theory. This reproduces the multi-branch structure (6.12) of the ground state energies:

$$E_{\text{G.S.}}(\theta) = \min_{k=0,1,\dots,Nq-1} \left(-2m_\psi e^{-S_{\mathcal{F}}} \cos \frac{\theta + 2\pi k}{Nq} \right). \quad (6.24)$$

We can summarize the main result of this section as follows.

- The existence of fractional topological charge instantons along with the fact that we need to perform a sum over $U(1)$ gauge configurations with integer topological charges leads to multi-branched observables both in quantum mechanics and corresponding QFT.
- If we refer to the action of winding number one configuration as $S_{W=1}$, the first non-perturbative saddle that contributes to the semi-classical expansion (6.21) has action $2S_{\mathcal{F}} = \frac{2S_{W=1}}{Nq}$. In other words, in the $W = 0$ zero sector, minimal action is zero (perturbative vacuum), but non-perturbative saddles have action $\frac{2S_{W=1}n}{Nq}$, $n = 1, 2, \dots$

Note that, if we take $m_\psi \rightarrow 0$ limit, the vacuum family composed of Nq -branches become degenerate.

7 Volume independence in $N \rightarrow \infty$ limit and quantum distillations

A sub-class of QFTs with large degrees of freedom have properties which are independent of compactification radius of spacetime $\mathbb{R}^{d-1} \times S^1$. This property is called large- N volume independence [89]. The extreme version of volume independence, where space-time (lattice) is reduced to a single point, is called Eguchi-Kawai reduction or large- N reduction [126–128]. There are two necessary and sufficient conditions for the validity of the volume independence. In a lattice formulation, these can be phrased as:

- Translation symmetry of lattice L^d is not spontaneously broken.
- Center symmetry is not spontaneously broken.

Provided these conditions are satisfied, expectation values and connected correlators of certain interesting observables are independent of compactification radius. In the charge- q Schwinger model, this includes flavor and center singlet observables.

A working realization of volume independence is a non-trivial phenomenon. It demands absence of *any* phase transitions when the theory is compactified. For example, in 4d gauge theory, it demands the absence of deconfinement transition when the theory is compactified on $\mathbb{R}^3 \times S^1$. Deconfinement is a generic behavior with the thermal partition function. However, if one considers a graded partition function such as $\text{tr}[(-1)^F e^{-LH}]$, there is a special class of gauge theory in 4d that satisfies volume independences. These theories are gauge theories with adjoint fermions. In these theories, there must exist profound spectral cancellations [84, 99, 111, 129] to avoid phase transitions. This is a version of quantum distillation, where only a subset of states contribute to the graded partition function.

Below, we comment on the realization of volume independence in the charge- q N -flavor Schwinger model in the large- N limit. In particular, we will provide evidence that:

- Thermal compactification of charge- $q \geq 1$ models does not obey volume independence.
- Ω_F twisted compactification respects volume independence.

First, we provide a perturbative argument. In the thermal compactification, the KK modes are quantized in the usual manner in units of $\frac{2\pi}{L}$ as shown in Fig. 2. In the twisted compactification, the usual KK-modes intertwine with the flavor-holonomy, and refined KK-modes are now quantized in units of $\frac{2\pi}{LN}$, as shown in Fig. 5. At fixed L , in the $N \rightarrow \infty$ limit, the modes become arbitrarily dense and form a continuum. This is just like perturbative spectrum of the theory on \mathbb{R}^2 with one-flavor, and this is sometimes called flavor-momentum transmutation.

Next, let us now discuss the center-symmetry realization of the thermal boundary condition. For simplicity, we discuss the case when we turn on a soft mass term for the fermion m_ψ . In this case, the minima of the holonomy potential remains unaltered, despite the fact that the potential is weakened. Furthermore, the fermionic zero modes of the fractons are lifted so that the transition amplitude between two consecutive minima is non-zero.

$$\langle n+1 | e^{-\beta H} | n \rangle \sim e^{-S_{\mathcal{F}}} m_\psi^N = e^{-\frac{\pi N}{m_\psi L}} m_\psi^N. \quad (7.1)$$

In charge- q model with N massive flavor, the one-loop potential (6.15) implies that the \mathbb{Z}_q center-symmetry is broken to all orders in perturbation theory. However, non-perturbatively, it is restored due to tunnelings between the q perturbative minima.

In the limit $N \rightarrow \infty$, however, we observe that the barrier in the potential (6.15) becomes arbitrarily large while the location of the minima is unaltered. In this case,

$$\lim_{N \rightarrow \infty} \left[\langle n+1 | e^{-\beta H} | n \rangle \sim e^{-S_{\mathcal{F}}} = e^{-\frac{\pi N}{m_\psi L}} \right] = 0 \quad (7.2)$$

and the tunneling amplitude is zero. Therefore, in the $N \rightarrow \infty$ limit of charge- q theory, the \mathbb{Z}_q center-symmetry is spontaneously broken. This implies that in the thermal case, large- N volume independence fails. Indeed, just inspecting the free energy density, we observe the temperature dependence, $\mathcal{F}_{\text{thermal}} = -NT^2 \frac{\pi}{6}$ at leading order in N .

Lastly, we show that, by using the twisted boundary condition with Ω_F , we can keep center-symmetry intact in the $N \rightarrow \infty$ thermodynamic limit, and volume independence is established.

As described in Sec. 4.2.2, with the twist, there are Nq type fractons, each of which has exactly two-fermionic zero modes. Again, turning on a soft mass term for the fermion m_ψ , the chiral symmetry is explicitly broken. The zero modes of fracton can be soaked up by the soft mass term and the fracton amplitudes take the form $\mathcal{F}_j \sim e^{-S_j} m_\psi$.

As described around (2.76), the zero-form part $\mathbb{Z}_q^{[0]}$ of the 1-form center symmetry $\mathbb{Z}_q^{[1]}$ is enhanced to $\mathbb{Z}_{qN}^{[0]}$ in the compactified theory due to Ω_F background. Below, we would like

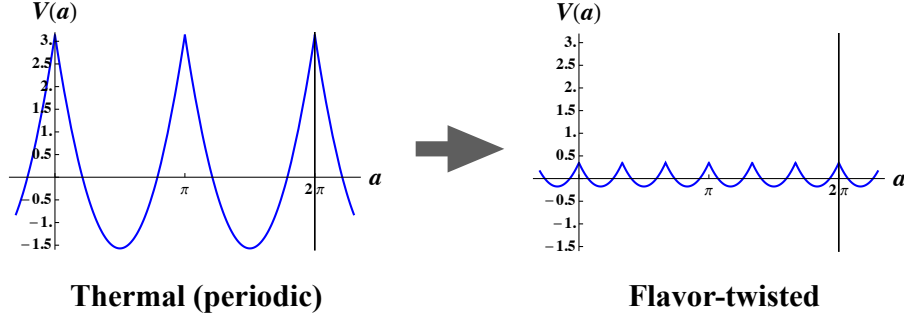


Figure 9. The holonomy potential and free energy for thermal and twisted theory $q = 2, N = 3$. With the inclusion of the twist Ω_F , potential is suppressed by a factor $\frac{1}{N^2}$. The image of this process in Hilbert space is cancellation among states in the graded state sum, a process that we refer to as quantum distillation.

to discuss the realization of this symmetry. Again, at finite- N , to all orders in perturbation theory, the $\mathbb{Z}_{qN}^{[0]}$ center-symmetry is broken, and non-perturbatively it is restored due to tunneling. The question is whether this restoration remains intact in the $N \rightarrow \infty$ limit. In this case,

$$\langle n+1 | e^{-\beta H} | n \rangle \sim e^{-\frac{\pi}{Nm_\gamma L}} m_\psi, \quad (7.3)$$

which remains finite even for large- N , implying unbroken center at large- N . Despite the fact that this conclusion is correct, the reasoning is not. In fact, we cannot even take $N \rightarrow \infty$ limit with the fracton action at fixed L , because semi-classical dilute instanton gas approximation breaks down when $S_{\mathcal{F}} = \frac{\pi}{Nm_\gamma L} \sim 1$.

In the large- N limit, we can reliably state that $V_{\Omega_F}(a) \rightarrow 0$ and holonomy field a direction becomes flat. The ground state wave function becomes the one of particle on a circle with no barriers in between. Since the tunneling becomes irrelevant in this regime, the \mathbb{Z}_{qN} center-symmetry is perturbatively unbroken. This guarantees that in the large- N limit of the QED₂ with Ω_F twist, volume-independence holds.

As a test, note the free energy in the Ω_F twisted background. In this case, free energy becomes $\mathcal{F}_{\Omega_F} = -\frac{1}{N}T^2\frac{\pi}{6}$ at leading order in large- N expansion. Indeed, both $O(N^1)$ and $O(1)$ parts of the free energy is temperature independent. This can be clearly seen in Fig. 9.

7.1 Interpretation as quantum distillation of Hilbert space

So far, we have discussed the $O(N^{-2})$ suppression of the twisted free energy compared with the thermal free energy in microscopic viewpoint. In this section, we provide its reinterpretation in view of physical Hilbert space.

In operator formalism, the thermal and graded partition functions correspond to

$$Z(\beta) = \text{tr} \left[e^{-\beta H} \right]$$

$$Z_{\Omega_F}(\beta) = \text{tr} \left[e^{-\beta H} (-1)^F \prod_{f=1}^N e^{i \frac{2\pi(f-1)}{N} Q_f} \right], \quad (7.4)$$

where Q_f is the fermion number operator for species f , and H is the Hamiltonian of QFT on \mathbb{R}^1 or its compactification to S_ℓ^1 . Note that we consider QFT on $\mathbf{T}^2 = S_\beta^1 \times S_\ell^1$ and assume boundary condition is twisted in the β circle. S_ℓ^1 provides a regularization for \mathbb{R} . The Hilbert space data that enters to these partition functions are identical, and concerns the spectrum of the Hamiltonian $H = H_{\mathbb{R}}$. However, in the graded sum, there are significant cancellations among states.

As an explicit example, consider a state in the adjoint representation of the $SU(N)_V$, created by

$$M_f^{f'} = \bar{\psi}_f \psi^{f'}, \quad f, f' = 1, \dots, N \quad (7.5)$$

In thermal case, these state would contribute to free energy as $e^{-\beta E_{\text{adj}}(N^2 - 1)}$. However, in the graded sum, $\prod_{f=1}^N e^{i \frac{2\pi(f-1)}{N} Q_f}$ assigns different phases to different states. For the adjoint representation, this assignment is

$$M_f^{f'} \rightarrow e^{-2\pi i(f-f')/N} M_f^{f'} \quad (7.6)$$

modifying the terms in the state sum into

$$(N^2 - 1)e^{-\beta E_{\text{adj}}} \longrightarrow \left(\sum_{f, f'=1}^N e^{-2\pi i(f-f')/N} - 1 \right) e^{-\beta E_{\text{adj}}} = (-1)e^{-\beta E_{\text{adj}}} \quad (7.7)$$

reducing the effect of $(N^2 - 1)$ degree of freedom to (-1) . This type of cancellation will occur in the graded partition function for all states, except for the singlets, including the ground states.

In order to understand the effect of these type of cancellation in thermodynamics, we recall the relation between partition functions and density of states following [129]. The inverse Laplace transform of the partition function is density of states. In the thermal case, the theory will exhibit a density of state expected from the Cardy formula for 2d massless Dirac fermions,

$$Z(\beta) \sim e^{\frac{N}{\beta} \frac{\pi}{6} \ell} \quad \underset{\text{Laplace transform}}{\Longleftrightarrow} \quad \rho(E) \sim e^{\sqrt{\frac{2\pi}{3}} NE \ell}, \quad (7.8)$$

where the central charge is N . In the graded case, we perform a graded sum over the Hilbert space of the theory. There are many cancellation and what is left out of these cancellations is the thermodynamic worth of the graded partition function. We find that

$$Z_{\Omega_F}(\beta) \sim e^{\frac{1}{N\beta} \frac{\pi}{6} \ell} \quad \underset{\text{Laplace transform}}{\Longleftrightarrow} \quad \rho_{\text{twisted}}(E) \sim e^{\sqrt{\frac{2\pi}{3N}} E \ell} \quad (7.9)$$

The density of states (7.8) is the largest growth expected from a 2d-local QFT with N degrees of freedom, corresponding to Stefan-Boltzmann growth. In the twisted case, the density of states will correspond to counting of states after cancellations triggered by the grading over Hilbert space. This growth is clearly extremely small compared to the thermal case. In particular, in the $N \rightarrow \infty$ limit, it is as if all states are eliminated after twisting and grading.

Normally, the competition between the growth in the density of states against the Boltzmann suppression is responsible for the changes in the saddles of the partition function and phase transition. At large- β , only ground states and low lying states contribute. But at low- β , many states may contribute on the same footing resulting possibly in phase transitions. In the graded case, the growth of density of states is effectively diminished and only a hand full of states contribute to state sum both at large- and small- β . This can and does prevent the possibility of phase transitions. These type of spectral cancellations, reminiscent of supersymmetric QFTs, is at the very origin of the working realizations of large- N volume independence, both in QED₂ or 4d gauge theories such as QCD(adj).

8 Twisted-compactification of $SU(N)_k$ Wess-Zumino-Witten model

As we have explained in Sec. 2.3, the low-energy behavior of charge-1 multi-flavor Schwinger model is described by the level-1 Wess-Zumino-Witten (WZW) model. More generally, the $SU(N)_k$ WZW model is defined as

$$S = \frac{1}{2g} \int_{M_2} \text{tr}[dU^\dagger \wedge \star dU] + ik\Gamma_{\text{WZ}}[U], \quad (8.1)$$

where the Wess-Zumino term is defined as

$$\Gamma_{\text{WZ}} = \frac{1}{12\pi} \int_{M_3} \text{tr}[(U^\dagger dU)^3]. \quad (8.2)$$

The RG flow has the conformal fixed point at $g = 4\pi/k$.

In this section, we show that this conformal behavior is responsible for the extra \mathbb{Z}_N degeneracy of the ground states under the flavor-twisted boundary condition. We therefore consider the twisted boundary condition (2.70),

$$u_{ij}(x, \tau + L) = \omega^{i-j} u_{ij}(x, \tau), \quad (8.3)$$

with $U = [u_{ij}]$. The case $k = 0$ with twisted boundary condition is studied in [100]. The theory with this boundary condition has the \mathbb{Z}_N symmetry, $u_{ij} \mapsto u_{i+1,j+1}$, and also the maximal Abelian subgroup of G .

8.1 Wess-Zumino term and topological θ terms

Let us evaluate the Wess-Zumino term under the flavor-twisted boundary condition at small compactification radius.

8.1.1 $SU(2)$ case

We first compute the $SU(2)$ case. In order to look at the classical vacua under the twisted boundary condition, it is convenient to take the Hopf coordinate,

$$U = \begin{pmatrix} e^{i\phi} \sin \eta & e^{i\xi} \cos \eta \\ -e^{-i\xi} \cos \eta & e^{-i\phi} \sin \eta \end{pmatrix}. \quad (8.4)$$

Here, ϕ and ξ are 2π periodic variables, and $\eta \in [0, \pi/2]$. The twisted boundary condition says

$$\phi(x, \tau + L) = \phi(x, \tau), \quad \eta(x, \tau + L) = \eta(x, \tau), \quad (8.5)$$

and

$$\xi(x, \tau + L) = \xi(x, \tau) + \pi. \quad (8.6)$$

Thus, only ξ should have nontrivial τ dependence in the small compactification limit, i.e. it does not have KK zero mode.

The kinetic term is given as

$$\text{tr}[\partial_\mu U^\dagger \partial_\mu U] = 2[\sin^2 \eta (\partial_\mu \phi)^2 + \cos^2 \eta (\partial_\mu \xi)^2 + (\partial_\mu \eta)^2]. \quad (8.7)$$

Because of the twisted boundary condition, the classical configuration of ξ satisfies

$$(\partial_2 \xi)^2 = \left(\frac{\pi}{L}\right)^2, \quad (8.8)$$

and thus $\eta = \pi/2$ is energetically favored so that $\cos \eta = 0$. We therefore approximate the kinetic term as

$$\text{tr}[\partial_\mu U^\dagger \partial_\mu U] = 2(\partial_\mu \phi)^2, \quad (8.9)$$

by neglecting quantum fluctuations around $\xi = \pi\tau/L$ and $\eta = \pi/2$, i.e.

$$U|_{M_2} = \begin{pmatrix} e^{i\phi} & 0 \\ 0 & e^{-i\phi} \end{pmatrix}. \quad (8.10)$$

Strictly speaking, this naive manipulation is subtle quantum mechanically [107], and this is carefully considered in Ref. [130] in the context of principal chiral model. It, however, turns out to be useful to understand the role of the WZ term under the twisted boundary condition. Especially, the structure of symmetry and 't Hooft anomaly is maintained.

Next, let us evaluate the WZ term setting $\phi = \phi(x)$, $\xi = \pi\tau/L$, and $\eta = \pi/2$ on $M_2 = M_1 \times S^1$. Using the Hopf coordinate, the WZ term becomes

$$\Gamma_{\text{WZ}} = -\frac{1}{2\pi} \int_{M_3} \sin(2\eta) d\phi \wedge d\xi \wedge d\eta. \quad (8.11)$$

We take $M_3 = M_2 \times [0, 1]$ and regard $M_2 \times \{1\}$ as a point so that $\partial M_3 = M_2 \times \{0\} \simeq M_2$. For this purpose, we need to set $U|_{M_2 \times \{1\}} = \mathbf{1}$, while satisfying the boundary condition, and we pick up the following extension along $x^3 \in [0, 1]$,

$$\begin{aligned} x^3 : \quad & 0 \longrightarrow \frac{1}{2} \longrightarrow 1, \\ U : \quad & \begin{pmatrix} e^{i\phi(x^1)} & 0 \\ 0 & e^{-i\phi(x^1)} \end{pmatrix} \xrightarrow{\eta: \frac{\pi}{2} \rightarrow 0} \begin{pmatrix} 0 & e^{\frac{i\pi\tau}{L}} \\ -e^{\frac{-i\pi\tau}{L}} & 0 \end{pmatrix} \xrightarrow{\eta: 0 \rightarrow \frac{\pi}{2}} \mathbf{1}. \end{aligned} \quad (8.12)$$

Using this parametrization, we get

$$\Gamma_{\text{WZ}} = \frac{\pi}{2\pi} \int d\phi, \quad (8.13)$$

and the theory becomes the particle on a circle with the theta angle $\theta = \pi k$:

$$S = \frac{L}{g} \int |d\phi|^2 + \frac{i\pi k}{2\pi} \int d\phi. \quad (8.14)$$

When k is even, i.e. $k = 0, 2, \dots$, the compactified WZW model has the unique ground state, and the energy gap is explained perturbatively with the formula $\sim g/2L$. When $k = 0$, the model is nothing but the $SU(2)$ principal chiral model, and its perturbative nature of the energy gap is emphasized in Ref. [130].

8.1.2 $SU(N)$ case

We extend the previous discussion to the case of general N . As in the $SU(2)$ case, we can argue that the classical moduli locates at the maximal torus $U(1)^{N-1} \subset SU(N)$ because of the flavor-twisted boundary condition, and we denote such a matrix as

$$U = \begin{pmatrix} e^{i\phi_1} & 0 & 0 \\ 0 & e^{i\phi_2} & 0 \\ 0 & 0 & e^{-i(\phi_1+\phi_2)} \end{pmatrix} = \begin{pmatrix} e^{i\phi_1} & 0 & 0 \\ 0 & e^{-i\phi_1} & 0 \\ 0 & 0 & 1 \end{pmatrix} \begin{pmatrix} 1 & 0 & 0 \\ 0 & e^{i(\phi_1+\phi_2)} & 0 \\ 0 & 0 & e^{-i(\phi_1+\phi_2)} \end{pmatrix}. \quad (8.15)$$

That is, we regard the classical vacua U as the successive multiplication of 2×2 Cartan factors. Here, we explicitly work on $SU(3)$ case, but the generalization is straightforward.

We consider the extension of U to extra dimension successively. That is, we take $M_3 = M_2 \times ([0, 1] \cup [1, 2])$. On $M_2 \times [0, 1]$, we parametrize U as

$$U = \begin{pmatrix} e^{i\phi_1} \sin \eta & e^{i\frac{2\pi\tau}{3L}} \cos \eta & 0 \\ -e^{-i\frac{2\pi\tau}{3L}} \cos \eta & e^{-i\phi_1} \sin \eta & 0 \\ 0 & 0 & 1 \end{pmatrix} \begin{pmatrix} 1 & 0 & 0 \\ 0 & e^{i(\phi_1+\phi_2)} & 0 \\ 0 & 0 & e^{-i(\phi_1+\phi_2)} \end{pmatrix}, \quad (8.16)$$

and the first 2×2 factor is set identity at $x^3 = 1$ as we did in the $SU(2)$ case. On $M_2 \times [1, 2]$, we parametrize

$$U = \begin{pmatrix} 1 & 0 & 0 \\ 0 & 1 & 0 \\ 0 & 0 & 1 \end{pmatrix} \begin{pmatrix} 1 & 0 & 0 \\ 0 & e^{i(\phi_1+\phi_2)} \sin \eta' & e^{i\frac{2\pi\tau}{3L}} \cos \eta' \\ 0 & -e^{-i\frac{2\pi\tau}{3L}} \cos \eta' & e^{-i(\phi_1+\phi_2)} \sin \eta' \end{pmatrix}, \quad (8.17)$$

and perform the same trick for the second 2×2 factor to set it identity at $x^3 = 2$. Since this is the inductive procedure, this computation also generalizes to $SU(N)$ cases in a straightforward manner.

As a consequence, we find that

$$\begin{aligned} \Gamma_{\text{WZ}} &= \frac{2\pi}{N} \frac{1}{2\pi} \int [(d\phi_1) + (d\phi_1 + d\phi_2) + \dots + (d\phi_1 + \dots + d\phi_{N-1})] \\ &= -\frac{1}{2\pi} \int \sum_{n=1}^{N-1} \frac{2\pi n}{N} d\phi_n \quad (\text{mod } 2\pi), \end{aligned} \quad (8.18)$$

and thus the problem becomes the $(N - 1)$ particles on a circle with the theta angles $\theta_n = 2\pi kn/N$. When the level of WZW model is $k = 0$ modulo N , we again find that the ground state is unique and the energy gap at the leading order is explained perturbatively, $\Delta E \sim g/2L$, which generalizes the result of Ref. [130].

8.2 Symmetry, Anomaly, and Energy spectrum

The $\mathbb{Z}_N^{[0]}$ symmetry acts as

$$\mathbb{Z}_N^{[0]} : \phi_n \mapsto \phi_{n+1} \ (n = 1, \dots, N-2), \quad \phi_{N-1} \mapsto -(\phi_1 + \dots + \phi_{N-1}), \quad (8.19)$$

which changes the θ angles as

$$\theta_n \mapsto \theta_{n-1} - \theta_{N-1} = \theta_n - 2\pi k \quad (n = 2, \dots, N-1), \quad (8.20)$$

$$\theta_1 \mapsto -\theta_{N-1} = \theta_1 - 2\pi k. \quad (8.21)$$

The difference of the action is

$$\Delta S = ik \int (d\phi_1 + \dots + d\phi_{N-1}) = 0 \text{ mod } 2\pi i, \quad (8.22)$$

and thus this transformation is the symmetry. The theory also has the symmetry $U(1)^{N-1} \subset SU(N)_R$, which acts on ϕ_n as

$$\phi_n \mapsto \phi_n + \alpha_n. \quad (8.23)$$

Let us gauge the $U(1)^{N-1}$ symmetry by introducing $U(1)$ gauge fields A_n , and then the gauged action is

$$\begin{aligned} S_{\text{gauged}} = & \frac{L}{2g} \int \left(\sum_{n=1}^{N-1} |d\phi_n + A_n|^2 + \left| \sum_{n=1}^{N-1} (d\phi_n + A_n) \right|^2 \right) \\ & - \frac{ik}{2\pi} \sum_{n=1}^{N-1} \frac{2\pi n}{N} \int (d\phi_n + A_n). \end{aligned} \quad (8.24)$$

We define the $\mathbb{Z}_N^{[0]}$ transformation on gauge fields as $A_n \mapsto A_{n+1}$ for $n = 1, \dots, N-2$, and $A_{N-1} \mapsto -(A_1 + \dots + A_{N-1})$. The partition function $Z[A_n]$ changes under the $\mathbb{Z}_N^{[0]}$ transformation as

$$Z[A_n] \mapsto Z[A_n] \exp \left(-ik \int (A_1 + \dots + A_{N-1}) \right), \quad (8.25)$$

and this is the mixed 't Hooft anomaly between $\mathbb{Z}_N^{[0]}$ and $U(1)^{N-1}$.

We can find the energy $E_{\{m_n\}}$ of $U(1)^{N-1}$ charges $\{m_n\} \in \mathbb{Z}^{N-1}$ by [54, 123]

$$\exp(-\beta E_{\{m_n\}}) = \int \mathcal{D}A_n Z[A_n] \exp \left(-i \sum_n m_n \int A_n \right), \quad (8.26)$$

where β is the imaginary time, where $E_{\{m_n\}}$ are given by

$$E_{\{m_n\}} = \frac{L}{2g} \left[\sum_{n=1}^{N-1} \left(m_n - k \frac{n}{N} \right)^2 - \frac{1}{N} \left(\sum_{n=1}^{N-1} \left(m_n - k \frac{n}{N} \right) \right)^2 \right]. \quad (8.27)$$

Performing the $\mathbb{Z}_N^{[0]}$ transformation, the $U(1)^{N-1}$ charges are changed as

$$m_1 \mapsto -m_{N-1} + k, \quad m_n \mapsto m_{n-1} - m_{N-1} + k \quad (n = 2, \dots, N-2). \quad (8.28)$$

This explains the N -fold degeneracy for $k \neq 0 \bmod N$; for example, when $k = 1$, the ground states are N -fold degenerate with

$$(m_1, \dots, m_{N-1}) = (0, \dots, 0), (0, \dots, 0, 1), (0, \dots, 0, 1, 1), \dots, (1, \dots, 1). \quad (8.29)$$

The coordinate expression of the state $|m_1, \dots, m_{N-1}\rangle$ is given as

$$\langle \phi_1, \dots, \phi_{N-1} | m_1, \dots, m_{N-1} \rangle = e^{im_1\phi_1 + \dots + im_{N-1}\phi_{N-1}}, \quad (8.30)$$

and thus

$$\langle m'_1, \dots, m'_{N-1} | e^{i\hat{\phi}_n} | m_1, \dots, m_{N-1} \rangle = \delta_{m'_1, m_1} \cdots \delta_{m'_n, m_n+1} \cdots \delta_{m'_{N-1}, m_{N-1}}. \quad (8.31)$$

Let us compute the vacuum expectation value of the fermion-bilinear scalar operator,

$$\bar{\psi}_R \psi_L \sim e^{i\phi_1} + \dots + e^{i\phi_{N-1}} + e^{-i(\phi_1 + \dots + \phi_{N-1})}. \quad (8.32)$$

By taking the following superposition of the N ground states,

$$|n\rangle = |0, \dots, 0\rangle + \omega^n |0, \dots, 0, 1\rangle + \dots + \omega^{n(N-1)} |1, \dots, 1\rangle, \quad (8.33)$$

with $\omega = e^{2\pi i/N}$, we find that

$$\langle n | \bar{\psi}_R \psi_L | n \rangle \sim e^{2\pi i n/N}. \quad (8.34)$$

We can compare this result with that of Sec. 4, especially Sec. 4.2.1. Especially, we have clearly shown that the extra \mathbb{Z}_N degeneracy of the ground states under the flavor-twisted boundary condition comes out of the 2d conformal behavior.

9 Conclusion and Outlook

What we have newly shown or obtained in the present work on the charge- q N -flavor Schwinger model (2d QED) are summarized as follows;

- full 't Hooft anomaly consistent with the results obtained analytically,
- $1/N^2$ -suppressed holonomy potential for flavor-twisted cases under compactification,
- Nq vacua and chiral condensate with fractional θ dependence for flavor-twisted cases,

- the expression of chiral condensate valid for all the range of the circumference
- the direct consequence of (fractional) quantum instantons on the physical quantities,
- the Nq -branch structure and the pattern of symmetry breaking for massive cases,
- new insights into the volume independence in the model,
- understanding on the WZW model as a dual theory of the Schwinger model.

These results themselves are of great significance for understanding 2d quantum field theory. We below discuss their implications on other theories including 4d QCD and string theory.

4d QCD: It is worth while to investigate the vacuum structure of 4d N -flavor QCD with \mathbb{Z}_N -twisted boundary condition on $\mathbb{R}^3 \times S^1$ (\mathbb{Z}_N -QCD) [50, 106, 131–136] in comparison to our results for the 2d N -flavor Schwinger model with the flavor twist on $\mathbb{R} \times S^1$. In particular the θ vacuum structures in the two theories could share common properties. Since the \mathbb{Z}_N -QCD results in the usual N -flavor QCD in a decompactification limit, this avenue also has potential impact on the study of non-supersymmetric gauge theory on \mathbb{R}^4 .

Brane configurations: $O1^- - \overline{D1}$ brane configurations corresponding to the charge-2 8-flavor Schwinger model are investigated in [26], where 8-flavor fermions and scalars are associated with eight dimensions transverse to $\overline{D1}$ brane. We can raise a question whether one can construct the brane configuration corresponding to the flavor-twisted Schwinger model, which has been the main topic in this work. One here needs to consider how to introduce \mathbb{Z}_8 holonomy of the $U(1)$ gauge field in the brane configuration. On the other hand, the brane configurations for the twisted CP^{N-1} and Grassmann models on $\mathbb{R} \times S^1$ were discussed in [103], where multiple D4 branes are introduced to realize the T-dualized configurations. It is still an open problem whether we can apply a similar technique to the present problem.

Resurgent structure: One of striking properties in the charge- q N -flavor Schwinger model is that fractional quantum instantons have direct consequence on physical quantities. The recent progress in the resurgent structure of quantum mechanics and field theories indicates the significance of fractional instantons and their composite objects called bions [85, 94–96], whose contributions cancel out the imaginary ambiguities arising from perturbation series of physical quantities. It is quite intriguing to derive the bion contributions and compare them to the perturbative calculation in order to investigate the resurgent structure in the charge- q N -flavor Schwinger model.

Acknowledgments

The authors thank S. Sugimoto, M. Anber, A. Cherman, and T. Sulejmanpasic for useful discussion. Especially, T. M. appreciates discussion with S. Sugimoto, and thanks the organizers of “KEK Theory workshop 2018” for giving them the opportunity. The work of T. M. was in part supported by the Japan Society for the Promotion of Science (JSPS) Grant-in-Aid for Scientific Research (KAKENHI) Grant Numbers 16K17677, 18H01217 and 19K03817. The work of T. M. was also supported by the Ministry of Education,

Culture, Sports, Science, and Technology(MEXT)-Supported Program for the Strategic Research Foundation at Private Universities “Topological Science” (Grant No. S1511006). The work of Y. T. was partly supported by JSPS Overseas Research Fellowships. M. U. acknowledges support from U.S. Department of Energy, Office of Science, Office of Nuclear Physics under Award Number DE-FG02-03ER41260. This work was performed in part at “Higher Symmetries conference 2019” at Aspen Center for Physics, which is supported by National Science Foundation grant PHY-1607611. The authors appreciate their hospitality during the program.

A Two-dimensional Dirac spinor

Throughout this paper, we take the following convention for the 2-dimensional Dirac spinor in Euclidean metric.

Let γ^μ be 2×2 matrices, satisfying

$$\{\gamma^\mu, \gamma^\nu\} = 2\delta^{\mu\nu}, \quad (\gamma^\mu)^\dagger = \gamma^\mu, \quad (\text{A.1})$$

for $\mu, \nu = 1, 2$. These relations can be satisfied by using Pauli matrices as

$$\gamma^1 = \sigma_1 = \begin{pmatrix} 0 & 1 \\ 1 & 0 \end{pmatrix}, \quad \gamma^2 = \sigma_2 = \begin{pmatrix} 0 & -i \\ i & 0 \end{pmatrix}. \quad (\text{A.2})$$

We define the chirality matrix γ by

$$\gamma = -i\gamma^1\gamma^2, \quad (\text{A.3})$$

and this satisfies $\{\gamma^\mu, \gamma\} = 0$, $\gamma^\dagger = \gamma$, and $(\gamma)^2 = 1$. Using the Pauli matrix, it is given by

$$\gamma = \sigma_3 = \begin{pmatrix} 1 & 0 \\ 0 & -1 \end{pmatrix}. \quad (\text{A.4})$$

The right/left-handed projectors $P_{\text{R/L}}$ are given by

$$P_{\text{R}} = \frac{1+\gamma}{2} = \begin{pmatrix} 1 & 0 \\ 0 & 0 \end{pmatrix}, \quad P_{\text{L}} = \frac{1-\gamma}{2} = \begin{pmatrix} 0 & 0 \\ 0 & 1 \end{pmatrix}, \quad (\text{A.5})$$

respectively.

The Dirac Lagrangian is given by

$$\mathcal{L} = \bar{\psi}(\not{\partial} + m)\psi, \quad (\text{A.6})$$

where ψ is the two-component spinor field and $\bar{\psi}$ is its conjugate field, $\not{\partial} = \gamma^\mu \partial_\mu$, and m is the fermion mass. We define the right-handed fermion and its conjugate as

$$\psi_{\text{R}} = P_{\text{R}}\psi, \quad \bar{\psi}_{\text{R}} = \bar{\psi}P_{\text{L}}, \quad (\text{A.7})$$

and the left-handed ones as

$$\psi_{\text{L}} = P_{\text{L}}\psi, \quad \bar{\psi}_{\text{L}} = \bar{\psi}P_{\text{R}}. \quad (\text{A.8})$$

The Dirac Lagrangian is then written in the following form:

$$\begin{aligned}\mathcal{L} &= \bar{\psi}_R \not{\partial} \psi_R + \bar{\psi}_L \not{\partial} \psi_L + m(\bar{\psi}_R \psi_L + \bar{\psi}_L \psi_R) \\ &= \bar{\psi}_R (\partial_1 + i\partial_2) \psi_R + \bar{\psi}_L (\partial_1 - i\partial_2) \psi_L + m(\bar{\psi}_R \psi_L + \bar{\psi}_L \psi_R).\end{aligned}\tag{A.9}$$

Here, we slightly abuse the notation: In the first line, ψ_R denotes the two-component spinor but it only has the upper component, while ψ_R in the second line denotes its upper component. The similar notice holds for others.

The motivation of the above definition for conjugate fields comes from the fact that, under the temporal reflection $\Theta : (x^1, x^2) \mapsto (-x^1, x^2)$, the reflection positivity $\langle \Theta(\mathcal{O})\mathcal{O} \rangle \geq 0$ is satisfied with the anti-linear operation Θ generated by

$$\Theta : \psi(x) \mapsto (\bar{\psi}(\Theta \cdot x) \gamma^1)^T, \quad \bar{\psi}(x) \mapsto (\gamma^1 \psi(\Theta \cdot x))^T.\tag{A.10}$$

With the above definition, we find that $\Theta : \psi_R \mapsto (\bar{\psi}_R \gamma^1)^T$ and $\psi_L \mapsto (\bar{\psi}_L \gamma^1)^T$ since γ anti-commutes with γ^μ . We note, in this notation, that $\gamma \psi_R = \psi_R$ but $\bar{\psi}_R \gamma = -\bar{\psi}_R$.

B Holonomy potential via bosonization

Below, we show that the holonomy potential (3.6) can also be obtained by using Abelian bosonization. In the original description, holonomy potential arises from integrating out fermions in the background $U(1)$ gauge field $a_2(\tau, x) = a(\tau)$, and is a one-loop effect. In the bosonized description, it is a tree level effect.

First, let us summarize the setup. For simplicity, we consider $N = 1$ -flavor charge- q Schwinger model, and we set $\theta = 0$. The bosonized action is given in (2.37), and integration-by-part gives;

$$S = \int_{M_2} \left(\frac{1}{2e^2} |da|^2 + \frac{1}{8\pi} |d\phi|^2 - \frac{iq}{2\pi} d\phi \wedge a \right).\tag{B.1}$$

Completing the square in terms of $d\phi$, we can find that the gauge field gets the mass $m_\gamma = qe/\sqrt{\pi}$.

We take $M_2 = T^2 \ni (\tau, x)$, with the identification $\tau + \beta \sim \tau$, $x + L \sim x$, and $L \ll \beta$. We will take $\beta \rightarrow \infty$ in the end, so we work on the temporal gauge $a_1 \equiv 0$ (Precisely speaking, we cannot take temporal gauge naively at finite β , but this does not affect our discussion on the effective potential). Assuming $eL \ll 1$, we would like to derive the effective potential for the holonomy $\exp(iLa_2)$. For that purpose, we put a_2 to be a constant, $a_2 \equiv h$, so that

$$a = h dx.\tag{B.2}$$

We denote the compact scalar field ϕ as

$$\phi(\tau, x) = \frac{2\pi n}{\beta} \tau + \tilde{\phi}(\tau),\tag{B.3}$$

where $\tilde{\phi}$ is the \mathbb{R} -valued scalar, and we neglect its non-zero KK modes. We shall see that it is important to keep the winding number n along the temporal direction even how β is large.

Substituting our approximation on the fields into the bosonized action, we obtain

$$\begin{aligned} S &= L \int d\tau \left(\frac{1}{8\pi} \left(\frac{2\pi}{\beta} n + \dot{\tilde{\phi}} \right)^2 - \frac{iq}{2\pi} \left(\frac{2\pi}{\beta} n + \dot{\tilde{\phi}} \right) h \right) \\ &= L \int d\tau \frac{1}{8\pi} \dot{\tilde{\phi}}^2 + \frac{L\pi}{\beta} \frac{n^2}{2} - iLnqh, \end{aligned} \quad (\text{B.4})$$

and we drop the total-derivative terms to obtain the second line. The effective potential $V(h)$ is obtained as

$$\begin{aligned} \exp(-\beta LV(h)) &= \sum_{n \in \mathbb{Z}} \int \mathcal{D}\tilde{\phi} \exp(-S) = \sum_n \exp \left[-\frac{L\pi}{2\beta} n^2 + inqLh \right] \\ &= \sum_k \exp \left[-L\beta \frac{q^2}{2\pi} \left(h - \frac{2\pi k}{qL} \right)^2 \right], \end{aligned} \quad (\text{B.5})$$

up to an overall normalization constant, or constant shift of V . To find the last expression, we use Poisson summation formula. As a consequence, by taking $\beta \rightarrow \infty$, we obtain the effective action,

$$V(a) = \min_k \frac{q^2}{2\pi} \left(a - \frac{2\pi k}{qL} \right)^2. \quad (\text{B.6})$$

This coincides with (3.6) for $N = 1$ by shifting $a \rightarrow a + \pi/qL$, and this shift corresponds to adding the imaginary chemical potential to make the fermion boundary condition to be periodic.

References

- [1] G. V. Dunne and M. Unsal, “New Nonperturbative Methods in Quantum Field Theory: From Large-N Orbifold Equivalence to Bions and Resurgence,” *Ann. Rev. Nucl. Part. Sci.* **66** (2016) 245–272, [arXiv:1601.03414 \[hep-th\]](#).
- [2] J. S. Schwinger, “Gauge Invariance and Mass. 2.,” *Phys. Rev.* **128** (1962) 2425–2429.
- [3] J. S. Schwinger, “Gauge Invariance and Mass,” *Phys. Rev.* **125** (1962) 397–398.
- [4] J. H. Lowenstein and J. A. Swieca, “Quantum electrodynamics in two-dimensions,” *Annals Phys.* **68** (1971) 172–195.
- [5] A. Casher, J. B. Kogut, and L. Susskind, “Vacuum polarization and the absence of free quarks,” *Phys. Rev.* **D10** (1974) 732–745.
- [6] S. R. Coleman, R. Jackiw, and L. Susskind, “Charge Shielding and Quark Confinement in the Massive Schwinger Model,” *Annals Phys.* **93** (1975) 267.
- [7] N. S. Manton, “The Schwinger Model and Its Axial Anomaly,” *Annals Phys.* **159** (1985) 220–251.
- [8] J. E. Hetrick and Y. Hosotani, “QED ON A CIRCLE,” *Phys. Rev.* **D38** (1988) 2621.
- [9] C. Jayewardena, “SCHWINGER MODEL ON $S(2)$,” *Helv. Phys. Acta* **61** (1988) 636–711.
- [10] I. Sachs and A. Wipf, “Finite temperature Schwinger model,” *Helv. Phys. Acta* **65** (1992) 652–678, [arXiv:1005.1822 \[hep-th\]](#).

- [11] M. C. Banuls, K. Cichy, J. I. Cirac, K. Jansen, and H. Saito, “Thermal evolution of the Schwinger model with Matrix Product Operators,” *Phys. Rev.* **D92** no. 3, (2015) 034519, [arXiv:1505.00279 \[hep-lat\]](#).
- [12] M. C. Banuls, K. Cichy, K. Jansen, and H. Saito, “Chiral condensate in the Schwinger model with Matrix Product Operators,” *Phys. Rev.* **D93** no. 9, (2016) 094512, [arXiv:1603.05002 \[hep-lat\]](#).
- [13] B. Buyens, F. Verstraete, and K. Van Acoleyen, “Hamiltonian simulation of the Schwinger model at finite temperature,” *Phys. Rev.* **D94** no. 8, (2016) 085018, [arXiv:1606.03385 \[hep-lat\]](#).
- [14] B. Buyens, J. Haegeman, F. Hebenstreit, F. Verstraete, and K. Van Acoleyen, “Real-time simulation of the Schwinger effect with Matrix Product States,” *Phys. Rev.* **D96** no. 11, (2017) 114501, [arXiv:1612.00739 \[hep-lat\]](#).
- [15] Y. Tanizaki and M. Tachibana, “Multi-flavor massless QED₂ at finite densities via Lefschetz thimbles,” *JHEP* **02** (2017) 081, [arXiv:1612.06529 \[hep-th\]](#).
- [16] A. Alexandru, G. Basar, P. F. Bedaque, H. Lamm, and S. Lawrence, “Finite Density QED₁₊₁ Near Lefschetz Thimbles,” *Phys. Rev.* **D98** no. 3, (2018) 034506, [arXiv:1807.02027 \[hep-lat\]](#).
- [17] S. L. Adler, “Axial vector vertex in spinor electrodynamics,” *Phys. Rev.* **177** (1969) 2426–2438.
- [18] J. S. Bell and R. Jackiw, “A PCAC puzzle: $\pi^0 \rightarrow \gamma \gamma$ in the sigma model,” *Nuovo Cim.* **A60** (1969) 47–61.
- [19] S. R. Coleman, “More About the Massive Schwinger Model,” *Annals Phys.* **101** (1976) 239.
- [20] I. Affleck, “On the Realization of Chiral Symmetry in (1+1)-dimensions,” *Nucl. Phys.* **B265** (1986) 448–468.
- [21] S. R. Coleman, “There are no Goldstone bosons in two-dimensions,” *Commun. Math. Phys.* **31** (1973) 259–264.
- [22] N. D. Mermin and H. Wagner, “Absence of ferromagnetism or antiferromagnetism in one-or two-dimensional isotropic Heisenberg models,” *Phys. Rev. Lett.* **17** (1966) 1133.
- [23] J. M. Kosterlitz and D. J. Thouless, “Ordering, metastability and phase transitions in two-dimensional systems,” *J. Phys.* **C6** (1973) 1181–1203. [,349(1973)].
- [24] M. M. Anber and E. Poppitz, “Anomaly matching, (axial) Schwinger models, and high-T super Yang-Mills domain walls,” *JHEP* **09** (2018) 076, [arXiv:1807.00093 \[hep-th\]](#).
- [25] M. M. Anber and E. Poppitz, “Domain walls in high- T $SU(N)$ super Yang-Mills theory and QCD(adj),” [arXiv:1811.10642 \[hep-th\]](#).
- [26] A. Armoni and S. Sugimoto, “Vacuum structure of charge k two-dimensional QED and dynamics of an anti D-string near an $O1^-$ -plane,” *JHEP* **03** (2019) 175, [arXiv:1812.10064 \[hep-th\]](#).
- [27] D. Gaiotto, A. Kapustin, Z. Komargodski, and N. Seiberg, “Theta, Time Reversal, and Temperature,” *JHEP* **05** (2017) 091, [arXiv:1703.00501 \[hep-th\]](#).
- [28] Y. Tanizaki, T. Misumi, and N. Sakai, “Circle compactification and ’t Hooft anomaly,” *JHEP* **12** (2017) 056, [arXiv:1710.08923 \[hep-th\]](#).
- [29] E. Witten, “Constraints on Supersymmetry Breaking,” *Nucl. Phys.* **B202** (1982) 253.

- [30] A. V. Smilga, “Instantons in Schwinger model,” *Phys. Rev. D* **49** (1994) 5480–5490, [arXiv:hep-th/9312110 \[hep-th\]](#).
- [31] M. A. Shifman and A. V. Smilga, “Fractons in twisted multiflavor Schwinger model,” *Phys. Rev. D* **50** (1994) 7659–7672, [arXiv:hep-th/9407007 \[hep-th\]](#).
- [32] Y. Tanizaki, “Anomaly constraint on massless QCD and the role of Skyrmions in chiral symmetry breaking,” *JHEP* **08** (2018) 171, [arXiv:1807.07666 \[hep-th\]](#).
- [33] K. Fujikawa, “Path Integral Measure for Gauge Invariant Fermion Theories,” *Phys. Rev. Lett.* **42** (1979) 1195–1198.
- [34] K. Fujikawa, “Path Integral for Gauge Theories with Fermions,” *Phys. Rev. D* **21** (1980) 2848. [Erratum: *Phys. Rev. D* **22**, 1499 (1980)].
- [35] D. Gaiotto, A. Kapustin, N. Seiberg, and B. Willett, “Generalized Global Symmetries,” *JHEP* **02** (2015) 172, [arXiv:1412.5148 \[hep-th\]](#).
- [36] G. ’t Hooft, “Naturalness, chiral symmetry, and spontaneous chiral symmetry breaking,” in *Recent Developments in Gauge Theories. Proceedings, Nato Advanced Study Institute, Cargese, France, August 26 - September 8, 1979*, vol. 59, pp. 135–157. 1980.
- [37] Y. Frishman, A. Schwimmer, T. Banks, and S. Yankielowicz, “The Axial Anomaly and the Bound State Spectrum in Confining Theories,” *Nucl. Phys. B* **177** (1981) 157–171.
- [38] X.-G. Wen, “Classifying gauge anomalies through symmetry-protected trivial orders and classifying gravitational anomalies through topological orders,” *Phys. Rev. D* **88** no. 4, (2013) 045013, [arXiv:1303.1803 \[hep-th\]](#).
- [39] A. Kapustin and R. Thorngren, “Anomalies of discrete symmetries in various dimensions and group cohomology,” [arXiv:1404.3230 \[hep-th\]](#).
- [40] J. C. Wang, Z.-C. Gu, and X.-G. Wen, “Field theory representation of gauge-gravity symmetry-protected topological invariants, group cohomology and beyond,” *Phys. Rev. Lett.* **114** no. 3, (2015) 031601, [arXiv:1405.7689 \[cond-mat.str-el\]](#).
- [41] C. G. Callan, Jr. and J. A. Harvey, “Anomalies and Fermion Zero Modes on Strings and Domain Walls,” *Nucl. Phys. B* **250** (1985) 427–436.
- [42] E. Witten, “The ”Parity” Anomaly On An Unorientable Manifold,” *Phys. Rev. D* **94** no. 19, (2016) 195150, [arXiv:1605.02391 \[hep-th\]](#).
- [43] Y. Tachikawa and K. Yonekura, “On time-reversal anomaly of 2+1d topological phases,” *PTEP* **2017** no. 3, (2017) 033B04, [arXiv:1610.07010 \[hep-th\]](#).
- [44] Y. Tanizaki and Y. Kikuchi, “Vacuum structure of bifundamental gauge theories at finite topological angles,” *JHEP* **06** (2017) 102, [arXiv:1705.01949 \[hep-th\]](#).
- [45] Z. Komargodski, A. Sharon, R. Thorngren, and X. Zhou, “Comments on Abelian Higgs Models and Persistent Order,” [arXiv:1705.04786 \[hep-th\]](#).
- [46] Z. Komargodski, T. Sulejmanpasic, and M. Unsal, “Walls, anomalies, and deconfinement in quantum antiferromagnets,” *Phys. Rev. D* **97** no. 5, (2018) 054418, [arXiv:1706.05731 \[cond-mat.str-el\]](#).
- [47] H. Shimizu and K. Yonekura, “Anomaly constraints on deconfinement and chiral phase transition,” *Phys. Rev. D* **97** no. 10, (2018) 105011, [arXiv:1706.06104 \[hep-th\]](#).

- [48] J. Wang, X.-G. Wen, and E. Witten, “Symmetric Gapped Interfaces of SPT and SET States: Systematic Constructions,” *Phys. Rev.* **X8** no. 3, (2018) 031048, [arXiv:1705.06728 \[cond-mat.str-el\]](#).
- [49] D. Gaiotto, Z. Komargodski, and N. Seiberg, “Time-reversal breaking in QCD_4 , walls, and dualities in $2 + 1$ dimensions,” *JHEP* **01** (2018) 110, [arXiv:1708.06806 \[hep-th\]](#).
- [50] Y. Tanizaki, Y. Kikuchi, T. Misumi, and N. Sakai, “Anomaly matching for phase diagram of massless \mathbb{Z}_N -QCD,” *Phys. Rev.* **D97** (2018) 054012, [arXiv:1711.10487 \[hep-th\]](#).
- [51] M. Yamazaki, “Relating ’t Hooft Anomalies of 4d Pure Yang-Mills and 2d \mathbb{CP}^{N-1} Model,” *JHEP* **10** (2018) 172, [arXiv:1711.04360 \[hep-th\]](#).
- [52] M. Guo, P. Putrov, and J. Wang, “Time reversal, $\text{SU}(N)$ YangMills and cobordisms: Interacting topological superconductors/insulators and quantum spin liquids in $3+1\text{D}$,” *Annals Phys.* **394** (2018) 244–293, [arXiv:1711.11587 \[cond-mat.str-el\]](#).
- [53] T. Sulejmanpasic and Y. Tanizaki, “C-P-T anomaly matching in bosonic quantum field theory and spin chains,” *Phys. Rev.* **B97** (2018) 144201, [arXiv:1802.02153 \[hep-th\]](#).
- [54] Y. Tanizaki and T. Sulejmanpasic, “Anomaly and global inconsistency matching: θ -angles, $\text{SU}(3)/\text{U}(1)^2$ nonlinear sigma model, $\text{SU}(3)$ chains and its generalizations,” *Phys. Rev.* **B98** no. 11, (2018) 115126, [arXiv:1805.11423 \[cond-mat.str-el\]](#).
- [55] C. Cordova and T. T. Dumitrescu, “Candidate Phases for $\text{SU}(2)$ Adjoint QCD_4 with Two Flavors from $\mathcal{N} = 2$ Supersymmetric Yang-Mills Theory,” [arXiv:1806.09592 \[hep-th\]](#).
- [56] M. M. Anber and E. Poppitz, “Two-flavor adjoint QCD,” *Phys. Rev.* **D98** no. 3, (2018) 034026, [arXiv:1805.12290 \[hep-th\]](#).
- [57] M. Hongo, T. Misumi, and Y. Tanizaki, “Phase structure of the twisted $\text{SU}(3)/\text{U}(1)^2$ flag sigma model on $\mathbb{R} \times S^1$,” *JHEP* **02** (2019) 070, [arXiv:1812.02259 \[hep-th\]](#).
- [58] K. Yonekura, “Anomaly matching in QCD thermal phase transition,” [arXiv:1901.08188 \[hep-th\]](#).
- [59] T. Banks and N. Seiberg, “Symmetries and Strings in Field Theory and Gravity,” *Phys. Rev.* **D83** (2011) 084019, [arXiv:1011.5120 \[hep-th\]](#).
- [60] A. Kapustin and N. Seiberg, “Coupling a QFT to a TQFT and Duality,” *JHEP* **04** (2014) 001, [arXiv:1401.0740 \[hep-th\]](#).
- [61] R. Stora, “Algebraic Structure and Topological Origin of Anomalies,” in *Progress in Gauge Field Theory. Proceedings, NATO Advanced Study Institute, Cargese, France*. 1983.
- [62] B. Zumino, “Chiral Anomalies and Differential Geometry,” in *Relativity, groups and topology: Proceedings, 40th Summer School of Theoretical Physics - Session 40: Les Houches, France, June 27 - August 4, 1983, vol. 2*, pp. 1291–1322. 1983. <http://inspirehep.net/record/192970/files/5461614.pdf>.
- [63] J. Stern, “Light quark masses and condensates in QCD,” [arXiv:hep-ph/9712438 \[hep-ph\]](#). [Lect. Notes Phys.513,26(1998)].
- [64] J. Stern, “Two alternatives of spontaneous chiral symmetry breaking in QCD,” [arXiv:hep-ph/9801282 \[hep-ph\]](#).
- [65] I. I. Kogan, A. Kovner, and M. A. Shifman, “Chiral symmetry breaking without bilinear condensates, unbroken axial $\text{Z}(N)$ symmetry, and exact QCD inequalities,” *Phys. Rev.* **D59** (1999) 016001, [arXiv:hep-ph/9807286 \[hep-ph\]](#).

- [66] T. Kanazawa, “Chiral symmetry breaking with no bilinear condensate revisited,” *JHEP* **10** (2015) 010, [arXiv:1507.06376 \[hep-ph\]](#).
- [67] F. D. M. Haldane, “Nonlinear field theory of large spin Heisenberg antiferromagnets. Semiclassically quantized solitons of the one-dimensional easy Axis Neel state,” *Phys. Rev. Lett.* **50** (1983) 1153–1156.
- [68] F. D. M. Haldane, “Continuum dynamics of the 1-D Heisenberg antiferromagnetic identification with the $O(3)$ nonlinear sigma model,” *Phys. Lett.* **A93** (1983) 464–468.
- [69] I. Affleck and E. H. Lieb, “A Proof of Part of Haldane’s Conjecture on Spin Chains,” *Lett. Math. Phys.* **12** (1986) 57.
- [70] I. Affleck and F. D. M. Haldane, “Critical Theory of Quantum Spin Chains,” *Phys. Rev.* **B36** (1987) 5291–5300.
- [71] D. Bykov, “Haldane limits via Lagrangian embeddings,” *Nucl. Phys.* **B855** (2012) 100–127, [arXiv:1104.1419 \[hep-th\]](#).
- [72] M. Lajkó, K. Wamer, F. Mila, and I. Affleck, “Generalization of the Haldane conjecture to $SU(3)$ chains,” *Nucl. Phys.* **B924** (2017) 508–577, [arXiv:1706.06598 \[cond-mat.str-el\]](#).
- [73] Y. Yao, C.-T. Hsieh, and M. Oshikawa, “Anomaly matching and symmetry-protected critical phases in $SU(N)$ spin systems in 1+1 dimensions,” [arXiv:1805.06885 \[cond-mat.str-el\]](#).
- [74] K. Ohmori, N. Seiberg, and S.-H. Shao, “Sigma Models on Flags,” [arXiv:1809.10604 \[hep-th\]](#).
- [75] S. R. Coleman, “The Quantum Sine-Gordon Equation as the Massive Thirring Model,” *Phys. Rev.* **D11** (1975) 2088.
- [76] M. M. Anber, E. Poppitz, and T. Sulejmanpasic, “Strings from domain walls in supersymmetric Yang-Mills theory and adjoint QCD,” *Phys. Rev.* **D92** no. 2, (2015) 021701, [arXiv:1501.06773 \[hep-th\]](#).
- [77] T. Sulejmanpasic, H. Shao, A. Sandvik, and M. Unsal, “Confinement in the bulk, deconfinement on the wall: infrared equivalence between compactified QCD and quantum magnets,” *Phys. Rev. Lett.* **119** no. 9, (2017) 091601, [arXiv:1608.09011 \[hep-th\]](#).
- [78] H. Nishimura and Y. Tanizaki, “High-temperature domain walls of QCD with imaginary chemical potentials,” [arXiv:1903.04014 \[hep-th\]](#).
- [79] J. Wess and B. Zumino, “Consequences of anomalous Ward identities,” *Phys. Lett.* **37B** (1971) 95–97.
- [80] E. Witten, “Global Aspects of Current Algebra,” *Nucl. Phys.* **B223** (1983) 422–432.
- [81] E. Witten, “Nonabelian Bosonization in Two-Dimensions,” *Commun. Math. Phys.* **92** (1984) 455–472. [,201(1983)].
- [82] A. M. Polyakov and P. B. Wiegmann, “Theory of Nonabelian Goldstone Bosons,” *Phys. Lett.* **B131** (1983) 121–126. [,195(1983)].
- [83] A. M. Polyakov and P. B. Wiegmann, “Goldstone Fields in Two-Dimensions with Multivalued Actions,” *Phys. Lett.* **141B** (1984) 223–228.
- [84] G. V. Dunne, Y. Tanizaki, and M. Ünsal, “Quantum Distillation of Hilbert Spaces, Semi-classics and Anomaly Matching,” *JHEP* **08** (2018) 068, [arXiv:1803.02430 \[hep-th\]](#).

- [85] G. V. Dunne and M. Unsal, “Resurgence and Trans-series in Quantum Field Theory: The CP(N-1) Model,” *JHEP* **11** (2012) 170, [arXiv:1210.2423 \[hep-th\]](#).
- [86] M. Unsal, “Magnetic bion condensation: A New mechanism of confinement and mass gap in four dimensions,” *Phys. Rev.* **D80** (2009) 065001, [arXiv:0709.3269 \[hep-th\]](#).
- [87] M. Unsal and L. G. Yaffe, “Center-stabilized Yang-Mills theory: Confinement and large N volume independence,” *Phys. Rev.* **D78** (2008) 065035, [arXiv:0803.0344 \[hep-th\]](#).
- [88] M. Unsal, “Abelian duality, confinement, and chiral symmetry breaking in QCD(adj),” *Phys. Rev. Lett.* **100** (2008) 032005, [arXiv:0708.1772 \[hep-th\]](#).
- [89] P. Kovtun, M. Unsal, and L. G. Yaffe, “Volume independence in large N(c) QCD-like gauge theories,” *JHEP* **06** (2007) 019, [arXiv:hep-th/0702021 \[HEP-TH\]](#).
- [90] M. Shifman and M. Unsal, “QCD-like Theories on R(3) x S(1): A Smooth Journey from Small to Large r(S(1)) with Double-Trace Deformations,” *Phys. Rev.* **D78** (2008) 065004, [arXiv:0802.1232 \[hep-th\]](#).
- [91] M. Shifman and M. Unsal, “Multiflavor QCD* on R(3) x S(1): Studying Transition From Abelian to Non-Abelian Confinement,” *Phys. Lett.* **B681** (2009) 491–494, [arXiv:0901.3743 \[hep-th\]](#).
- [92] G. Cossu and M. D’Elia, “Finite size phase transitions in QCD with adjoint fermions,” *JHEP* **07** (2009) 048, [arXiv:0904.1353 \[hep-lat\]](#).
- [93] G. Cossu, H. Hatanaka, Y. Hosotani, and J.-I. Noaki, “Polyakov loops and the Hosotani mechanism on the lattice,” *Phys. Rev.* **D89** no. 9, (2014) 094509, [arXiv:1309.4198 \[hep-lat\]](#).
- [94] P. C. Argyres and M. Unsal, “The semi-classical expansion and resurgence in gauge theories: new perturbative, instanton, bion, and renormalon effects,” *JHEP* **08** (2012) 063, [arXiv:1206.1890 \[hep-th\]](#).
- [95] P. Argyres and M. Unsal, “A semiclassical realization of infrared renormalons,” *Phys. Rev. Lett.* **109** (2012) 121601, [arXiv:1204.1661 \[hep-th\]](#).
- [96] G. V. Dunne and M. Unsal, “Continuity and Resurgence: towards a continuum definition of the CP(N-1) model,” *Phys. Rev.* **D87** (2013) 025015, [arXiv:1210.3646 \[hep-th\]](#).
- [97] E. Poppitz, T. Schafer, and M. Unsal, “Continuity, Deconfinement, and (Super) Yang-Mills Theory,” *JHEP* **10** (2012) 115, [arXiv:1205.0290 \[hep-th\]](#).
- [98] M. M. Anber, S. Collier, E. Poppitz, S. Strimas-Mackey, and B. Teeple, “Deconfinement in $\mathcal{N} = 1$ super Yang-Mills theory on $\mathbb{R}^3 \times S^1$ via dual-Coulomb gas and ”affine” XY-model,” *JHEP* **11** (2013) 142, [arXiv:1310.3522 \[hep-th\]](#).
- [99] G. Basar, A. Cherman, D. Dorigoni, and M. Ünsal, “Volume Independence in the Large N Limit and an Emergent Fermionic Symmetry,” *Phys. Rev. Lett.* **111** no. 12, (2013) 121601, [arXiv:1306.2960 \[hep-th\]](#).
- [100] A. Cherman, D. Dorigoni, and M. Unsal, “Decoding perturbation theory using resurgence: Stokes phenomena, new saddle points and Lefschetz thimbles,” *JHEP* **10** (2015) 056, [arXiv:1403.1277 \[hep-th\]](#).
- [101] T. Misumi and T. Kanazawa, “Adjoint QCD on $\mathbb{R}^3 \times S^1$ with twisted fermionic boundary conditions,” *JHEP* **06** (2014) 181, [arXiv:1405.3113 \[hep-ph\]](#).

- [102] T. Misumi, M. Nitta, and N. Sakai, “Neutral bions in the \mathbb{CP}^{N-1} model,” *JHEP* **06** (2014) 164, [arXiv:1404.7225 \[hep-th\]](#).
- [103] T. Misumi, M. Nitta, and N. Sakai, “Classifying bions in Grassmann sigma models and non-Abelian gauge theories by D-branes,” *PTEP* **2015** (2015) 033B02, [arXiv:1409.3444 \[hep-th\]](#).
- [104] G. V. Dunne and M. Unsal, “Resurgence and Dynamics of $O(N)$ and Grassmannian Sigma Models,” *JHEP* **09** (2015) 199, [arXiv:1505.07803 \[hep-th\]](#).
- [105] T. Misumi, M. Nitta, and N. Sakai, “Non-BPS exact solutions and their relation to bions in \mathbb{CP}^{N-1} models,” *JHEP* **05** (2016) 057, [arXiv:1604.00839 \[hep-th\]](#).
- [106] A. Cherman, T. Schafer, and M. Unsal, “Chiral Lagrangian from Duality and Monopole Operators in Compactified QCD,” *Phys. Rev. Lett.* **117** no. 8, (2016) 081601, [arXiv:1604.06108 \[hep-th\]](#).
- [107] T. Fujimori, S. Kamata, T. Misumi, M. Nitta, and N. Sakai, “Nonperturbative contributions from complexified solutions in \mathbb{CP}^{N-1} models,” *Phys. Rev.* **D94** no. 10, (2016) 105002, [arXiv:1607.04205 \[hep-th\]](#).
- [108] T. Fujimori, S. Kamata, T. Misumi, M. Nitta, and N. Sakai, “Exact resurgent trans-series and multibion contributions to all orders,” *Phys. Rev.* **D95** no. 10, (2017) 105001, [arXiv:1702.00589 \[hep-th\]](#).
- [109] T. Fujimori, S. Kamata, T. Misumi, M. Nitta, and N. Sakai, “Resurgence Structure to All Orders of Multi-bions in Deformed SUSY Quantum Mechanics,” *PTEP* **2017** no. 8, (2017) 083B02, [arXiv:1705.10483 \[hep-th\]](#).
- [110] T. Fujimori, S. Kamata, T. Misumi, M. Nitta, and N. Sakai, “Bion non-perturbative contributions versus infrared renormalons in two-dimensional \mathbb{CP}^{N-1} models,” *JHEP* **02** (2019) 190, [arXiv:1810.03768 \[hep-th\]](#).
- [111] T. Sulejmanpasic, “Global Symmetries, Volume Independence, and Continuity in Quantum Field Theories,” *Phys. Rev. Lett.* **118** no. 1, (2017) 011601, [arXiv:1610.04009 \[hep-th\]](#).
- [112] M. Yamazaki and K. Yonekura, “From 4d Yang-Mills to 2d \mathbb{CP}^{N-1} model: IR problem and confinement at weak coupling,” *JHEP* **07** (2017) 088, [arXiv:1704.05852 \[hep-th\]](#).
- [113] E. Itou, “Fractional instanton of the $SU(3)$ gauge theory in weak coupling regime,” [arXiv:1811.05708 \[hep-th\]](#).
- [114] P. V. Buividovich and S. N. Valgushev, “Lattice study of continuity and finite-temperature transition in two-dimensional $SU(N) \times SU(N)$ Principal Chiral Model,” [arXiv:1706.08954 \[hep-lat\]](#).
- [115] K. Aitken, A. Cherman, E. Poppitz, and L. G. Yaffe, “QCD on a small circle,” *Phys. Rev.* **D96** no. 9, (2017) 096022, [arXiv:1707.08971 \[hep-th\]](#).
- [116] A. Behtash, E. Poppitz, T. Sulejmanpasic, and M. Ünsal, “The curious incident of multi-instantons and the necessity of Lefschetz thimbles,” *JHEP* **11** (2015) 175, [arXiv:1507.04063 \[hep-th\]](#).
- [117] N. K. Nielsen and B. Schroer, “Topological Fluctuations and Breaking of Chiral Symmetry in Gauge Theories Involving Massless Fermions,” *Nucl. Phys.* **B120** (1977) 62–76.
- [118] M. Hortacsu, K. D. Rothe, and B. Schroer, “Generalized QED in Two-dimensions and Functional Determinants,” *Phys. Rev.* **D20** (1979) 3203.

- [119] K. D. Rothe and J. A. Swieca, “Path Integral Representations for Tunneling Amplitudes in the Schwinger Model,” *Annals Phys.* **117** (1979) 382.
- [120] N. V. Krasnikov, V. A. Matveev, V. A. Rubakov, A. N. Tavkhelidze, and V. F. Tokarev, “DOUBLE THETA VACUUM STRUCTURE AND THE FUNCTIONAL INTEGRAL IN THE SCHWINGER MODEL,” *Phys. Lett.* **97B** (1980) 103–106.
- [121] S. Iso and H. Murayama, “Hamiltonian Formulation of the Schwinger Model: Nonconfinement and Screening of the Charge,” *Prog. Theor. Phys.* **84** (1990) 142–163.
- [122] T. H. Hansson, H. B. Nielsen, and I. Zahed, “QED with unequal charges: A Study of spontaneous Z_n symmetry breaking,” *Nucl. Phys.* **B451** (1995) 162–176, [arXiv:hep-ph/9405324 \[hep-ph\]](#). [Erratum: Nucl. Phys. B456,757(1995)].
- [123] Y. Kikuchi and Y. Tanizaki, “Global inconsistency, ’t Hooft anomaly, and level crossing in quantum mechanics,” *Prog. Theor. Exp. Phys.* **2017** (2017) 113B05, [arXiv:1708.01962 \[hep-th\]](#).
- [124] J. E. Hetrick, Y. Hosotani, and S. Iso, “The Massive multi - flavor Schwinger model,” *Phys. Lett.* **B350** (1995) 92–102, [arXiv:hep-th/9502113 \[hep-th\]](#).
- [125] J. E. Hetrick, Y. Hosotani, and S. Iso, “The Interplay between mass, volume, vacuum angle and chiral condensate in N flavor QED in two-dimensions,” *Phys. Rev.* **D53** (1996) 7255–7259, [arXiv:hep-th/9510090 \[hep-th\]](#).
- [126] T. Eguchi and H. Kawai, “Reduction of Dynamical Degrees of Freedom in the Large N Gauge Theory,” *Phys. Rev. Lett.* **48** (1982) 1063.
- [127] A. Gonzalez-Arroyo and M. Okawa, “The Twisted Eguchi-Kawai Model: A Reduced Model for Large N Lattice Gauge Theory,” *Phys. Rev.* **D27** (1983) 2397.
- [128] G. Bhanot, U. M. Heller, and H. Neuberger, “The Quenched Eguchi-Kawai Model,” *Phys. Lett.* **113B** (1982) 47–50.
- [129] A. Cherman, M. Shifman, and M. Unsal, “Bose-Fermi cancellations without supersymmetry,” *Phys. Rev.* **D99** no. 10, (2019) 105001, [arXiv:1812.04642 \[hep-th\]](#).
- [130] J. Evslin and B. Zhang, “Mass-gap in the compactified principal chiral model,” *Phys. Rev.* **D98** no. 8, (2018) 085016, [arXiv:1809.10973 \[hep-th\]](#).
- [131] H. Kouno, Y. Sakai, T. Makiyama, K. Tokunaga, T. Sasaki, and M. Yahiro, “Quark-gluon thermodynamics with the $Z(N(c))$ symmetry,” *J. Phys.* **G39** (2012) 085010.
- [132] Y. Sakai, H. Kouno, T. Sasaki, and M. Yahiro, “The quarkyonic phase and the Z_{N_c} symmetry,” *Phys. Lett.* **B718** (2012) 130–135, [arXiv:1204.0228 \[hep-ph\]](#).
- [133] H. Kouno, T. Makiyama, T. Sasaki, Y. Sakai, and M. Yahiro, “Confinement and Z_3 symmetry in three-flavor QCD,” *J. Phys.* **G40** (2013) 095003, [arXiv:1301.4013 \[hep-ph\]](#).
- [134] H. Kouno, T. Misumi, K. Kashiwa, T. Makiyama, T. Sasaki, and M. Yahiro, “Differences and similarities between fundamental and adjoint matters in $SU(N)$ gauge theories,” *Phys. Rev.* **D88** no. 1, (2013) 016002, [arXiv:1304.3274 \[hep-ph\]](#).
- [135] H. Kouno, K. Kashiwa, J. Takahashi, T. Misumi, and M. Yahiro, “Understanding QCD at high density from a Z_3 -symmetric QCD-like theory,” *Phys. Rev.* **D93** no. 5, (2016) 056009, [arXiv:1504.07585 \[hep-ph\]](#).
- [136] T. Iritani, E. Itou, and T. Misumi, “Lattice study on QCD-like theory with exact center symmetry,” *JHEP* **11** (2015) 159, [arXiv:1508.07132 \[hep-lat\]](#).